Understanding Complex Flooding Dynamics in Low-Gradient Coastal Watersheds Using Hybrid 1D/2D Hydrodynamic Modeling and Implications for Flood Risk Mitigation

A Dissertation

Presented to the

Graduate Faculty of the

University of Louisiana at Lafayette

In Partial Fulfillment of the

Requirements for the Degree

Doctor of Philosophy

Haitham Abdel Hakeem Saad

Spring 2022

Understanding Complex Flooding Dynamics in Low-Gradient Coastal Watersheds Using Hybrid 1D/2D Hydrodynamic Modeling and Implications for Flood Risk Mitigation

Haitham Abdel Hakeem Saad

APPROVED:

Emad Habib, Chair
Professor of Civil Engineering

Robert L. Miller
Assistant Professor of Civil Engineering

Mohammad Jamal Khattak
Professor of Civil Engineering

Xiaoduan Sun
Professor of Civil Engineering

Durga D. Poudel
Professor of Environmental Science

Brian Miles
Senior Research Project Engineer
Center for Coastal and Ocean Mapping
University of New Hampshire

Mary Farmer-Kaiser
Dean of the Graduate School

To the loves of my Life
Parents, family, wife, and my kids

Acknowledgments

All praise is due to the almighty God ALLAH, the Most Gracious and the Most Merciful for his blessings bestowed upon me (as well as mankind) and for giving me the strength to achieve what I have accomplished in my life.

First and foremost, I would like to acknowledge and extend my sincerest gratitude to my major advisor, Professor Emad Habib. In addition to being a great source of expertise in his own field, he had the confidence, encouragement, and patience to support me as I ventured into areas that were unfamiliar to me.

I would also like to thank the rest of my committee, Dr. Mohammad Khattak, Dr. Robert Miller, Dr. Xiaoduan Sun, Dr. Durga Poudel, and Dr. Brian Miles for their support and encouragement throughout this process. A special thanks go out again to Dr. Brian Miles for his support and continuous offer to help while I was doing my research and preparing my dissertation.

Special thanks to my labmate and friend Mohamed Salah who not only aided in brainstorming, preparing my defense presentation, and overall advice, but formed a support network that made completing this research possible.

Lastly, I would like to express my appreciation to my wife and better half, Yasmin Sakr, who has given me unwavering support, love, and encouragement throughout every step of the way. She took care of the whole family lifting a huge weight off my shoulders for me to clear my head and focus on my research. Yasmin, I owe you!

Table of Contents

List of Tables

List of Figures

Chapter 1: Introduction

1.1 Motivation

Coastal regions are vital for the advancement of society by supporting capital flows for tourism, industrialization, transportation, and urban development (Santiago-Collazo et al., 2019). Current projections for the United States (U.S.) population that resides in low-gradient coastal zones forecast an increase of 145% by 2030 compared to 2000 (Neumann et al., 2015). In addition, the U.S. has 17 port cities with a population greater than 1 million (Wahl et al., 2015). Extreme coastal flooding is one element that poses a significant threat to human life and infrastructure (Bhaskaran et al., 2014; Moussa and Bocquillon, 2009). When combined with the typical low-gradient nature of these watersheds, such extreme flooding conditions exhibit a complex hydrodynamic nature manifested in bi-directional riverine flows, multiple-peak flows, local stagnations, significant backwater effects, and prolonged flood recession episodes. However, the relative significance of the different physical drivers behind complex flood dynamics in low gradient systems on a reach scale is challenging to define. Backwater effects are highly significant (Dalrymple and Choi, 2007); wind and tidal effects, combined with the low-gradient topography in such systems, also play a critical role in the overall flood response in such settings (Maskell et al., 2013). Significant runoff contributions produced from developed and heavily urbanized areas situated around the river. Extensive swamp areas with significant river-swamp interactions lead to unique flow regimes with significant implications for flooding in the main river and its tributaries. Besides its research significance, developing a comprehensive understanding of complex flood dynamics in low-gradient riverine systems is essential for designing effective flood mitigation strategies.

1.2 Overarching Goal and Main Objectives

The overarching goal of this dissertation is to develop a comprehensive understanding of the complex flood dynamics in low-gradient riverine systems using a modeling-based approach. Using this approach, the study will also provide a deep insight into the value of different strategies for flood mitigation and how they perform in the context of extreme rainfall events and changing landscapes. The study starts by investigating the level of model complexity required for reproducing complex flood regimes in low-gradient watersheds and quantitatively assessing them using reliable numerical models. Following that, we utilize the modeling approach that allows for a more accurate representation of the flow dynamics to evaluate the performance of riverine dredging as a traditional flood mitigation strategy in response to decreased channel capacities. Finally, the study examines a more nature-based approach by maximizing the role of riverine-connected natural storage areas (swamps and wetlands) in mitigating the flooding impact.

The current dissertation focused on three main objectives, as listed below. Each objective is thoroughly investigated in a separate chapter and presented in the format of a manuscript that has already been published or submitted for peer-reviewed publication.

1.2.1 Objective 1: Assessment of model complexity required to simulate flood dynamics in low-gradient coastal watersheds.

Flooding can emerge from several mechanisms or driving forces. A wide variety of modeling approaches have been proposed and implemented in terms of scale and representation of physical processes to simulate such mechanisms. However, selecting the proper level of detail in the model setup continues to pose challenges, particularly in low gradient basins. Previous studies highlighted the need to develop reliable and representative numerical models that can be used to understand complex flood dynamics and propose effective flood mitigation strategies in low-gradient riverine systems. This part of the dissertation focuses on developing a hydrodynamic model that can reproduce the complex flood dynamics in the Vermillion Watershed, a representative system of low-gradient watersheds in coastal regions. The model development and assessment will concentrate on the following specific aspects:

1.2.1.1 Effect of flow routing methodology. Practically, adopting a specific numerical model within the context of studying floods requires selecting a runoff generation, both surface and subsurface, and a runoff routing component. The runoff generation component manages the amount of water that gets into the stream and flows towards the catchment outlet within the time frame of the storm and the period that follows, while the runoff routing deals with the routing of the runoff from the source areas to the outlet. Typically, hydrologic and hydrodynamic models are responsible for the runoff generation and runoff routing components, respectively. However, the boundary between runoff generation and runoff routing is not a very precise one (Beven, 2011), and it is widely accepted among the community of practitioners that the runoff generation problem is the more difficult to adjust (Kim et al., 2012). Thus, practical experience suggests that a

comprehensive hydrologic model simulating the rainfall-runoff mechanism, combined with relatively simple models for the routing, may suffice (Hooper et al., 2017). However, simplified models have several limitations for applications in cases such as: models for urban flooding inundation (Abderrezzak et al., 2009), low-gradient regions in which backwater effects are significant (Tsai, 2005), or flow into large reservoirs (Kim et al., 2012). Therefore, it is critical to quantify the role and dependence between the flooding mechanisms when studying flooding in coastal watersheds (Bilskie and Hagen, 2018).

1.2.1.2 Selection of model dimensionality. Model dimensionality presents another challenge. Different physical processes may govern at different spatial scales. While 1-D hydrodynamic models may be appropriate for large-scale applications, explicit modeling of floodplain flows using 2-D models can be vital for more local assessments. Earlier studies focused on comparisons of 1D versus 2D hydrodynamic models (e.g., Benjankar et al., 2015; Leandro et al., 2009), cross-comparisons of multiple 2D models (e.g., Vanderkimpen et al., 2008), and assessing the exact model under different configurations of topographic resolution (e.g., Bates et al., 2003; Cook and Merwade, 2009). Research is still needed to assess the value of increasing the dimensional complexity and how it impacts the models' ability to capture the local flow dynamics.

1.2.1.3 Effect of tailwater conditions. The physical processes that drive flooding in coastal watersheds and the internal interaction between such processes are still relatively understudied. Flood mechanisms in these regions are typically due to the following factors: (i) Precipitation where intense or prolonged precipitation induces surface runoff that, when it reaches streams, increases the streamflow rate to the point that exceeds the channel capacity and produces an out-of-bank flow that inundates the floodplain, (ii) Storm surge produced by

high winds and low atmospheric pressure drives oceanic waters to interact with the local coastal geometry and (iii) Compound flooding due to rainfall-runoff and storm surge. Typically, storm surge or coast conditions are represented in flood models as downstream boundary conditions. In flood models, simplifications for boundary conditions often involve disregarding enforcing an exact downstream boundary condition (that represents tides or storm surges) and considering a normal depth assumption downstream. According to this assumption, a rating curve is generated internally within the model routine and imposed as a downstream boundary condition. Despite studies investigating the probability of the co-occurrence of storm surge and rainfall-runoff or in close succession highlighted that these flooding mechanisms are present over different length scales (Santiago-Collazo et al., 2019), the significance of such normal depth assumption in low-gradient watersheds is not fully understood. The significance of boundary uncertainty on the performance of a flood model presents a challenge in flood modeling and investigating the level of detail required for such representation is needed.

1.2.2 Objective 2: Assessment of riverine dredging as a traditional mitigation approach within low-gradient watersheds.

The typical low gradients that characterize the main rivers and their tributaries in coastal or inland-coastal transition zones further intensify flooding along these rivers. The flow regimes under low-gradient conditions typically lead to channel sedimentation and reduction of channel conveyance capacity, and thus an increase in fluvial flooding during moderate and extreme storms.

Flood mitigation measures are often sought in these regions to alleviate the impact of riverine-induced flooding. One of the traditional and most common flood mitigation practices in coastal watersheds is watercourse dredging or channelization (Liao et al., 2019).

Dredging refers to activities that include any combination of removing instream and riparian sediment and vegetation, modifying channel width, depth, and gradient, and straightening the river (Brookes, 1988). By structurally altering one or more of the hydraulic variables that govern channel flow and its conveyance capacity (e.g., slope, depth, width, roughness), water stages are typically decreased, reducing the spatial extent of the flood inundation and associated flood risk. Early studies on watercourse dredging provided empirical and theoretical evidence that channelization can be quite effective as a flood mitigation measure if appropriately designed to prevent bank erosion and channel silting (Nunnally, 1978; Shankman and Pugh, 1992). Recent feasibility studies examined potential dredging scenarios for tidally-dominated sections of coastal rivers in the southwest U.K. These studies demonstrated that dredging did not significantly lower the peak flood levels during winter storms (Webster et al., 2014). The study showed that the shape of the river cross-section and the heights of the riverbanks played a significant role in determining the actual flood level reduction. Other studies showed that dredging could have unintended consequences in other watersheds, especially in downstream communities. For example, (Prestegaard et al., 1994) reported that areas downstream of a modified section of the Raccoon River in Iowa had experienced higher-magnitude floods compared to sections from rivers that have upstream similarly-sized drainage areas. (Rose and Peters, 2001) showed that channel cross-section enlargement increases the flood wave velocity, speeding downstream flood peaks' arrival time.

Other studies have focused primarily on the adverse effects of channelization on water quality (Schoof, 1980), ecological alterations of the stream and the riparian corridor (Juan et al., 2020), and stream degradation (Pierce and King, 2013). Another potential aspect

of river dredging activities is the effect on tidal propagation. (Cai et al., 2012) applied an analytical model to show that a reduction in river discharge and degradation of the riverbed leads to a significant decrease in the travel time of the tidal wave. The study also highlighted that the amplification of the tidal amplitude due to dredging could facilitate the penetration of storm surges into the estuary. Likewise, (Ralston et al., 2019) studied the effect of dredging on New York Harbor and the tidal Hudson River and found that such modification doubled the tidal amplitude and increased the landward conveyance of coastal storms surge.

While dredging can increase the hydraulic efficiency of river channels and potentially reduce overbank flooding, the impact on flow hydrodynamics and the overall flooding regime needs to be better understood, especially in watersheds located within inland-coastal transition zones. In such regions, river systems are typically characterized with complex flow dynamics due to factors such as flow reversals and bi-directional flows (e.g., Watson et al., 2017), dynamic connectivity, and flow exchanges with large natural storage areas such as swamps and wetlands; tidal influences, and the large volumes of synchronized tributary flows from urbanized sub-watersheds (e.g., Pattison et al., 2014; Wang et al., 2019). The complexity of flow regimes in these regions has implications for flood mitigation; therefore, it is imperative to develop a comprehensive understanding of the impacts of riverine dredging that emerge as a possible mitigation strategy in response to decreased channel capacities and increased flood risk.

1.2.3 Objective 3: Examining the Role of Natural Water Storage Areas for Flood Mitigation in Low-Gradient Watersheds.

Natural storage areas such as wetlands and swamps that exist throughout a watershed play an essential role in hydrological functions and processes that underlie a range of potential ecosystem services (Kadykalo and Findlay, 2016). However, perhaps the most cited natural storage areas services are their impact on flow regimes, specifically their potential to reduce flood peaks and increase flood return period, augment low flows, and reduce runoff and streamflow. However, such expectation of flood control or reduction is quite controversial. Indeed, there is evidence that floodplain wetlands reduce the frequency (Acreman et al., 2003; Hillman, 1998) and magnitude (Ferrari et al., 1999) of flood events and increase the time to peak of these events.

On the other hand, literature does not only include evidence that wetland drainage has little impact on flooding (for example, Bengtson and Padmanabhan, 1999; Ehsanzadeh et al., 2012) but also show some evidence that in some circumstances, wetlands may increase flood peaks (Acreman and Holden, 2013; Brauman et al., 2007). Previous research argues that flood regulation relies on available water storage, and permanently saturated habitats with little or no storage capacity may generate or augment floods relative to semi-saturated or unsaturated habitats (Morris and Camino, 2011). Hence, it is unclear to what extent floods are attenuated or enhanced by wetlands of different types and sizes located in areas of different topographies. This dependence of water storage capacity on wetland type and topography makes it difficult to generalize the flow regulation services of wetlands (Acreman and Holden, 2013). In their synthesis of the hydrological functions of wetlands, Bullock and Acreman, 2003, concluded that although there are many qualitative assessments of the impact on flood flow regulation, there are few quantitative assessments.

Additionally, past research about the flood mitigation effect of sizable natural storage areas such as swamps or wetlands mainly focused on how the natural storage capacity of the wetlands affects flood peak and volume and that natural available storage capacity may become more limited for some areas in rainy seasons when mild to heavy rainfall events occur continuously for days or weeks (Tang et al., 2020). Another attribute of storage areas that definitely affects its flood protection services is how river-to-natural storage areas flow is controlled (Tang et al., 2020). In on-channel swamp areas where the main stem of the river crosses through the swamp as part of its normal route, the flow exchange between the river and surrounding swamps starts once the capacity of the river section is exceeded and water starts to overtop the banks. After the river flows start receding and stage drops within the river, the swamp drains back into the river. The amount, duration, and flow rate of the backflow depends on several factors, including the topography and structure of the swamp itself. Besides being relatively under-studied in general, such swamp behavior exhibits far more complex dynamics in low-lying topography. In such regions, river systems are typically characterized by complex flow dynamics such as flow reversals and bi-directional flows (Watson et al., 2017), dynamic connectivity, and flow exchanges with large natural storage areas, such as swamps. As the flood stages in the river reach just downstream of the swamp areas start to build up because of the inflows from lateral tributaries, the elevated water stage causes the flow to overtop the upstream banks towards the natural wetland areas located on both sides of the river. As this mechanism grows in low-lying topography, a steeper hydraulic gradient towards the swamp areas develops, and the floodwater moves upstream towards such an area rather than the normal downstream direction followed during normal conditions, thus causing the reverse flow to occur. Moreover, in most rivers, inundation of

floodplain swamps occurs when the discharge exceeds the channel's capacity, and floodwater overtops banks; however, in some settings, floodwaters leave the river via flow paths that laterally connect the river and the swamp and inundate the swamp prior to filling up the river section. It is critical to have a thorough understanding of the significance of this relationship and the physical processes that drive the flow exchange to arrive at feasible plans for sustainable management of the floodplain swamps.

1.3 Research Plan (DMAIC Approach)

The research plan for this study adapts the six-sigma DMAIC (Define, Measure, Analyze, Improve, and Control) approach as a problem-solving methodology for understanding flood dynamics and evaluating proposed flood mitigation options. DMAIC can be thought of as a roadmap for solving problems and improvement of system performance. The five phases of DMAIC implemented to establish the research framework for this study are listed below:

- Define (Problem statement – study goals): This project aims to develop a comprehensive understanding of the complex flood dynamics in low-gradient riverine systems, such as the Vermilion River in Louisiana, using a modeling-based approach. The study seeks to answer these questions: What is the level of model complexity needed for flood models in low-gradient coastal watersheds? What are the main drivers for the flooding dynamics? What are the flood benefits expected from applying different flood mitigation measures such as riverine dredging and increasing natural storage capacity?
- Measure (Data Collection – Metrics): Collect all flow and stage data from the three gauge stations located along the Vermilion River in the past storm

events. Hydrologic forcing datasets from the National Water Model and Multi-Radar/Multi-Sensor (MRMS) rainfall datasets are also collected to enforce the boundary conditions of the developed numerical model.

- Analyze (Performance objectives): Quantification of the impact of each level of model complexity on the overall model-predictive performance using model-performance measures, e.g. visual inspection of simulated hydrographs, goodness-of-fit for the peak values, and model results intercomparison.
- Improve (Potential solutions): Identify flood mitigation solutions to reduce the current level of flood risk in the system.
- Control (Monitoring performance): Assessment of the expected flood level under the proposed flood mitigation measures.

Chapter 2: Effect of Model Setup Complexity on Flood Modeling in Low-Gradient Basins

2.1 Abstract

The flat topography, large natural storage features, backwater effects and boundary conditions all play different roles in the flood response of rivers in low-gradient environments. The combined effects of these factors result in frequent episodes of reverse flows, slow recession of flood waters, and complex flow interactions. This study investigates the value of varying degrees of model complexity and setup features on the model ability to reproduce some of the unique flooding characteristics in low-gradient basins. The study focuses on (a) effect of streamflow routing techniques; (b) effect of incorporating large natural storage areas; (c) effect of model dimensionality; and (d) effect of downstream boundary conditions. The study applied the May-June 2014 storm events over six different model setups prepared for the Vermilion River in south Louisiana, USA. A successful simulation of the repetitive reverse flows in the river was only possible after incorporating the large swamp areas within the basin. The slow recession of the flood peaks was accurately reproduced with the use of a 2D representation in characterizing the swamp areas. The results of this study have implications for understanding flood dynamics in low-gradient basins, and for guiding the development of reliable flood models that take advantage of available technologies and information without adding unwarranted complexities that require extensive, yet typically unavailable calibration data.

2.2 Introduction

Extreme flood events are increasing on global and local scales (Hirabayashi et al., 2013; Lewis et al., 2011) with major economic losses and devastating socioenvironmental

impacts. Hydrologic and Hydraulic numerical models are commonly used to quantitatively simulate and predict the impacts of floods across multiple scales. A wide variety of modeling approaches, in terms of scale and representation of physical processes, have been proposed and implemented. However, the selection of the proper level of detail in the model setup continues to pose challenges, particularly in low gradient basins. In such basins, the concept of upstream and downstream direction is not well-defined (Habib and Meselhe, 2006), and the flow direction becomes a time-dependent variable controlled by the hydraulic gradient. The relative significance of the different physical drivers behind complex flood dynamics in low gradient systems on a reach scale is challenging to define. Backwater effects are highly significant (Dalrymple and Choi, 2007) and wind and tidal effects also play a critical role in the overall flood response in such settings (Maskell et al., 2013). A shallow water model (Sandbach et al., 2018) was applied to test different configurations for describing flow dynamics in the Columbia River Estuary where bi-directional flows and significant tidal influences are often encountered. The study showed a significant role for the topographic forcing in describing the location and extent of flow reversals in the estuary. A recent study applied a hydrodynamic model in a Pacific-dominated river basin and indicated the need to better understand the critical role that restored natural floodplains play in attenuating flood peaks (Ahilan et al., 2018). A study by the US Army Corps of Engineers on flooding in the Vermilion River basin in Louisiana, USA, attributed the repetitive flow reversals in the river to the mild longitudinal slopes and the inability of the river channel to accommodate lateral inflows (USACE, 1995). A recent study (Waldon, 2018) on the same river analyzed high-water marks from an extreme flood event and identified distinct locations of reverse flows. The preceding studies highlight the need for modeling-based analysis to better understand the

role of factors such as sedimentation and riverine interactions with natural storage areas in producing the complex flow dynamics commonly encountered in low-gradient basins.

Flood models serve as valuable tools to assess flood mitigation alternatives and to discern the effects of physical processes in low gradient basins. However, the accuracy and credibility of the model results strongly depend on professional judgment and practical experience in model selection, setup, validation, and analysis (Hodges, 2014). Recent advances in computational power, as well the increasing availability of remote sensing data (Bates, 2004), provide new opportunities for developing numerical models that can be used to simulate the complexity of flood regimes in low-gradient basins and better understand the interaction of different physical processes. Despite the potential benefits of such modeling advancements, they may add uncertainties by expanding the number of decisions required in the selection of the adequate level of detail in the model setup (Cook and Merwade, 2009). Due to an incomplete understanding of the runoff generation process (Kim et al., 2012), recent studies (e.g., Hooper et al., 2017) have suggested that a comprehensive hydrologic model combined with a relatively simple model for channel routing may suffice. However, simplified routing models have several limitations for applications in cases such as urban flood inundation (Abderrezzak et al., 2009), low-gradient regions with significant backwater effects (Tsai, 2005), or flow into large reservoirs (Kim et al., 2012).

The model complexity is also dependent on mechanisms used to account for boundary conditions and how they affect flooding regimes in low-gradient basins (Tsai, 2005). Representations of upstream rating curves and inflow hydrographs can result in significant uncertainties in model results. Recent studies (Bermúdez et al., 2017) suggested that further research is needed to understand the significance of the boundary uncertainty and

how they might depend on site-specific conditions. Focusing on urbanization effects in low-gradient catchments, (Wang et al., 2019) proposed a new model that is capable of accounting for typical characteristics of urban areas and the rapid generation of surface runoff. While the proposed model showed promising results in capturing the flow-reversal phenomenon when applied to the Vermilion River, the lack of proper boundary conditions didn't allow the model to fully explain the role and significance of different physical drivers behind the flow reversals.

Model dimensionality presents another challenge. Different physical processes may govern at different spatial scales. While 1-D hydrodynamic models may be appropriate for large-scale applications, explicit modeling of floodplain flows using 2-D models can be vital for more local assessments. Earlier studies focused on comparisons of 1D versus 2D hydrodynamic models (e.g., Benjankar et al., 2015; Leandro et al., 2009), cross comparisons of multiple 2D models (e.g., Vanderkimpen et al., 2008), and assessing the same model under different configurations of topographic resolution (e.g., Bates et al., 2003; Cook and Merwade, 2009). Further research is still needed to assess the value of increasing the dimensional complexity and how it impacts the models' ability to capture the local flow dynamics.

The potential increase in model dimensionality, and the uncertainties associated with the selection of proper levels of model setup complexity can generate major uncertainty in assessing current and future flood risk (Lewis et al. 2011). Therefore, in this article we address the question of model complexity in modeling applications in low-gradient watersheds with complex flood regimes. The study specially aims to assess the value of increasing complexity in the hydraulic model setup by testing a range of model spatial scale

dimensions and linkage combinations (1-D only and hybrid 1-D/2-D), boundary conditions, and the representation of large natural storage areas. The analysis is performed over the Vermilion River basin in South Louisiana, USA. The Vermilion River features a broad range of effects including rapid urbanization, tidal influence, flow regulation, and significant interaction with adjacent swamps during flood events. A series of numerical experiments are developed using a range of model setups featuring a HEC-RAS hydraulic model of varying complexity forced by hydrologic inputs furnished by the National Water Model (NWM). The model results are compared against available stage and streamflow observations during a series of flooding events that occurred in late spring of 2014. The outcomes of the various model experiments provide insight on the advantages and disadvantages of the range in model setup and the level of model complexity needed to reproduce complex flow regimes in low-gradient river basins. The results will also guide the development of flood models and contribute to our understanding of the different physical processes and how they impact the flood response in such environments. This paper is organized in the following manner. First, a description of the study site, data collection, and the available model forcing data is given. Next, the setup of the different approaches followed in the multi-model analysis is briefly explained. Finally, the results of the test setups are discussed followed by conclusions and suggestions for further research.

2.3 Study Area and Datasets

2.3.1 Study Area. The Vermilion River is located in the Gulf Coastal Plain along the central Louisiana coast (**Figure 2-1**). The headwaters of the Vermilion River are the confluence of Bayou Bourbeux and Bayou Fusilier in the north after which the river flows in a predominately south direction until it drains into the gulf through the Vermilion Bay. The drainage area of the Vermilion River watershed is about 1206 km2 and is represented with a single 8-digit hydrologic unit code. Pasture/hay, developed land, and cultivated croplands are the three dominant land uses in the basin (U.S. Geological Survey Gap Analysis Program, 2016) and cover 20.9%, 21.5%, and 38.3% of the total watershed area, respectively. Towards the outlet of the river at the Vermilion Bay, the dominant land use types give way to a band of coastal marshland that extends from east to west along the coastline (LA Department of Wildlife & Fisheries, 2005).

The Vermilion River basin is considered both a natural and controlled hydrologic system. Functioning as a major drainage artery in the area, the Vermilion River collects runoff from many intersecting lateral drainage channels, locally referred to as coulees, some of which are concrete-lined to facilitate quick drainage of tributary watersheds (Kim et al., 2012). During normal river stages, the Vermilion River collects inflows from the different tributaries and transport them downstream into the Vermilion Bay, and ultimately into the Gulf of Mexico (**Figure 2-1**). The Vermilion River is connected from the east to another river, Bayou Teche, through Bayou Fusilier and Ruth Canal. A control structure is located at the headwater of both channels. Bayou Fusilier is controlled by a fixed crest weir that permits about 25 percent of the flow of Bayou Teche to be diverted through this channel into the Vermilion River during non-flood conditions (Baker, 1988). Ruth canal also diverts

freshwater into Vermilion River from Bayou Teche through manually operated gates. A series of inter-connected swamps and lakes, locally known as the Bayou Tortue Swamp and Lake Martin, surround the Ruth Canal diversion channel. Historical connections between the Vermilion River watershed with the former Mississippi River alluvial floodplain resulted in the formation of the Bayou Tortue Swamp and Lake Martin (shown in **Figure 2-1**). These series of interconnected swamps and lakes occupy an area of ~35.2 km2 and function as a natural floodwater storage area by accepting overflow from the Vermilion River depending on the intensity of the storm event.

Several characteristics of the Vermilion River make it a viable test site for the current study. First, the low gradient (typical slope is 1:10,000 for the main stem) and the repeatedly eye-witnessed experiences of reverse flow that occur during moderate to heavy rainstorms, as well as during periods of storm surge (Waldon, 2018; Wang et al., 2019; Watson et al., 2017). During intense storm events, overland runoff is delivered through the system of lateral coulees to the Vermilion River within a small travel time, causing the river to quickly reach its capacity. Once the river capacity is exceeded, the flow starts to reverse its direction to the north towards the Bayou Tortue Swamp. During moderate storms, the flow reversal also occurs, but remains limited to a shorter river reach. This hydrodynamic regime, combined with the existence of large low-lying natural storage topographic features, make the river susceptible to multi-peak flows and prolonged flooding.

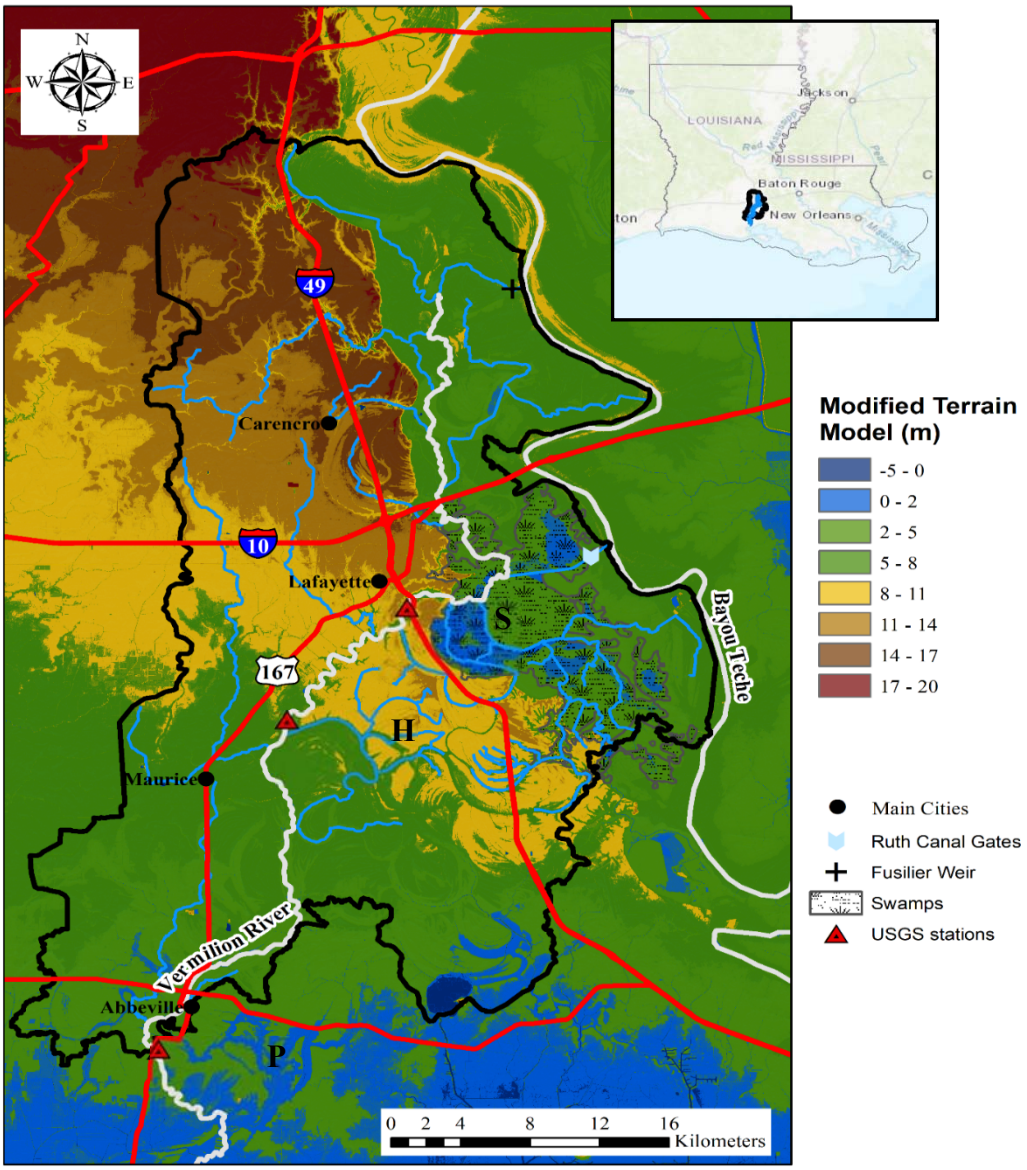

Figure 2-1: The Vermilion River watershed overlaying LiDAR-based Digital Elevation Model. The map shows different features within the river basin, including the Bayou Tortue swamps, the 15 main lateral coulees, and the Ruth Canal gates and Fuselier Weir that control flow from Bayou Teche to the Vermilion River. USGS river gauges are also shown (S: Surrey; H: Hwy733; P: Perry).

This basin, a representative of other low-gradient inland-coastal transitional basins, has a long history of severe flooding since the major flood that occurred in August 1940 until the most recent in August 2016 (major floods were recorded in 1940, 1953, 1955, 1966, 1971, 1973, 1977, 1980, 1982, 1989, 1993, 2014, and 2016) (USACE, 1995 and; Watson et al., 2017). The frequent severe disasters call for a more comprehensive understanding of

flood processes that take place in such basins and efficient modeling tools that can assist in mitigating flood risks.

2.3.2 Study Period and Data Sources. The flood events examined in this study occurred during May-June of 2014. A series of rainfall storms started on the 28th of May 2014, where a late-season cold front and slow-moving upper level system moved into the region (NCEI, 2015). The front pulled down deep atmospheric moisture across the area and caused heavy rain that lasted for two days resulting in a widespread flooding. During these two days, the storm dropped a total rain accumulation of 220 mm with a maximum hourly intensity of 37 mm/hr. Traffic disruptions and private properties were flooded, and rescues were conducted in areas where the most torrential rainfall occurred. Ten days later, from June 10th to the 13th, a strong upper-level disturbance dropped another 110 mm of rain across the city of Lafayette producing multiple rounds of severe weather and flooding.

Observations on river stage and streamflow during the study period are available from the U.S. Geological Survey (USGS) at three gauges (Surrey, Hwy733, and Perry) along the Vermilion River mainstem (**Figure 2-1**). Stage measurements are available at all three gauges, while streamflow measurements are available only at Surrey and Perry gauges. Records of water surface elevations upstream the of inlet control gates of Ruth canal are also available from the operational staff of the Teche-Vermilion Freshwater District. These records allow for estimation of flow exchanges across the Ruth Canal and Fusilier Weir. A summary of the data availability is shown in **Table 2-1**and **Figure 2-2**. During this event, the maximum observed stage at Surrey, Hwy733, and Perry gauges were 3.25, 3.38, and 1.88 m, respectively. These stages exceeded the flood stage of 2.21 m at Surrey gauge, as reported by the National weather Service, causing significant flooding where lateral coulees meet the

Vermilion River (AHPS, 2018). Additionally, the event is classified as a 10-yr return period flood based on the flood frequency analysis performed by the Federal Emergency Management Agency (FEMA) for the Vermilion River (FEMA, 2018). The stage and streamflow hydrographs (**Figure 2-2**) observed during the May-June period clearly illustrate the reverse flows that happen within the Vermilion River, as well as the extremely slow recession that continues for several days after the end of the rainfall storm. Actual flow records across the Fusilier weir and through the Ruth Canal gates are not available, instead they were estimated using structure characteristics and available water level observations as explained later.

Table 2-1: Summary of available stage and streamflow observations

	Surrey Gauge	Hwy733 Gauge	Perry Gauge	Ruth Canal gates	Fusilier Weir
Stage	5/18/14–6/20/14	5/30/14 – 6/20/14	5/18/14–6/20/14	5/18/14 – 6/20/14	5/18/14–6/20/14
Flow		N/A		N/A	N/A
Additional data	N/A	N/A	N/A	Gate operations; rating curves	Rating curves

While developing the hydrodynamic model for the Vermilion River, additional data on the river bathymetry, topographic data for the region outside the river mainstream, and hydraulic structure characteristics were collected. The US Army Corps of Engineers (USACE, 2015) performs routine hydrographic surveys to monitor local river and waterway navigation conditions. Due to the periodic update of the data published for the river surveys, this study used the 2015 river survey to represent the Vermilion bathymetry. Although this survey was conducted after the simulation period of the current study (Spring of 2014), it is the earliest version available from the US Army Corps of Engineers. This survey was also collected during an average-flow year, and therefore can be considered a representative of the average riverbed conditions. Due to the fact that the riverine bathymetric survey focused

primarily on the navigable reaches of the main river, survey data was absent in some locations, particularly in the upper reach of the river. At these locations, local cross-sectional surveys of the river were acquired from the tributary hydraulic models developed earlier as part of the FEMA program on flood insurance rate maps for the Vermilion River.

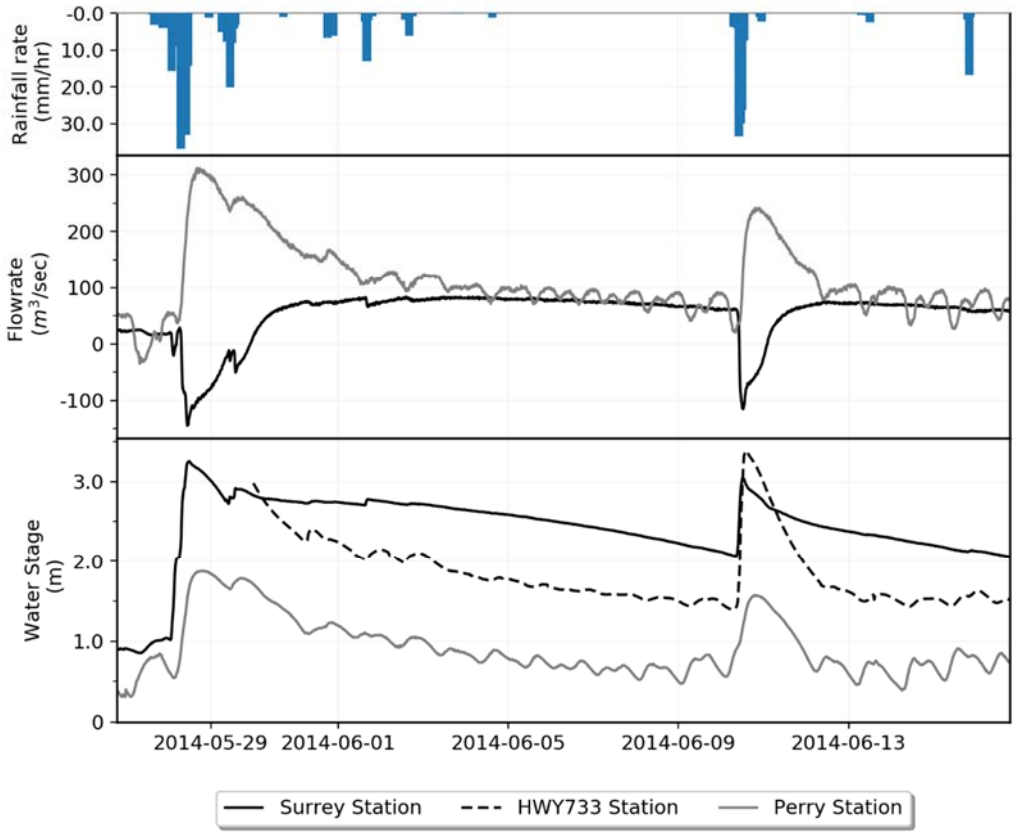

Figure 2-2: Observed streamflow and stage hydrographs at three river gauges (see **Figure 2-1** for gauge locations) during the 2014 storm.

The Louisiana Statewide LIDAR Project provides high-resolution elevation data for the entire state in the form of Digital Elevation Models (DEM) with a 5-m horizontal resolution and with a vertical accuracy of ~ 15–30 cm RMSE (Cunningham et al., 2009). One of the major problems when using DEMs in hydraulic modeling is that the terrain cannot represent the river main stem due to the inability of the LIDAR technology to "see through" the water surface (Cook and Merwade, 2009). Therefore, in this study both the LIDAR DEM and the riverine bathymetry were merged for the Vermilion River corridor, and an improved

terrain model was generated that includes the riverbed survey in the channel region and the DEM data elsewhere in the model domain. The merged terrain model was hydrodynamically-corrected following the procedure explained in (Jarihani et al., 2015). The Vermillion River watershed exhibits a significant heterogeneity in the land-use and land-cover patterns. To reliably model the flood response of the watershed, the 2011 30-m National Land Cover Database (NLCD) (Homer et al., 2015) was used to develop a lookup table that links each NLCD grid cell with a representative value of the Manning's roughness coefficient. This allowed the model to incorporate a spatially-distributed representation for overland and channel roughness characteristics.

2.3.3 Tributary Streamflow Hydrographs. The main reach of the Vermilion River receives lateral inflows from 15 main tributaries (**Figure 2-1**). Since the focus of the current study is on examining the complex flow regimes along the main river, the hydrodynamic simulations in the river relied on pre-generated hydrologic simulations available through the National Water Model (NWM) (Office Of Water Prediction, 2018).

Hourly streamflow hydrographs for all the tributaries that feed into the river were obtained from an online repository of the NWM through the NOAA National Water Model Reanalysis project. The repository archives the results of a 25-year retrospective simulation period (1993-2017) of version 1.2 of the National Water Model. The core of the NWM is the National Center for Atmospheric Research (NCAR)-supported community Weather Research and Forecasting Hydrologic model (WRF-Hydro), which is a coupled 1D vertical Land surface model and a fully-distributed hydrologic model (Gochis et al., 2018). WRF-Hydro is configured to use the Noah-MP Land Surface Model (LSM) to simulate land surface processes. The NWM uses diffusive wave surface routing and saturated subsurface flow

routing on a 250-m grid, and channel routing down the NHDPlus stream reaches using the Muskingum-Cunge (MC) method (Shastry et al., 2017). The NWM-derived streamflow hydrographs were extracted at the outlet of each of the 15 tributaries before they meet the river and were then used as boundary conditions that force the hydrodynamic simulations along the main river.

2.4 Methods

2.4.1 Hydraulic Model Simulations. In this study, the Hydrologic Engineering Center's River Analysis System (HEC-RAS) is used to implement the different hydraulic modeling approaches. The model domain encompasses a total of 87.9 km of the mainstream of the Vermilion River along which the river receives inflows from 15 main tributaries and about 23 minor lateral streams.

The model domain starts at the headwaters of the Vermilion River, where a flow hydrograph from the Fusilier weir provides an upstream boundary condition, and terminates at Perry near the Vermilion parish (**Figure 2-1**), where a stage hydrograph from a U.S. Geological Survey (USGS) gauge provides a downstream boundary condition.

HEC-RAS has been widely used in different types of flooding studies such as flood hazard mapping (Masood and Takeuchi, 2011) and prediction of flood depth hydrographs (Quirogaa et al., 2016; Timbadiya et al., 2014). The HEC-RAS can perform 1D and 2D unsteady flow simulations using either dynamic or diffusive wave approximations of the shallow water equations, as well as hybrid 1D/2D models. We used these features to test varying complexity levels in modeling the Vermilion River under different spatial configurations and dimensions (1D or hybrid 1D/2D) and assess the ability to reproduce the complex flow regimes during flood events. In this study, the HEC-RAS 1D unsteady

equation solver was used in the case of 1D simulations (e.g., the main channel of the river. In this case, the HEC-RAS model solves the full 1D St. Venant equations for unsteady open channel flow. These equations are discretized using the finite difference method and solved using a four point implicit method (USACE, 2016). In the case of 2D simulations, the HEC-RAS uses an extended version of the St. Venant equation, also known as Shallow Water equations. For faster computations, this study opted to use the diffusive wave approximation of the shallow water equations as similar results were obtained when the full dynamic solver was used. While performing the 2D computations, the HEC-RAS uses an implicit finite difference scheme to discretize time derivatives and a combination of finite difference and finite volume solver (hybrid discretization) to solve for spatial derivatives.

The 2D areas within the model (e.g., in the swamp areas and the channel floodplains) were discretized into a computational mesh using both structured and un-structured cells, but with a maximum of 8 sides per cell for efficiency and memory considerations. The flexibility in mesh generation allowed for capturing topographic details and abrupt changes in terrain (e.g., river banks, levees) as precisely (un-structured cells) and parsimoniously (square cells) as possible. In the case of hybrid models, HEC-RAS allows for full control over the mechanisms of flow exchanges between the 1D and 2D parts of the domain. This was done via direct connection at the endpoints between 1D channels and 2D flow areas, or weir-based lateral connections between the channels and adjacent floodplains.

The Vermillion River includes key hydraulic structures that affect the flow regime in the basin. These include multiple bridges and road crossings, and more importantly the Fusilier weir and the Ruth canal gates, which both allow for flow exchanges between the Vermillion River and its neighboring Teche River. The Fusilier weir was included in the

model as an uncontrolled overflow broad-crested weir using the standard weir equation. Using the weir stage-discharge curves, visually inspecting satellite images for the weir location, and through model calibration, the weir characteristics were deduced (crest length=7m, crest level = 5.67, and weir coefficient = 2.65). The standard gate modeling features in HEC-RAS can't account for capturing the dependency of flow across the gate on tailwater conditions and the possibility of having reverse flows. Therefore, special scripts were developed to explicitly define the flow through the gates based on gate dimensions and openings, while accounting for tailwater and headwater conditions that can dynamically change during run-time. As part of all unsteady flow simulations performed during the study, a 10-days warm-up period prior to the actual simulation period is applied. This period was found to be enough for the model to settle down to consistent water surface elevations and flows, and for the structures to reach their full computed flow and reduce computational instabilities.

2.4.2 Description of Model Complexity Tests. The model complexity analysis utilized six different hydrodynamic modeling approaches. These approaches were designed to represent varying ranges of model dimensionality and spatial geometry, effects of tailwater boundary conditions, and different ways for representation of natural storage features within the basin.

The design of this analysis is summarized in **Table 2-2:** Summary of six modeling approaches used in model complexity analysisand **Figure 2-3**. The results of these modeling approaches will be inter-compared to assess their skill in reproducing the complex flow dynamics in the Vermilion River, such as those encountered during the May-June 2014 flooding period (**Figure 2-2**). As described earlier, the same hydrologic model, the NWM,

was used to provide the streamflow hydrographs that drive the six hydrodynamic model setups. This neutralizes the effects of the hydrologic component and lets all models to run with identical spatial and temporal hydrologic forcings.

The first and most simple approach (A0) implements the Muskingum-Cunge method for hydrograph routing over a one-dimensional channel network and doesn't include any HEC-RAS components. The flow out of each channel reach is determined based on flow hydraulics, channel storage and an inflow contribution that is only allowed at the beginning and end of each reach. The static hydraulic properties used to describe each channel reach are based on a trapezoidal section assumption. These properties are prescribed as a function of Strahler stream order for each reach. The Strahler stream order is obtained from the National Hydrography Dataset (NHDPlus V2) developed by the USEPA Office of Water and US Geological Survey (McKay et al., 2012). In this approach, no downstream boundary condition is needed, and no topographic features other than the river network itself is incorporated in the model. This setup is similar to how channel routing is implemented in the current operational setup of the NWM.

The second approach (A1; **Figure 2-3**a) increases the model complexity compared to approach (A0) by adopting the full dynamic 1-D Saint Venant equation (FSV) available in HEC-RAS. Solving the FSV equations, unlike the Muskingum-Cunge method, requires imposing both downstream and upstream boundary conditions. Therefore, in the A1 approach, a normal depth is assigned to the model as the simplest downstream boundary condition. The normal depth assumption is one of the most commonly used downstream boundary conditions in both steady and unsteady numerical simulations, particularly in models used to develop regulatory flood insurance maps. According to this assumption, a

rating curve is generated internally within the model routine and imposed as a downstream boundary condition. The rating curve is based on using the Manning's equation with a friction slope equal to that of the last river reach to solve for the river stage. This simplification avoids the need for actual stage data that are often lacking at the downstream end in most practical applications. In this test, effects of the natural storage areas within the Vermilion River basin are not considered.

The third approach (A2; **Figure 2-3**b) uses the same setup of approach (A1) while incorporating the effects natural storage of the Bayou Tortue Swamp system. These off-channel swamps provide vast floodplain storage for the Vermilion River during extreme events. In this approach, the storage area is modeled as a spatially-lumped compartment using a stage-versus-volume curve connected to the main river via a weir equation. This is basically equivalent to the commonly-used reservoir level-pool routing method. The next approach (A3; **Figure 2-3**b) uses the same setup of approach (A2) and substitutes the simplified normal depth downstream boundary condition with an actual stage hydrograph observed at the Perry gauge.

The final two approaches, (A4;**Figure 2-3**c) and (A5;**Figure 2-3**d), increase the model complexity by introducing 2D modeling components. In approach A4, while the main river is still modeled as a 1D network using the FSV formulation, the Bayou Tortue Swamp, represented as lumped compartments in approach A3, are now represented with 2D grids where the depth-averaged dynamic flow equations are solved. The final approach (A5) also uses a 2D setup for the Bayou Tortue Swamp but implements a hybrid 1D-2D model along the main stem of the Vermilion River. This design emulates the increasing trend in using 2D modeling approaches but can also allow for a better representation of the local channel

features and interactions with the floodplain. In this case, both the middle reach (spanning the urban center of the City of Lafayette between I-10 and Hwy733 gauge), and the lower reach (extending from Hwy733 gauge until Perry gauge) of the Vermilion River are represented by a 1D bankfull channel connected laterally with 2D overbank floodplain areas. The main river and its floodplains communicate through 2D connections that are positioned on each bank side of the 1D network for the whole reach length. These connections allow for flow exchange between 1D and 2D areas using the 2D shallow water equations in order to conserve momentum. The diffusive wave approximation was applied in the 2D regions of the model. The 2D depth-averaged shallow water equations is solved based on an unstructured finite volume solver with an implicit finite difference scheme in time. This allowed the 2D model areas to be represented using both structured and un-structured cells (see Figure 4a for some representative 2D areas). Such flexibility in mesh generation allowed for capturing topographic details and abrupt changes in terrain (e.g., river banks, crossing road embankments) as precisely (un-structured cells) and parsimoniously (square cells) as possible, and for the faces of model cells to work as "virtual cross-sections" that regulate the propagation of flood wave. The final design of the computational 2D mesh consisted of 58,634 cells with an average element size of 2109 m2 in the swamp area, and 366,375 cells with a finer average element size of 238 m2 in the 2D areas of the main river. The 2D representation of the Bayou Tortue Swamp system in approaches A4 and A5 also allowed for spatially distributed representation of surface and channel roughness. Using the 2011 30-m National Land Cover Database (NLCD) (Homer et al., 2015), a lookup table was developed to assign each grid cell within the swamp areas a representative value of the Manning's

roughness coefficient that accounts for different land-use types (see **Figure 2-4**b for some representative areas).

Given the large area of the Bayou Tortue Swamp system, a precipitation boundary condition was enforced for all approaches that included the swamps as a part of the model domain (approaches A2, A3, A4, and A5). The precipitation hyetograph was directly used without accounting for any infiltration losses. The continuous inundation of the swamps, and the low-permeability substrates restrict the infiltration losses causing the difference between the precipitation and net runoff hyetographs to be insignificant. The spatial discretization of the swamp system into several interconnected zones allowed for using spatially varying precipitation hyetographs.

Table 2-2: Summary of six modeling approaches used in model complexity analysis

	(A0)	**(A1)**	**(A2)**	**(A3)**	**(A4)**	**(A5)**
RIVER CORRIDOR	1D	1D	1D	1D	1D	1D-2D
1D ROUTING METHOD	MC	FSV	FSV	FSV	FSV	FSV
DOWNSTREAM B/C	N/A	Normal depth	Normal depth	Stage hydrograph	Stage hydrograph	Stage hydrograph
SWAMP REPRESENTATION	N/A	N/A	Lumped compartment with level-pool routing		2D grid	
2D ROUTING METHOD	N/A	N/A	N/A	N/A	Diffusive wave	

It is noted that only a limited level of model calibration was possible due to the lack of adequate streamflow observations across the model domain of the Vermilion River. Flow observations that can be used for calibration were available at one gauge only (Surrey) and stage observations were available at another gauge (Hwy733). A visual calibration was performed where the model parameters were adjusted to primarily capture the magnitudes and timings of flow and stage peaks at the two gauges.

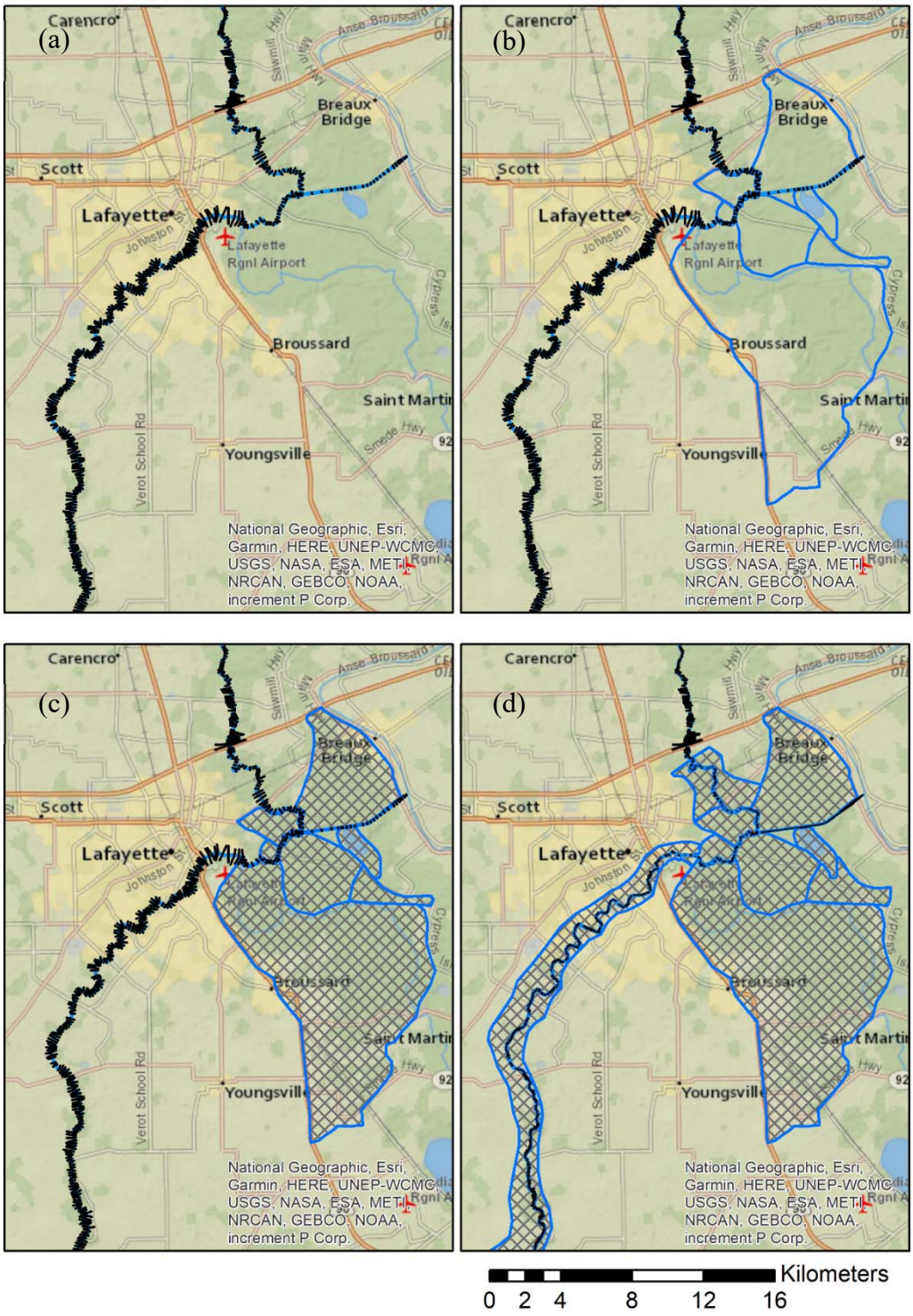

Figure 2-3: Different modeling approaches used for simulating the Vermilion River and the Bayou Tortue Swamp System: (a) approach A1, (b) approaches A2 and A3, (c) approach A4, and (d) approach A5. The polygons in part (b) represent the extent of the Bayou Tortue Swamps. The dark lines across the main river show the locations of the cross sections used in the 1D part of the model. The cross-hatched polygons are the areas that were modeled using 2D representation.

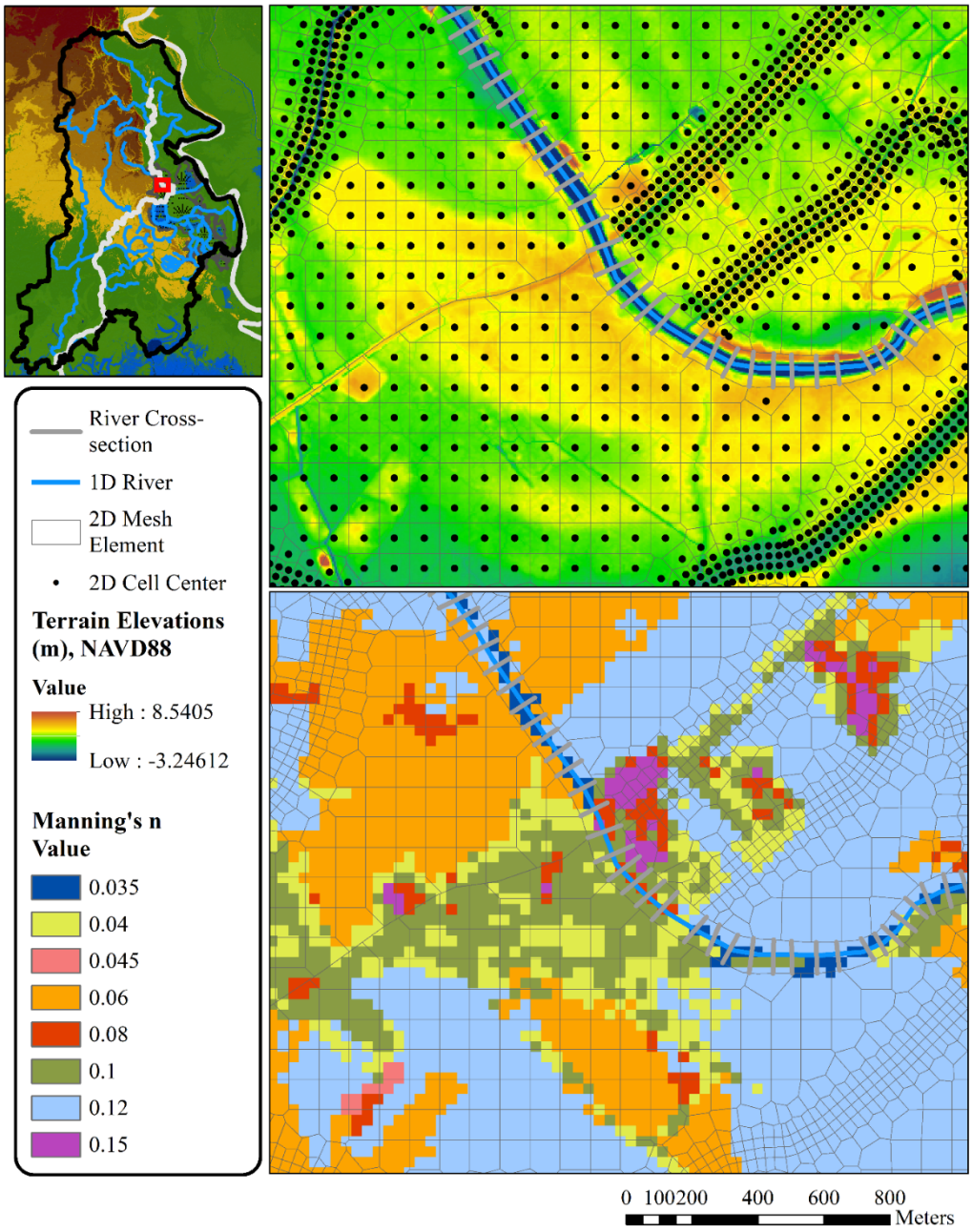

Figure 2-4: (a) Example of the computational 2D mesh generated over the Bayou Tortue Swamp areas and its connection to the main river, (b) Spatially varied Manning's layer based on land cover dataset (Manning's Value between brackets)

Special attention was also paid to calibrate the model to re-produce the prolonged recession of the receding flood wave, a typical behavior of the river during extreme events (**Figure 2-2**). The model parameters that were adjusted during the visual calibration process were the Manning's roughness coefficients. In the channel reaches that were simulated as

1D, the roughness coefficient was adjusted for the main channel as well as for the right and left overbanks. Similarly, the roughness coefficients were also adjusted spatially over the swamp areas that were simulated using a 2D grid. The adjustments were primarily focused on capturing the slow recession of the flow hydrographs, which is largely attributed to river-swamp flow exchanges, while maintaining a physically reasonable roughness values that reflect the land-use characteristics within the model domain.

2.5 Results And Discussion

This section presents the results of the model complexity tests via comparison against available observations at two gauging stations (Surrey and Hwy733 Gauges; **Figure 2-1** and **Figure 2-2**) and cross-comparisons amongst the individual tests. The results are all reported for the May-June 2014 storm; however, the same analysis was also performed for another extreme event that occurred during August 2016. The overall results of the 2016 storm were consistent with those of the 2014 storm and are not reported here due to space limitations. The comparison will primarily focus on examining streamflow hydrographs (observed only at Surrey Gauge) and stage hydrographs (available at both Surrey and Hwy733 gauges) since these are the two model-internal locations that were not used for any boundary conditions. To gain more insights on the differences amongst the different approaches, we will also examine two primary model products: the longitudinal profiles of maximum water surface elevation (WSE), and the spatial extent of flood inundation.

2.5.1 Simplified versus Fully Dynamic Routing. We first analyze the results obtained from simulating the Vermilion River using approaches A0 and A1. Approach A0 utilizes the MC routing methodology with simplified channel geometry. This case was considered to generally assess how far low-complexity models would behave in comparison to running a detailed FSV hydrodynamic model as in the case of approach A1. Recall that both approaches account for the main channel only and do not include the storage areas associated with the in the Bayou Tortue Swamp system.

Despite the differences in the way each approach represents the flow physics, both approaches clearly failed to reproduce the reverse flows recorded at Surrey Gauge in the two flow peaks during the simulation period (**Figure 2-5**). The results show that both approaches peaked positively (i.e., flowing towards Perry gauge) with a peak discharge of 186.2 m3/sec and 147.9 m3/sec on 05/29/2014, which correspond to a relative peak flow error (PFE) of 29.96% and 5.8% for approaches A0 and A1, respectively. Similar behavior is observed for the second flood peak in early June. The overestimation of flow peaks in approach A0, compared to approach A1, is probably contributed to the limitations of the MC method. The MC method is incapable of accommodating a downstream boundary condition or capturing any possible backwater effect (Koussis, 2009), especially if the reverse flow is considered as an extreme case of backwater effects where the hydraulic gradient shifts causing the flow to move upstream. On the other hand, Approach A1 shows some signs of flow reversals in the very early parts of the storm in both peaks, but these reverse flows are short-lived compared to the observations and the river revert back quickly to its usual downstream direction. The overall unsatisfactory performance of approach A1 could possibly be attributed to the lack of

representing storage areas and the use of normal depth as a downstream boundary condition. This is examined in the next sections.

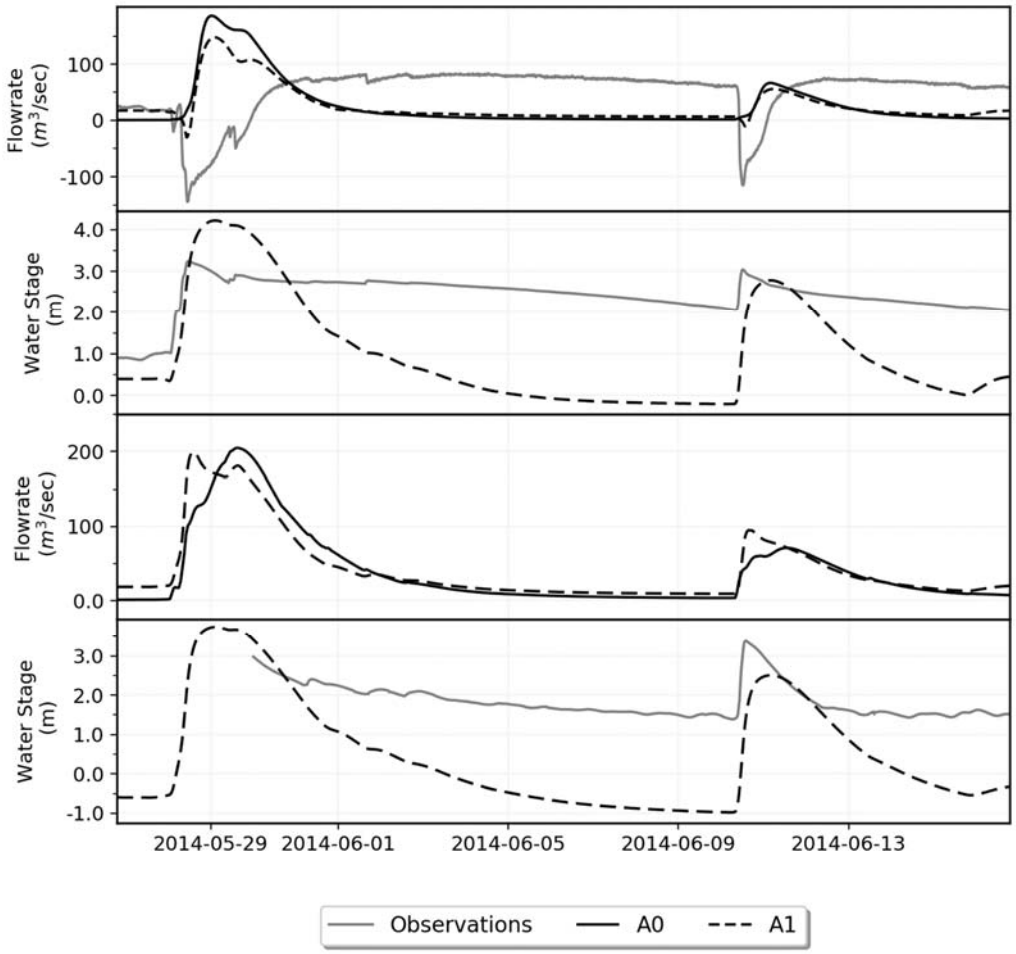

Figure 2-5: Simulated flow and stage hydrographs using modeling approaches A0 and A1 at Surrey gauge (top two plots) and at Hwy733 gauge (bottom two plots). Note, Hwy733 gauge doesn't record streamflow.

2.5.2 Effects of Natural Storage Areas. Approaches A1 and A2 are compared to examine the effect of incorporating the natural storage areas into the model setup. Going from approach A1 to approach A2 (**Figure 2-6**) highlights the critical role played by the vast storage areas associated with the Bayou Tortue Swamp system.

The inclusion of the natural storage areas in approach A2 resulted in an immediate improvement in the model behavior and allowed it to reproduce the reverse flows. Note that

the swamps were represented as spatially lumped compartments. Compared to approach A1, it is also interesting to see a relative improvement with approach A2, in terms of simulating the slow recession of the stage and streamflow hydrographs at both Surrey and Hwy733 gauges; however, approach A2 still shows a relatively faster recession than the observation, with a difference close to 2 m by the end of the first rainfall event.

Examining the longitudinal maximum water surface profiles (**Figure 2-7**) shows a clear difference in stage along the entire reach of the river. This difference reflects an overestimation of approach A1 in moving the flow downstream due to the absence of the upstream storage areas. The lack of storage representation caused approach A1 to build up an unrealistic water level at upstream locations (i.e. Surrey gauge) and produce hydraulic gradient that is large enough to drive the flow to the only outlet in the downstream direction. This caused the model to completely miss the reverse flow phenomenon and to systematically overestimate the stage along the longitudinal profile (**Figure 2-6** and **Figure 2-7**). The inclusion of the natural storage features also significantly affected the spatial extent of flood inundation associated with each approach (**Table 2-3**). Approach A1, which did not include the swamps as a part of the model, yielded an inundation area that is 64% and 38% higher than the inundation area estimated by approach A2 for the middle and lower reaches of the river, respectively.

Table 2-3: Effect of including natural storage features on the inundation extent

	MAX WSE (M)		**INUNDATED AREA (KM^2)**	
APPROACH	Middle Reach	Lower Reach	Middle Reach	Lower Reach
A1	4.39	3.45	3.73	2.63
A2	2.97	2.52	2.28	1.91
A3	3.13	2.87	2.41	2.79
A4	3.20	2.93	2.56	2.82
A5	4.16	2.98	2.86	3.02

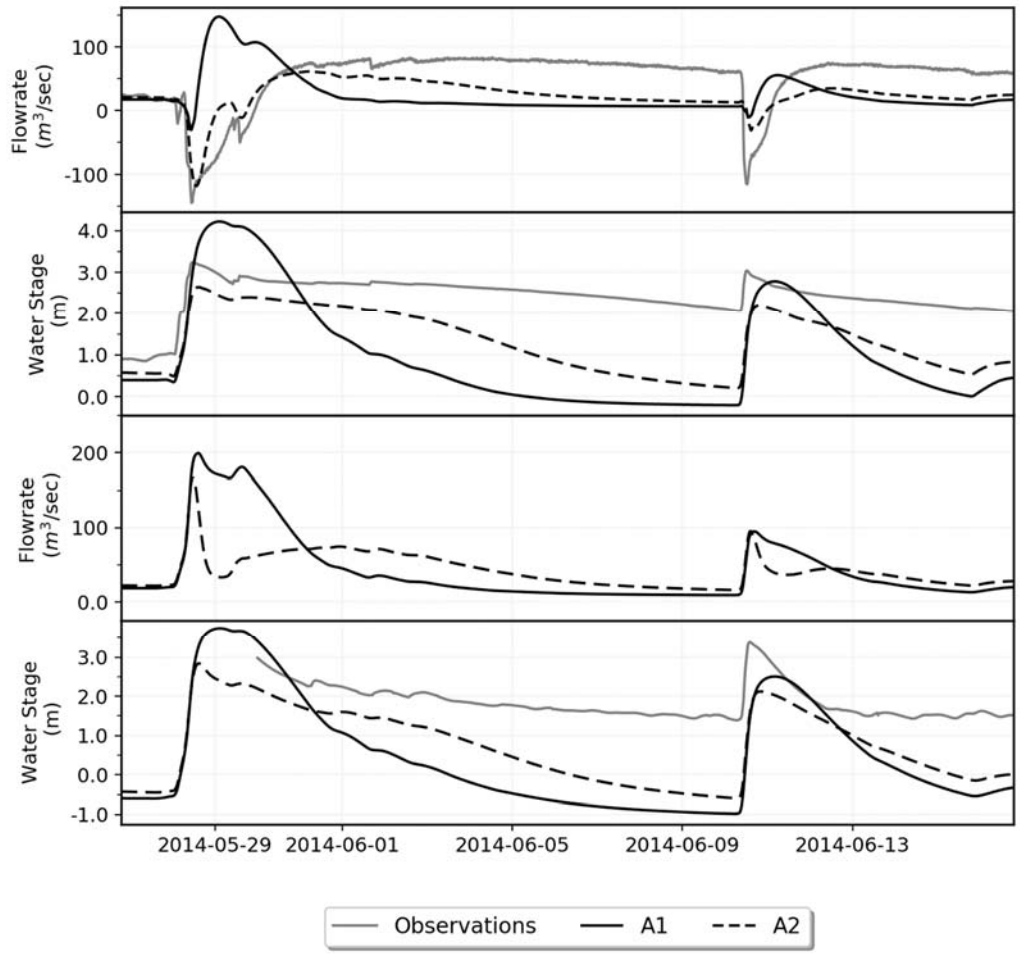

Figure 2-6: Simulated flow and stage hydrographs using modeling approaches A1 and A2 at Surrey gauge (top two plots) and at Hwy733 gauge (bottom two plots). Note, Hwy733 gauge doesn't record streamflow.

2.5.3 Impact of Downstream Boundary condition. It is a common modeling practice to locate the boundary condition "far enough" from the area of interest (Alemseged and Rientjes, 2007). The tailwater (downstream) boundary condition is typically represented using either a rating curve, or an observed stage hydrograph.

Due to limited data availability and inability to specify accurate boundary conditions especially for modeling alternative scenarios (e.g., design storm), a rating curve is usually implemented based on the normal depth boundary condition (NDBC) assumption. In order to examine the impact of this assumption in low gradient systems, we examine the results of

approaches A2 and A3. The two approaches are identical in each aspect, except for the downstream boundary condition where NDBC is used with approach A2 while an actual stage hydrograph is used in approach A3. The difference between the two types of boundary conditions was equivalent to a difference of 3 m in the stage at the downstream end of the model at Perry Gauge (**Figure 2-7**).

As shown in **Figure 2-8**, both approaches are successful in capturing flow reversal regime and peak arrival time at Surrey gauge (both arrived at 18.5h on 05/28/2014). However, approach A2 with the NBDC assumption, shows lower peaks in the reverse flows and higher positive (i.e., downstream) flowrates than approach A3. Switching from a normal-depth assumption to an actual stage hydrograph in the downstream boundary condition resulted in flow peaks (both negative and positive) and more realistic recession of the stage throughout the simulation period at both gauges, Surrey and Hwy733 (**Figure 2-8**).

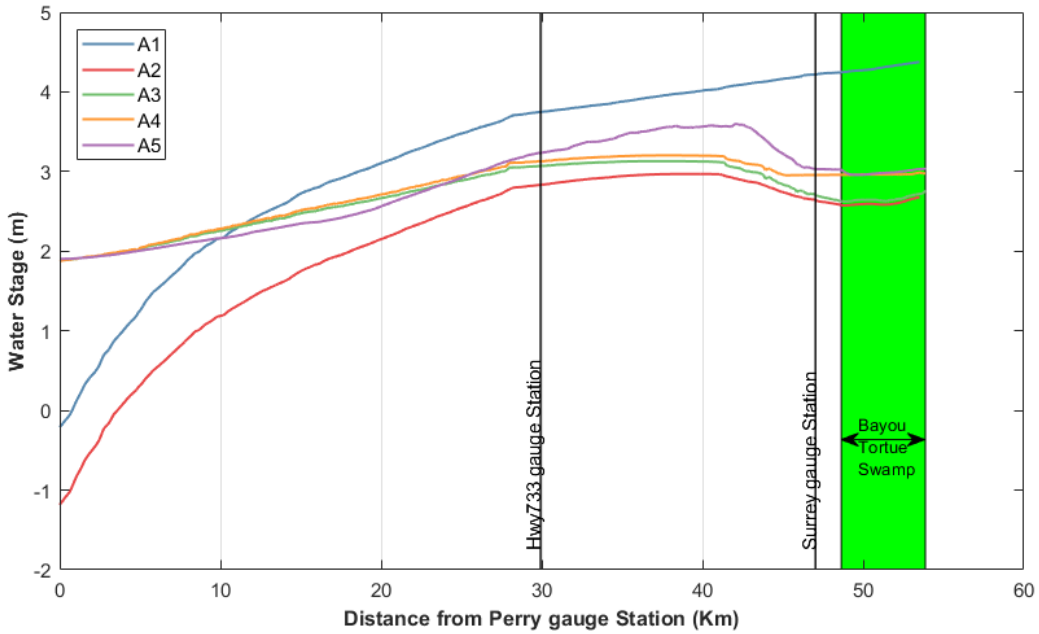

Figure 2-7: Maximum water surface profiles for modeling approaches A1 to A5.

These results suggest that approach A2 pushed more flows towards the downstream end of the modeled domain. The impact of the downstream boundary condition is further evident in the longitudinal profile of the maximum water surface along the entire reach (**Figure 2-7**). The stage profile for both approaches is quite similar at the upstream end of the model domain where Bayou Tortue swamp, which was incorporated in both approaches, apparently dominates the behavior of the model in that area. Moving away from the swamp area, the impact of boundary condition becomes more evident with a much steeper downstream hydraulic gradient for approach A2 compared to that of approach A3. As illustrated in Figure 8, this has translated into a systematic overestimation for peak flows in the reaches with downstream flow direction (i.e. Hwy733 and further downstream) and underestimation for peak flows in the reverse flow reaches (i.e., at Surrey Gauge location and further upstream).

The significance of the downstream boundary condition is further highlighted when comparing the hydrograph recession. The difference between approaches A2 and A3 was more pronounced during the recession limb and the inter-storm period compared to the rising limb and the peak of the storm. These results have practical implications (e.g., flood forecasting applications, flood mapping products) and emphasize the importance of having representative downstream boundary conditions and initial model conditions in low-gradient hydraulic simulations. The downstream boundary conditions have a direct impact on the prediction of flood inundation, especially in the lower reaches of the model domain (**Table 2-3**). The increase in the area of inundation is a direct consequence of the persistent higher water level that resulted from using the observed stage hydrograph as a downstream boundary condition.

2.5.4 Impact of 2D versus 1D Model Dimensional Representation.

Approaches A3, A4, and A5 incorporate storage areas using different model dimensionality and spatial resolutions (**Table 2-2** and **Figure 2-4**).

The primary differences between the three approach are in the representation of the swamp areas (a lumped compartment in approach A3, versus a 2D distributed grid in approaches A4 and A5) and in how the river corridor is represented (1D along the full length of the river, versus using a 2D grid for the overbank floodplains). To maintain consistency, the same downstream boundary condition (actual stage hydrograph) was applied for all three approaches.

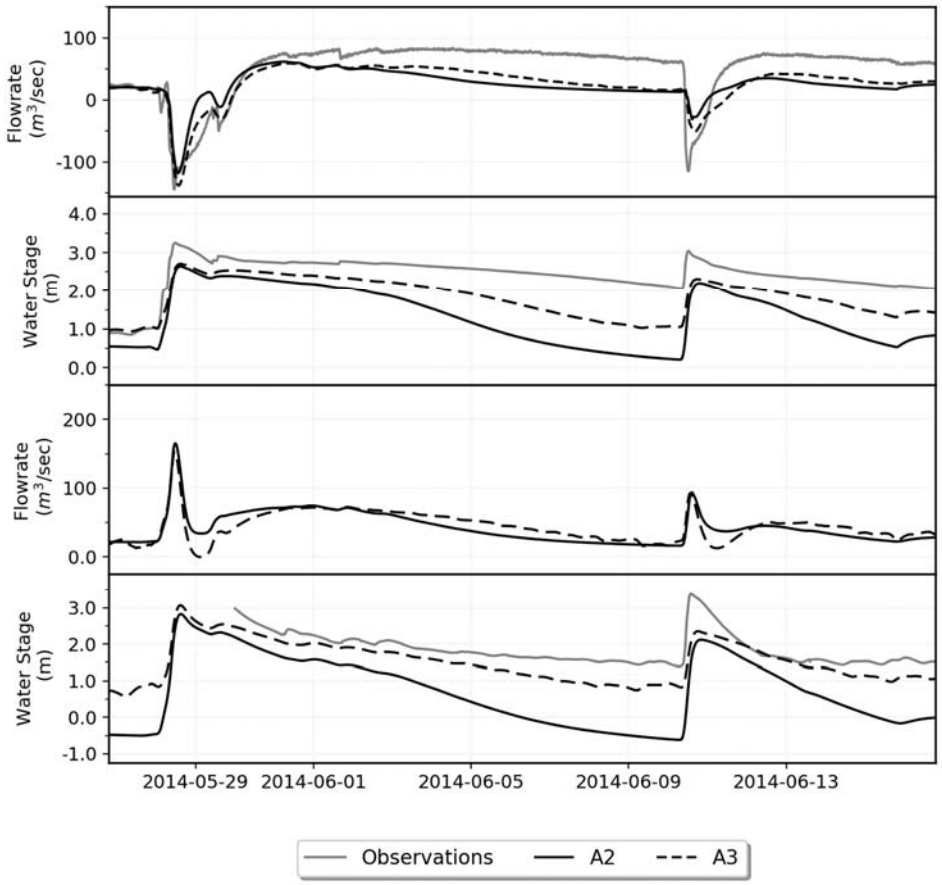

Figure 2-8: Simulated flow and stage hydrographs using modeling approaches A2 and A3 at Surrey gauge (top two plots) and at Hwy733 gauge (bottom two plots). Note, Hwy733 gauge does not record streamflow.

The results (Figure 9) show that the three approaches were equally capable of capturing the reverse flow regime regardless of increasing the model dimensionality. The three approaches showed some differences in the peak magnitudes and timing, with approach A5 being the most different from approaches A3 and A4, as well as from the observed peaks. Approach A5 underestimated the negative peak flow magnitude (the reverse flow) at Surrey gauge, while showed higher positive peak flow (i.e the downstream flow) when compared to other approaches A3 and A4. Compared against the observed peak flows at Surrey gauge, the results show PFE values of 4.33%, 8.41%, and 33.15% for the three approaches A3, A4 and A5, respectively. Examining the flow hydrographs for both Surrey and Hwy733 gauges (**Figure 2-9**), it seems that approach A5 distributed the flow among multiple flow directions, longitudinally and transversally, including upstream and downstream the Vermilion River with a tendency to divert more flow towards the normal downstream direction.

The impact of the three different approaches is more pronounced in the stage hydrographs (**Figure 2-9**) and the longitudinal water surface profiles (**Figure 2-8**). Representing the swamp area using a spatially distributed approach (A4), instead of a lumped compartment approach (A3), has resulted in a noticeable improvement in reproducing the prolonged and slow recession of the hydrographs after the two major flow peaks. Interestingly, and compared to approach A4, adding more 2D representation into the model to represent the overbank floodplains along the main river (approach A5) resulted in a deterioration in simulating the receding periods of the flow hydrographs. This is apparent in both the stage and flow hydrographs. The use of a lumped representation of the Bayou Tortue Swamp area in approach A3 produced higher water surface elevations than those of approaches A4 or A5. The longitudinal water surface profiles suggest that the maximum

water surface elevations (WSE's) in the lower and upper reaches of the river are similar across the three approaches. However, the max WSE's exhibited greater variation in the middle reach, with approach A5 showing a higher WSE and a shorter extent for the reversal flow. Despite the scarcity of observations along the Vermilion River, eyewitness observations and USGS reports of high-water marks (Watson et al., 2017), as well as analysis of the FEMA flood insurance studies for the Vermilion River, all substantiate that the reversal flow stretch extends longer downstream for a storm comparable to May-June 2014 period (FEMA, 2018). The overestimation in water levels by approach A5 is also evident in the spatial extent of the flood inundation (**Table 2-3**). Besides inundation along the river, examining the inundation spatial extents over the Bayou Tortue swamps reveals some interesting differences (**Figure 2-10**). While approaches A4 and A5 showed very similar inundation pattern over the swamp domain, approach A3 shows a much smaller area (52.8% less when compared to approach A4). Such smaller area of inundation, and in turn the stored volume of water inside the swamps, impacted the recession curve of the hydrographs at Surrey gauge. As the rain ceases and incoming runoff volume decreases, the flow in the river becomes more dominated by the outflow capacity of the connected swamps causing a prolonged recession limb.

The results also suggest a slight decline in the comparative performance of approach A5 which (paradoxically) includes more 2D features (i.e., both the swamp and the overbank floodplains are represented in 2D) than the other approaches. While some previous studies demonstrated that a full 2D approach can have benefits over 1D modeling in simulating flow dynamics in floodplains (for example Tayefi et al., 2007), we believe that the lower performance by approach A5 can be attributed to challenges introduced by the additional

model parameters and geometrical modifications needed in the 1D/2D setup. Since the floodplains of the Vermilion River are typically ranged between a few hundreds of meters up to one kilometer in width, we decided that a model of a 100m grid size for the floodplains area will represent these floodplains particularly well. As it is vital that the model represents the floodplain available for storage realistically if the floodwave is to be precisely predicted, a small part of the decline in performance can be assigned to errors arising from such mesh size uncertainty, and better model performance might occur using higher spatial resolution to represent the flooplains. Fictitious weirs were introduced to characterize the lateral flow exchange between the main channel of the river, represented as 1D, and the channel floodplains, represented as 2D. The selection of appropriate weir coefficients to model the exchange between 1D (channel) and 2D (floodplain) areas is not entirely physically-based and requires extensive calibration datasets. Flow interactions between the main channel and active conveyance areas in the floodplain may also require further control by manipulating the overland resistance coefficients to avoid unrealistic flow patterns leaving the main channel. Without adequate high-resolution observational data, the manipulation of these coefficients remains highly subjective and may introduce model uncertainties, which can sometimes lead to a deterioration in the model performance.

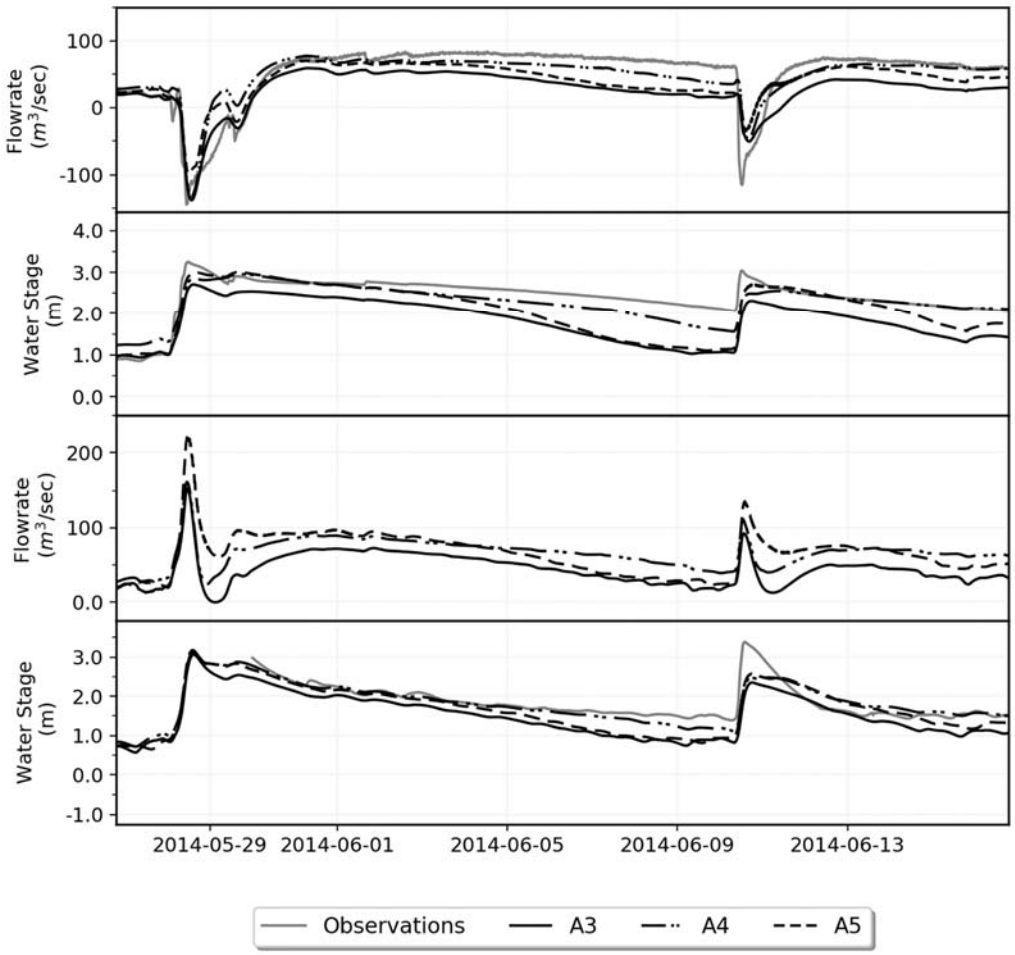

Figure 2-9: Simulated flow and stage hydrographs using modeling approaches A3, A4, and A5 at Surrey gauge (top two plots) and at Hwy733 gauge (bottom two plots). Note, Hwy733 gauge doesn't record streamflow.

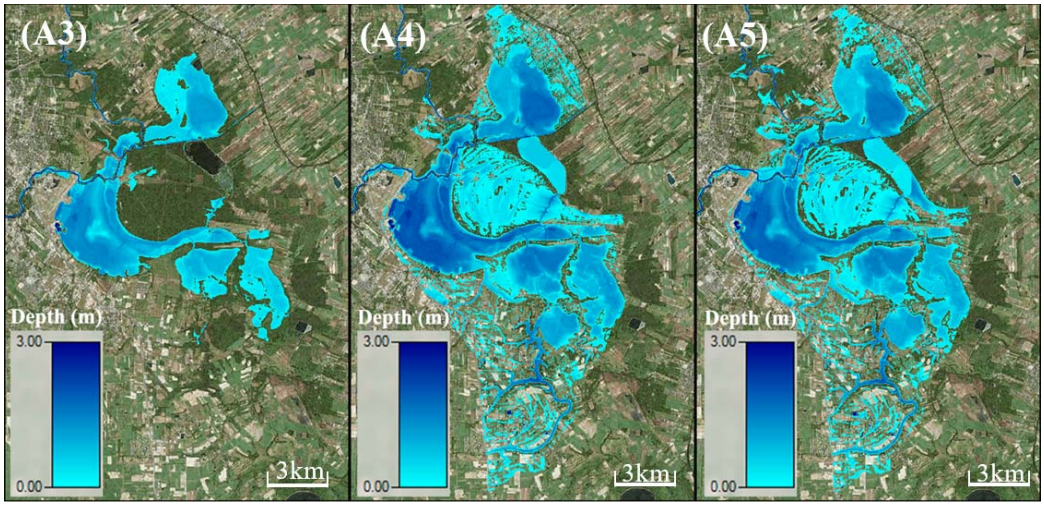

Figure 2-10: Comparison of inundation extent based on modeling approaches A3, A4, and A5.

2.6 Conclusions And Future Recommendations

This study provides an assessment of the effect of increasing complexity in model setup in low-gradient river basin flood simulations. We based the analysis on comparing results from numerical simulations from six different modeling approaches built using the best-known modeling practices. Each modeling approach is characterized by different model setup complexity, external boundary condition specification, and spatial representation of large natural storage areas. The analysis also provides insight on the causes behind unique low-gradient flood phenomena, such as reverse flows and prolonged flood recession episodes. The analysis was performed during a flood-active period in May-June 2014 along the Vermilion River in south Louisiana. The main conclusions that can be deduced from the results are summarized as follows:

1. Incorporating large natural storage areas, such as swamps and wetlands, into the model domain was required to capture the complex flow dynamics, especially the reverse flows. Explicitly incorporating storage elements also significantly improved the estimates of peak flow parameters (stage and flowrate). Such natural areas play a major role in rivers with low transport capacity and flat gradients. During the active part of the rainstorm, these areas offer significant temporary storage for the flood water and cause flow reversals into the upstream direction, and then drain back into the usual downstream direction resulting in a very slow and prolonged attenuation of the flood.
2. Increasing the model complexity by adopting a more superior flow routing approximation led to only minor improvements in capturing the reverse flow

dynamics. However, improved representation of the physical hydraulic processes led to a more realistic simulation of the stages and flowrates along the river.

3. Both discharge and water stage hydrograph simulations, and especially the stage, have benefitted from simulating the large natural storage areas using a 2D representation compared to 1D storage elements. Using a 2D representation resulted in more realistic flow exchanges, in terms of volume and timing, between storage areas and the main river. Such representation also allowed the model to better reproduce the slow recession of the hydrographs along the river reaches that are significantly affected by the storage areas. In modeling such large storage areas, consideration of the momentum terms and the spatial heterogeneity of friction, through a fully 2D representation improved the model predictions especially during the receding limb and inter-storm periods.
4. Unlike the case of representing the storage areas in 2D, increasing the model dimensionality along the mainstream of the river by representing the floodplain along the main channel using 2D didn't necessarily improve the model performance. Instead, it resulted in a slight deterioration in capturing the prolonged flood receding and the spatial extent of the reversal flows. These unexpected results are attributed to the added challenges in characterizing flow exchanges between the main channel and the floodplains, especially with the absence of calibration data at scales necessary to capture such fine-resolution local effects.

5. In low-gradient rivers, imposing a normal-depth assumption as a downstream boundary condition can significantly impact the stage and flow simulations and can result in inaccurate representation of the water surface profile and the extent of river-induced flooding at locations well within the domain of interest. Special care is needed when developing tailwater boundary conditions for low gradient flood simulation models.

While this study highlighted the role of large natural storage areas in low-gradient basins, further analysis is required to better understand the complex flood processes that occur between the river and the swamps and how such natural areas can be strategically managed as flood mitigation features. Analysis of the potential role of runoff timing and synchronization from major tributaries in controlling flooding is also warranted, especially in the context of increasing urbanization in low-gradient coastal environments.

Acknowledgments

This material is based upon work supported by the National Oceanic and Aviation Administration (NOAA) UCAR Subaward No. SUBAED001383 to the University of Louisiana at Lafayette and by the Louisiana Board of Regents Support Fund (BoRSF) under Award # LEQSF (2019-22)-RD-B-05. The authors would like to thank Mr. Donald Sagrera, the Executive Director of Teche-Vermilion Freshwater District, for providing information on the characteristics and operation of the Vermilion River hydraulic structures.

Chapter 3: Assessment of Riverine Dredging Impact on Flooding in Low-Gradient Coastal Rivers Using a Hybrid 1D/2D Hydrodynamic Model

3.1 Abstract

The current study investigates the effect of large-scale channel modifications via riverine dredging on flood dynamics in low-gradient river systems located in inland-coastal flood transition zones. The study site is the Vermilion River in south Louisiana, US, which is characterized by complex flow regimes, reversal and bi-directional flows, presence of large swamps with significant river-swamp interactions, and large volumes of runoff contributions from lateral tributaries. The study aims to understand the interplay of these factors and how they modulate and get affected by different dredging approaches that vary in spatial extent and the modifications introduced to the channel. The study deploys a hybrid, one-/two-dimensional (1D/2D), hydrodynamic model that simulates flow and stage dynamics in the main river and its major tributaries, as well as the flow exchanges with the interconnected swamp system. Overall, the results show that the dredging activities can significantly alter the flow regime in the watershed and affect flow exchanges between the river and the swamp system. In terms of flooding impact, only dredging approaches that are extensive in spatial extent and modifications to channel longitudinal slope can result in sizeable reductions in flood stages. However, these benefits come at the expense of significant increases in the amplitude and inland propagation of the Gulf tidal wave. On the other hand, less-extensive dredging can still provide moderate and spatially limited flood mitigation; however, they further expose downstream communities to increased levels of flooding, especially during more frequent events. The results reveal that while dredging can increase the hydraulic conveyance of the river system, the large runoff volumes delivered by the urbanized

tributaries seem to outweigh the added improvement in the in-channel storage, thus reducing the anticipated flood relief. The results suggest that a watershed-centered approach, instead of a riverine-centered approach is needed for flood management in these systems so that the relative benefits and tradeoffs of different mitigation alternatives can be examined.

3.2 Introduction

Watersheds that are located in inland-coastal transition zones (Bilskie and Hagen, 2018) are increasingly subject to extreme flooding due to both man-made alterations and natural processes. Examples of such processes include compound inland and coastal storms, accelerated relative sea-level rise, and increased population and urbanization (Crossett et al., 2013; NCEI, 2020). Flooding in these areas is further exacerbated by the typical low gradients that characterize the main rivers and their tributaries. Flow regimes under low-gradient conditions typically lead to channel sedimentation and reduction of the channel conveyance capacity, and thus an increase in fluvial flooding during moderate and extreme storms.

Flood mitigation measures are often sought in these regions to alleviate the impact of riverine-induced flooding. One of the traditional and most common flood mitigation practices in coastal watersheds is watercourse dredging or channelization (Liao et al., 2019). Dredging refers to activities that include any combination of removing instream and riparian sediment and vegetation, modifying channel width, depth, and gradient, and straightening the river (Hooke, 1990). By structurally altering one or more of the hydraulic variables that govern channel flow and its conveyance capacity (e.g., slope, depth, width, roughness), the water stages are typically decreased, which can reduce the spatial extent of the flood inundation and the associated flood risk.

Early studies on watercourse dredging provided empirical and theoretical evidence that channelization, if appropriately designed to prevent the bank erosion and channel silting, can be quite effective as a flood mitigation measure (Nunnally, 1978; Shankman and Pugh, 1992). However, recent feasibility studies examined potential dredging scenarios for tidally-dominated sections of coastal rivers in southwest UK and demonstrated that dredging did not lower the peak flood levels significantly during winter storms (Webster et al., 2014). The study showed that the shape of the river cross-section and the heights of the riverbanks played a significant role in determining the actual flood level reduction. Other studies showed that dredging can have unintended consequences in other parts of the watershed, especially in the downstream communities. For example, Prestegaard et al. (1994) reported that areas downstream of a modified section of the Raccoon River in Iowa had experienced higher-magnitude floods compared to sections from rivers that have upstream similarly-sized drainage areas. Rose and Peters (2001) showed that channel cross-section enlargement increases the flood wave velocity, thereby speeding the arrival time of flood peaks downstream.

Other studies have focused primarily on the adverse effects of channelization on water quality (Schoof, 1980), ecological alterations of the stream and the riparian corridor (Juan et al., 2020), and stream degradation (Pierce and King, 2013). Another potential aspect of river dredging activities is the effect on tidal propagation. Cai et al. (2012) applied an analytical model to show that a reduction in river discharge and degradation of the riverbed both lead to a significant reduction in the travel time of the tidal wave. The study also highlighted that the amplification of the tidal amplitude, as a result of dredging, could facilitate the penetration of storm surges into the estuary. Likewise, Ralston et al. (2019)

studied the effect of dredging on New York Harbor and the tidal Hudson River and found that such modification doubled the tidal amplitude and increased the landward conveyance of coastal storm surge.

While dredging can increase the hydraulic efficiency of river channels and potentially reduce overbank flooding, the impact on flow hydrodynamics and the overall flooding regime needs to be better understood, especially in watersheds that are located within inland-coastal transition zones. In such regions, river systems are typically characterized with complex flow dynamics due to factors, such as flow reversals and bi-directional flows (e.g., Burton and Demas, 2016; Watson et al., 2017), dynamic connectivity and flow exchanges with large natural storage areas, such as swamps and wetlands (Saad et al., 2020); tidal influences, and the large volumes of synchronized tributary flows from urbanized sub-watersheds (e.g., Pattison et al., 2014; Wang et al., 2019). The complexity of flow regimes in these regions has implications for flood mitigation; therefore, it is imperative to develop a comprehensive understanding of the impacts of riverine dredging that emerge as a possible mitigation strategy in response to decreased channel capacities and increased flood risk. This study deploys a hydrodynamic model to investigate the various impacts of channel dredging and their implications for flood mitigation and how it may alter the overall flow regime. The study site is in the Vermilion River in southern Louisiana, US, a representative of low-gradient tidally-influenced river systems that are located in flood transition zones. The study focuses on understanding the effect on flow regime and reduction in water surface elevations under a suite of dredging approaches that represent varying degrees of channel cross-sectional modifications, changes to the riverbed slope, and the spatial extent of the dredging along the river. The analysis will be performed for different storm conditions (e.g., 10-year

and >100-year return periods) to assess the dependence on the storm magnitude and the amount of runoff generated in the watershed. A special attention is given to how dredging may also alter the river-swamp interactions. Swamps, which are a common feature in low-gradient coastal watersheds, play a significant role in flood mitigation and provide flood relief in large river basins (Wu et al., 2020). The scientific literature shows a need for understanding the impact of riverine dredging on flow exchanges with swamp areas and their ecosystem viability. Given the direct connection with the Gulf of Mexico, the analysis will also examine the effects of the spatial location and extent of the dredging on the amplitude and propagation of the tidal wave along the river. Besides the main river, it is also of importance to assess the propagation of any potential flood mitigation benefits into the tributaries that are connected to the river. Unlike most previous studies that depended on 1-dimensional (1D) hydraulic modeling in simulating pre- and post-dredging conditions, the current study utilizes a hybrid 1D/2D approach that allows for more accurate representation of the flow dynamics in low-gradient complex river systems (Saad et al., 2020).

3.3 Methods

3.3.1 Study Area. The Vermilion River is a tidally-influenced river located in south central Louisiana, US, and has a watershed that covers an area of about 1,560 km2 (Figure 3-1). The Vermilion River basin, a representative of other low-gradient inland-coastal transitional basins (Bilskie and Hagen, 2018), has a long history of severe flooding since the major flood that occurred in August 1940 until the most recent in August 2016 (USACE, 1995; Watson et al., 2017).

The river starts at the confluence of Bayou Bourbeux and Bayou Fusilier, after which it travels ~115 km until it intersects with the Gulf Intracoastal Waterway (GIWW). The river

eventually drains into the Gulf of Mexico through the Vermilion Bay. The river functions as a major artery that collects runoff from many intersecting lateral tributaries, locally referred to as coulees (Kim et al., 2012). The Vermilion River receives flow diversions from another river in the east, Bayou Teche, through Bayou Fusilier and Ruth Canal (Figure 3-1). Flow diversions are regulated through a concrete weir and a manually operated gate that permits about 25% the flow of Bayou Teche to be diverted during non-flood conditions (Baker, 1988).

A major feature that adds complexity to flood dynamics in the basin is a series of inter-connected swamps and lakes, locally known as the Bayou Tortue Swamp and Lake Martin (Figure 1) that occupy a large area of the watershed (~35.2 km2). These swamps function as a natural storage area by accepting reverse flows (i.e., flow traveling upstream) from the Vermilion River. During low and normal river stages, the river collects inflows from its tributaries and travels downstream (south) toward the bay. However, during extreme flooding events, the river becomes bidirectional and shows a reverse flow toward the north where it drains into the Bayou Tortue swamps. The division point between downstream flows (toward the Vermilion Bay) and upstream flows (toward the Bayou Tortue swamps) depends on the severity of the flooding event. During high-frequency events, the bidirectional flow often initiates where one of the main tributaries, Coulee Mine, enters the river (Figure 3-1). If the storm event is extreme enough, a further downstream change in bidirectional flow division may occur where two other major tributaries, Coulee Ile des Cannes and Isaac Verot Coulee, enter the river. In both cases, extensive flooding occurs along many reaches of the river and its tributaries, and especially over the urbanized areas of the City of Lafayette and its surrounding communities. Examples of reverse flows are shown in **Figure 3-2**.

The hydrographs also show excessively slow recession of flood peaks, which are driven by outflows from the swamp after the river stage has started to recede. Observations on river stage and streamflow are available at four locations within the domain of interest to the current study (Figure 3-1). Stage measurements are available at three road crossings over the Vermilion river, namely Surrey, HWY733, and Perry, while the fourth location is just upstream the inlet control gates of Ruth canal (Figure 3-1). Streamflow (flow rate) data are available only at Surrey and Perry gauges.

The historically navigable reach of the Vermilion River extends between the City of Lafayette (river kilometer of 76, measured from the river mouth at the Vermilion bay) and the GIWW (river kilometer 5), and has periodically been subject to channel dredging for maintenance purposes. However, due to the declining navigation activities and other logistical reasons, the river has not been dredged for the last two decades. This has resulted in riverbed shoaling and reduction in the conveyance capacity of the river, especially in the central reaches that pass through the urbanized sub-watersheds in Lafayette.

3.3.2 Simulation Periods. The dredging analysis of this study was conducted for two multi-storm simulation periods, August 1st−30th, 2016 and May 15th–June 5th, 2014 (Figure 3-2), that capture different storm magnitudes and flooding impacts.The two simulation periods were associated with widespread flooding in different parts of the watershed. The stage and streamflow hydrographs observed during both periods clearly illustrate the reverse flows that happen within the Vermilion River, as well as the extremely slow recession that continue for several days after the end of the rainfall storm.

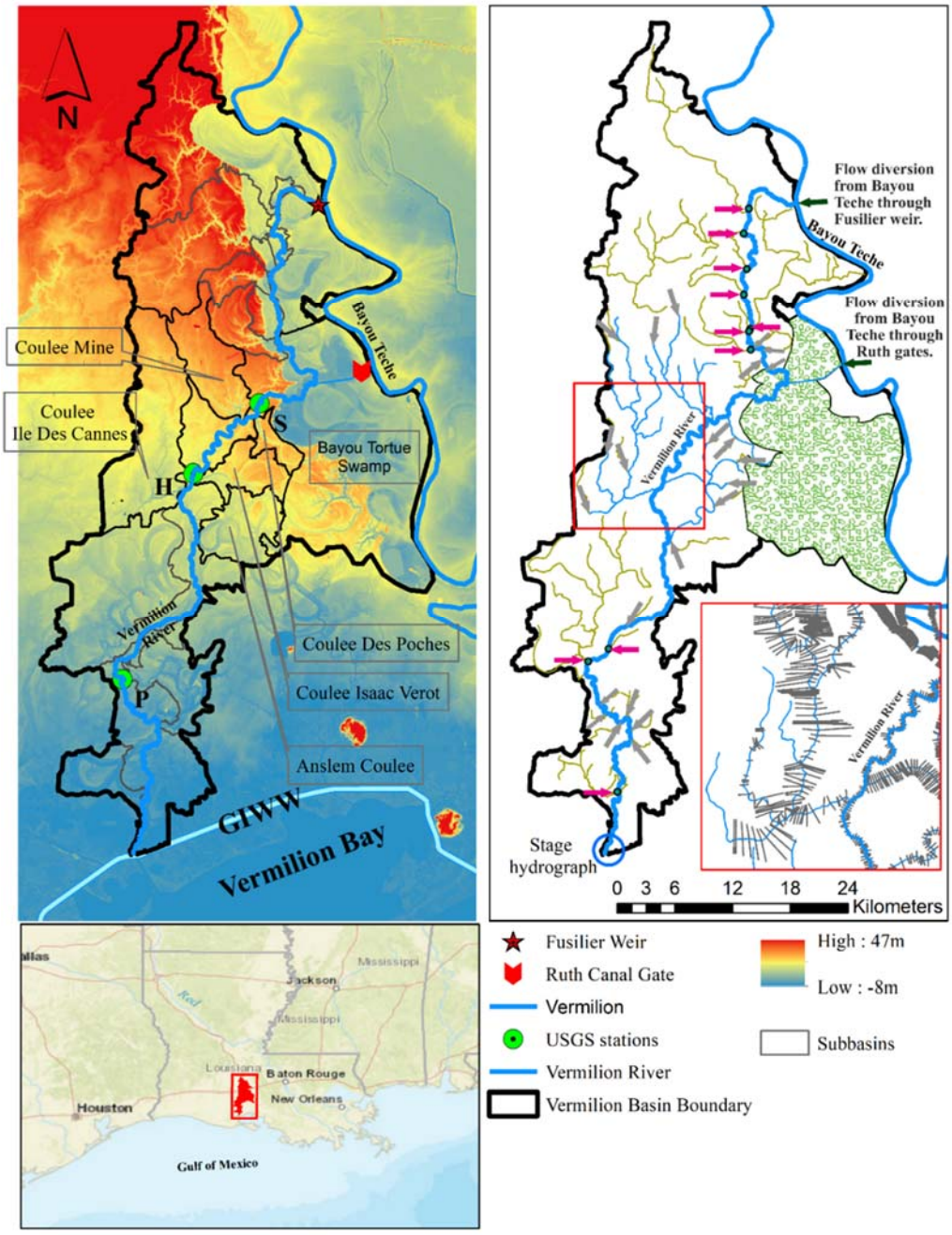

Figure 3-1: Left Panel: Digital Elevation Model of the Vermilion watershed in south Louisiana, US. The five lateral tributaries (coulees) that are simulated in the hydrodynamic model are shown. Locations of USGS gauges are also shown (S: Surrey, H: HYW733 and P: Perry). Right Panel: Stream network of the Vermillion River and its 15 tributaries. Streams in blue represent the main river and the five tributaries that are explicitly simulated in the hydrodynamic model as 1D reaches. The swamp area (hatched) is represented in the model using a 2D setup and is enforced by direct rainfall-over-grid from the Stage IV radar-rainfall product. The inset in the right panel shows an example representation of channel cross sections used in the 1D hydrodynamic simulations.

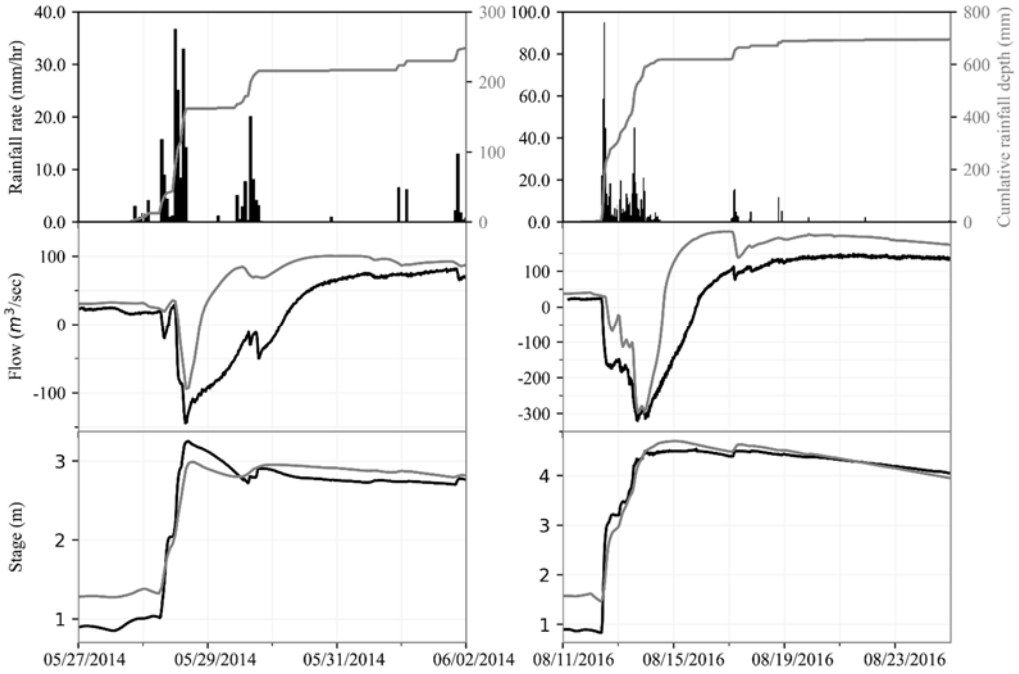

Figure 3-2: Top panels: Hourly rainfall rates (black) and accumulations (grey) extracted from the Stage IV radar product. Middle and lower panels: streamflow and stage hydrographs at the USGS Surrey gauge during the 2014 (left panels) and 2016 (right panels) simulation periods. Model simulations are in grey and USGS observations are in black.

The August 2016 storms generated devastating flooding within the basin and across many areas of the state (van der Wiel et al., 2017; Watson et al., 2017). Based on a rainfall duration-depth analysis, the August 2016 storm can be classified as a 100–200-year storm. A total of 762 mm of rainfall was recorded during the August 2016 period, with hourly rainfall intensities exceeding 90 mm/h. Rainfall events during the 2014 simulation period can be classified as a 2–10-year storm, depending on the duration considered. During the May–June 2014 period, a total rainfall depth of 250 mm was recorded, with hourly rainfall intensities reaching 37 mm/h, causing significant flooding where lateral coulees meet the Vermilion River (Advanced Hydrologic Prediction Service, 2018).

3.3.3 Hydrodynamic Model. In this study, an unsteady hybrid 1D/2D hydrodynamic model for the Vermilion River and its main tributaries was used to simulate the existing conditions and the proposed dredging scenarios. The model is an expansion of an earlier version (Saad et al., 2020) that was developed using the Hydrologic Engineering Center's River Analysis System (HEC-RAS) version 5.0.7. The HEC-RAS system allows for 1D and 2D unsteady flow simulations using either dynamic or diffusive wave approximations of the shallow water equations. For the purposes of this study, the HEC-RAS 1D solver was used in the case of 1D simulations (e.g., the main channel of the river) to solve the full 1D St. Venant equations for unsteady open channel flow.

These equations are discretized using the finite difference method and solved using a four point implicit method (USACE, 2016). For 2D simulations, this study opted to use the diffusive wave approximation of the shallow water equations since similar results were obtained when the full dynamic solver was used. While performing the 2D computations, the HEC-RAS uses an implicit finite difference scheme to discretize time derivatives and a combination of finite difference and finite volume solver (hybrid discretization) to solve for spatial derivatives.

3.3.4 Model 1D/2D Setup. The model encompasses a total of 115 km of the mainstream of the Vermilion River (Figure 1), starting at its headwaters, where a flow hydrograph from the Fusilier weir provides an upstream boundary condition.

The river also receives flows through the Ruth canal structure that conveys flows from Bayou Teche to Vermilion River. Time-series of flow diversions through the Ruth canal structure and over the Fusilier weir were constructed based on information provided by the Teche-Vermilion Freshwater District responsible for operation of the structures. The model

terminates at its intersection with the GIWW, where a stage hydrograph available from a Gulf monitoring station is used as downstream boundary condition.

The hybrid 1D-2D model setup includes the mainstem of the river and five of its major tributaries represented as 1D (Figure 3-1), while the Bayou Tortue swamp system and its surrounding areas were represented as 2D (Figure 3-3). The narrow and steep-sided channel of the Vermilion River (Kinsland and Wildgen, 2006) makes the 1D characterization of the river rather reasonable. Significant flow exchanges occur between the river and the Bayou Tortue swamp system through several tributaries as well as direct bank overflows. To simulate such exchanges, a 2D setup was used to represent the swamp using a total of eight 2D flow areas (**Figure 3-3**). An unstructured mesh was developed with varying resolutions of 30–90 m. The varying resolution was needed to address model stability and terrain representation. Generally, a fine mesh size was heavily enforced around breaklines and in areas where abrupt changes in the velocity field was encountered. Breaklines were used in the 2D areas to enforce key features of the terrain and ensure that the model reasonably simulates the movement of overland flow. Breaklines were used along channels with concentrated flows and ridgelines that allow flows to spill from one area to another across features, such as road embankments, levees, and natural ridgelines. On the other hand, a coarse mesh resolution was adopted in areas where the 2D flow is relatively uniform. Even in areas with relatively coarse computational grids, a reasonable representation of the swamp hydrodynamics is achieved due to the HEC-RAS implementation of a sub-grid approach that allows for a relatively coarse grid while capturing the finer scale underlying topography (Brunner, 2016). To allow for flow exchanges between the river and the swamp, the 1D (river) and 2D (swamp) parts of the model were coupled through lateral connections

represented in the model as fictitious weir structures. During the unsteady flow simulation, the solution algorithm allows for direct feedback at each time step between the 1D and 2D flow elements, which enables an accurate calculation of headwater, tailwater, flow, and any submergence that occurs at the hydraulic structure on a time-step-by-step basis.

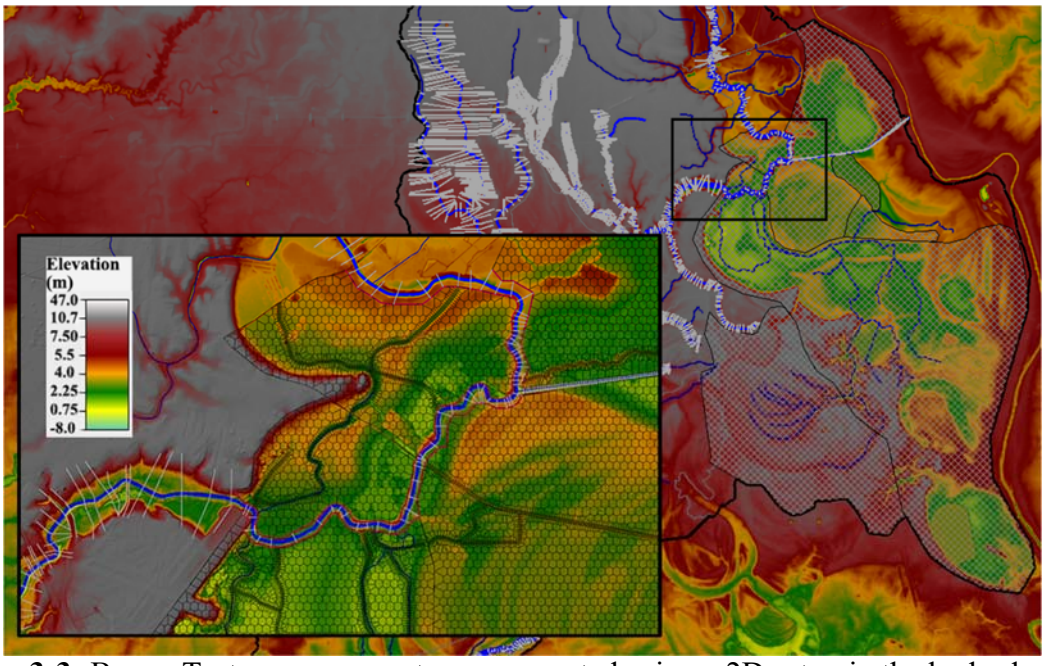

Figure 3-3: Bayou Tortue swamp system represented using a 2D setup in the hydrodynamic model. The close-up view shows the Vermilion River (modeled as 1D) flowing through the Bayou Tortue swamp. The red lines around the riverbanks represent a set of fictitious lateral structures that were used to simulate the connection between the river and the swamp.

3.3.5 Representation of Tributaries and Surface Runoff. Along its main course, the Vermilion River receives runoff contributions from 15 main tributaries and about 23 minor lateral streams.

Due to the absence of tributary streamflow observations, the current study depended on readily-available hydrologic simulations from the National Water Model (NWM) Reanalysis to obtain tributary streamflow hydrographs. These tributary hydrographs were then used to drive the hydrodynamic model simulations (red and gray arrows in Figure 3-1).

The NWM is a modeling framework that depends on a fully coupled surface/subsurface hydrological model called WRF-Hydro (Gochis et al., 2018). The NWM uses diffusive wave surface routing and saturated subsurface flow routing on a 250-m grid, and channel routing down the NHDPlus stream reaches using the Muskingum-Cunge (MC) method (Shastry et al., 2017). Only five major tributaries (Coulee Des Poches, Coulee Mine, Coulee Isaac Verot, Coulee Ile Des Cannes, and Anslem Coulee), were explicitly simulated in the hydraulic model as 1D reaches (Figure 3-1). These specific tributaries were selected since they play a key role in the river hydrodynamics. Hydrographs were extracted from the NWM dataset at the outlets of the lower-order streams of the five tributaries (gray arrows in Figure 3-1) and the outlets of the 10 main tributaries that were not fully included in the hydrodynamic model (red arrows in Figure 3-1). These hydrographs were then used to drive the 1D hydrodynamic simulations of the five tributaries and the main river. Examples of NWM hydrographs that were used to enforce the hydrodynamic model are shown in the Supplementary Material.

It is also noted that, besides the concentrated streamflow hydrographs, additional overland streamflow hydrographs were extracted from the spatially-distributed NWM outputs. These were then provided as laterally-distributed hydrographs to the 1D reaches of the five tributaries and the main river to capture overland surface runoff that drain directly to the channels (see Supplementary Material for more details). Additional surface runoff comes from direct rainfall over the Bayou Tortue swamps. Since the swamps were represented in the model using a 2D setup, a rainfall-on-grid HEC-RAS approach was adopted over the swamps. Rainfall data was available via the hourly, spatially distributed (4×4 km^2) Stage IV radar-rainfall product (Eldardiry et al., 2015). Hourly Stage IV rainfall data were extracted

over each of the eight 2D swamp areas and used to drive the 2D hydrodynamic simulations over the swamp domain.

3.3.6 Terrain and Land-use Representation. A modified terrain model was developed for the Vermilion River basin using a combination of cross sectional surveys, high-resolution LiDAR-based Digital Elevation Models (DEM; Cunningham et al., 2009), and detailed bathymetric surveys for the river (USACE, 2015). To compensate for the inability of the LiDAR technology to "see-through" the water surface (Cook and Merwade, 2009), the LiDAR DEM and the riverine bathymetry were merged to generate an improved terrain model that includes the riverbed survey along the channel reaches and the DEM data elsewhere in the model domain. The merged terrain model was hydrodynamically-corrected following Jarihani et al. (2015). Merging these elevation sources into a single DEM, while keeping the priority for the local surveys and river bathymetry in overlap areas, produces a base DEM that is used in the hydraulic modeling and subsequent analysis of dredging scenarios.

The Vermilion River watershed exhibits a significant heterogeneity in the land-use and land-cover characteristics. To reliably model the flood response of the watershed, the 2011 30-m National Land Cover Database (NLCD) (Homer et al., 2015) was used to develop a lookup table that links each NLCD grid cell with a representative value of the Manning's roughness coefficient. This allowed the model to incorporate a spatially distributed representation for overland and channel roughness characteristics.

3.3.7 Model Calibration. The model was calibrated using the May–June 2014 multi-storm simulation period, while the results were tested under the August 2016 simulation period (**Figure 3-2**).

Due to the lack of adequate flow and stage observations in the basin, only a limited level of model calibration was possible. A visual-based calibration was performed to adjust the model parameters by focusing on key attributes of the river flow regime during flood events (e.g., reverse flows, river-swamp flow exchanges, slow recession of flood waves). The calibration was done primarily by adjusting the Manning's roughness coefficient in the channel reaches that were simulated as 1D and the swamp areas that were simulated as 2D. In channel reaches, the roughness coefficient was adjusted for the main channel as well as for the overbanks. The calibration focused primarily on simulating the magnitudes and timings of flow and stage peaks at the two gauges. In calibrating the model, special attention was given to re-produce the reverse flows that were observed at the Surrey gauge, which is an indication of the model's ability to capture river-to-swamp flow exchanges. Adjustments roughness coefficients were also spatially adjusted over the swamp areas that were simulated using a 2D grid. The adjustments were key in improving the model's ability to simulate the prolonged recession of the receding flood waves, a typical behavior of the river during extreme events that is attributed to swamp-to-river flow exchanges. More details about the model performance and the calibration results are available in Saad et al. (2020).

3.3.8 Description of Dredging Scenarios. To investigate the impact of dredging on flow regime within the river, four different scenarios were considered. The scenarios reflect different combinations of spatial extents and changes to the dimensions of the river channel and its longitudinal slope (**Table 3-1** and **Figure 3-4**).

These combinations also reflect a wide range in the expected volume of the dredged material. Despite the differences between the four dredging scenarios, they all share some common features. All dredging scenarios intend to cut the river cross-section to a 30-m width and side slopes of 2H:1V, while maintaining the river alignment unchanged. These new channel dimensions were based on navigation and flood control criteria set by the Bayou Teche and Vermilion River Operations and Maintenance project (USACE, 1995). In all scenarios, the roughness coefficient was adjusted in the dredged sections to reflect the expected improvement in channel irregularity and bed roughness.

Table 3-1: The four dredging scenarios considered for evaluation. The numbers reported for each scenario represent the length of the dredged reach (km) and the volume of bed material that needs to be dredged (million cubic meters, Mm^3).

	Spatial Extent of Modifications	
Modifications to River Capacity	Partial	Full
Modify Channel Dimensions	Scenario (A) 27 km; 1.7 Mm^3	Scenario (C) 81.1 km; 3.0 Mm^3
Modify Channel Dimensions and Bed Slope	Scenario (B) 27 km; 2.9 Mm^3	Scenario (D) 81.1 km; 7.5 Mm^3

Dredging scenarios A and C focused on changing the channel dimensions only, while scenarios B and D included changes to both of the channel dimensions and the longitudinal bed slope. Modifying the channel dimensions intends to dredge the river bed to a fixed elevation of −3.35 m, based on the North American Vertical Datum of 1988 (NAVD 88), with a width of 30-m and side slopes of 2H:1V (**Figure 3-4**). However, if the existing bed

elevation located within the intended dredging reach was already lower than the −3.35-m elevation, which was the case for most of the dredged reaches, the bed elevation is kept unchanged while the new width is carved at the elevation of −3.35 m. In addition to increasing the channel cross-sectional dimensions, scenarios B and D included grading the river bed to achieve a downstream-oriented longitudinal slope (**Figure 3-4**).

The study also examined two spatial extents of river dredging, a partial dredging extent (scenarios A and B) and a full dredging extent (scenario C and D). The "Full" spatial extent applies dredging for the whole navigation reach of the river, starting from its intersection with the GIWW in the south, and extends north for 81.1 km where the Ruth Canal joins the river. Alternatively, the "Partial" dredging extent covers only 27 km of the river where it passes through the heavily urbanized areas within the City of Lafayette. The four dredging scenarios capture different degrees of modifications to the channel conveyance capacity and will allow a comprehensive evaluation of impacts on flow regimes and flooding in the river basin. Each dredging scenario will be tested separately using the hydrodynamic numerical model under the 2014 and 2016 simulation periods. The results will then be compared against those of a baseline scenario that represents the existing conditions of the river geometry.

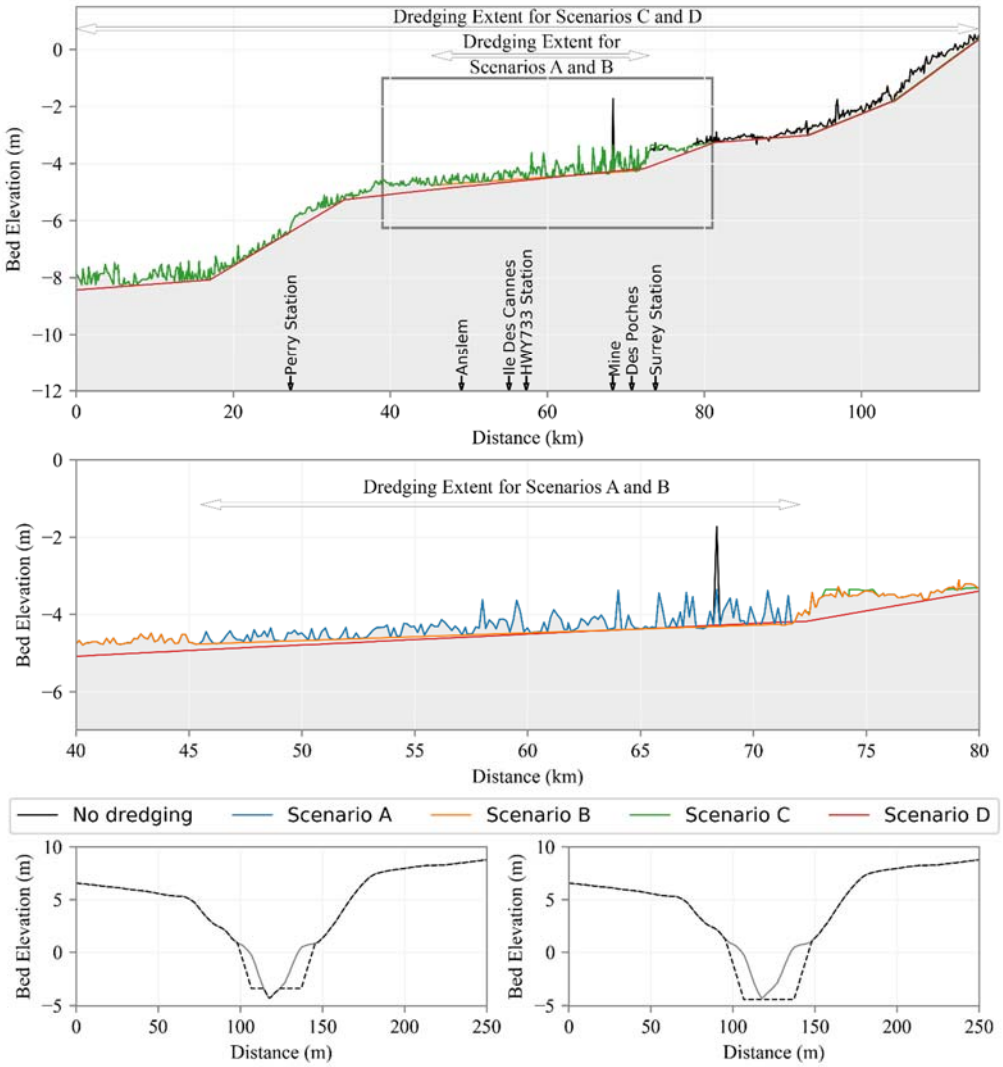

Figure 3-4: Top panel: Bed elevation of the Vermilion River starting from its downstream intersection with the GIWW until its most upstream station. The bed elevation is shown for the existing condition of the river (base scenario, black line in top panel) and the four dredging scenarios, A, B, C and D. Middle Panel shows a close-up view on the dredging extents of scenarios A and B. Note that the existing bed elevation follows the irregular bed profile and overlaps with some of the scenarios in certain reaches. Lower panels show examples of cross section modified for dredging (solid lines indicate the existing cross section while the dashed lines show the same section after dredging).

3.4 Results and Discussion

This section presents the results of the hydrodynamic model for the Vermilion River under the existing conditions (baseline scenario) in addition to the four proposed dredging scenarios. To isolate the effects of changing the river bathymetry, the forcing boundary conditions, including the tributary inflow hydrographs and tidal downstream boundary

conditions, were all kept the same in all scenarios including the baseline scenario. This approach will allow for inter-scenario comparisons and ensure that reflect only the effect of bathymetric changes due to river dredging.

3.4.1 Effect on Flow Regime in the Main River. Figure 3-5 and Figure 3-6 show the simulated flow hydrographs at three key locations along the Vermilion River for the two simulation periods, May–June 2014, and August 2016. The three locations (Surrey, HWY733, and Perry crossings) are selected in such a way to reflect different flow regimes along the river (e.g., reverse flows, upstream and downstream conditions, water surface gradients).

These figures illustrate flow hydrographs from simulating the baseline case (no dredging scenario), and those from the four proposed dredging scenarios (Table 1). Prior to discussing the effect of the different dredging scenarios, it is necessary to discuss the flow regime in the river under the existing conditions. The Vermilion River, under its current status, tends to show reverse (negative) flow values at Surrey station (top panels in Figure 3-5, Figure 3-6) under moderate and extreme rainfall storm events. These negative values indicate a reverse in flow direction where the river starts to travel north and exchange flows with the Bayou Tortue Swamp, rather than following its normal course south toward the Gulf of Mexico. The specific location where this flow inversion starts mostly depends on the severity of the storm and the spatial distribution of the rainfall over the watershed. This can be seen when comparing the simulated flow hydrographs at HWY733 during May–June 2014 period (moderate 2–10-year events) and August 2016 period (extreme >100-year events). The results suggest that the reach of the river where inversion in flow direction occurred extended much further downstream to reach south of HWY733 during the more extreme

August-2016 storm, while it was only limited to shorter reaches during more moderate rainfall events. The degree and spatial extent of the reverse flow are also apparent in the longitudinal water surface profiles shown later in **Figure 3-7** and **Figure 3-8**

Generally, the different dredging scenarios appear to alter the overall flow regime in the river, especially during moderate storms, such as the May–June 2014 period. All dredging four scenarios tend to reduce the reverse flows during the peak period of the storm while increasing the positive flows during the recession period. Despite differences in the spatial extent and degree of channel modification across the four dredging scenarios, the dredging activities tend to cause the main river to flow in its normal course toward the Gulf of Mexico. This is further evident in the simulated flow hydrographs at HWY733 and Perry locations (**Figure 3-5**) which experience a general promotion in the positive flow values. Increases in in the magnitudes of downstream flows are also apparent in the slow and elongated recession curve, indicating that the river is now accepting more flows coming from the swamp system and moving into the downstream direction.

The results under a more extreme storm (August 2016) provide other interesting insights on how dredging can significantly alter the flow regime in the river. Note that during this extreme flooding event, the extent of the reverse flow reached much further downstream (top and middle rows in **Figure 3-6**) than during the 2014 moderate events. During the August 2016 period, only the more aggressive Scenarios B and D, which involve implementing downstream-sloped riverbed grading, acted similar to the May–June 2014 period and reduced reverse flows. On the other hand, the less aggressive dredging Scenarios A and C showed an opposite behavior where some increases in the reverse flows were

obtained, indicating an increase in the peak flows traveling north toward the Bayou Tortue Swamp.

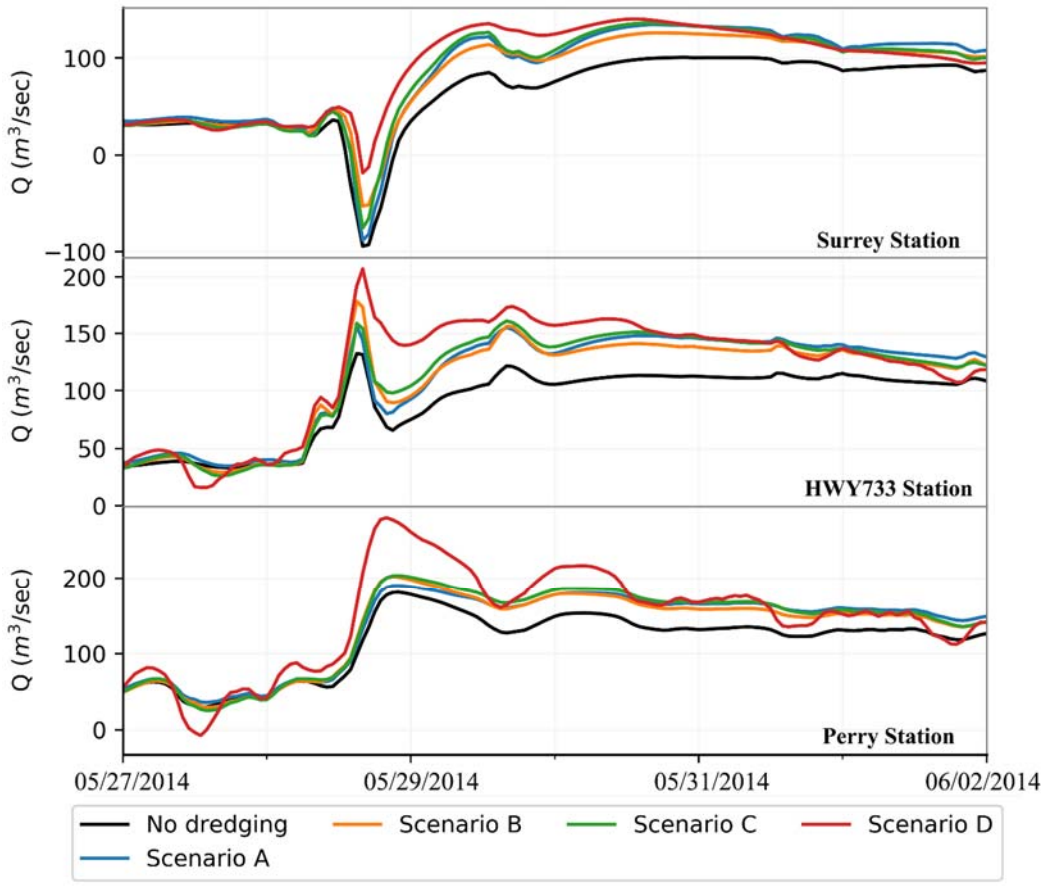

Figure 3-5: Simulated flow hydrographs at three key stations along the Vermilion River (top panel: Surrey, middle panel: HWY733, bottom panel: Perry; see Figure 1 for specific locations) during the May-June 2014 simulation period for the no-dredging baseline condition and the four dredging scenarios.

The dredging approach of scenarios A and C involve only enlarging the river cross-sectional dimensions without any grading of the longitudinal bed slope as was done in scenarios B and D. Apparently such approaches lead to an increase in the in-channel storage capacity within the dredged reach of the river without changes the bed slope. During extreme events, such as the August-2016 event, the in-channel storage of the river gets dominated by the amount of rainfall and thus plays a less significant role in controlling the water surface gradient. The runoff delivered to the river through its tributaries overwhelm the river storage

capacity and build a hydraulic gradient that makes it easier for the river to travel in the reverse direction toward the Bayou Tortue Swamp system.

The results clearly suggest that the dredging scenarios have an effect on flow exchanges between the river and the swamp system that provide a valuable flood mitigation service for the entire watershed (Saad et al., 2020). During the peak of the storm, the river flows north into the swamp providing relief for the downstream areas of the watershed. However, after the peak, the large volumes of water that were diverted into the swamp start to drain back into the river resulting in an extremely extended recession of the hydrograph, which leaves the downstream communities under high flood stages for several days. To further examine the impacts of the different dredging scenarios on the river-swamp interactions, hydrographs of flow exchange between the river and the swamp were examined. These hydrographs (not shown) were constructed by tracking the exchange flows through the tributaries and lateral connections that connect the swamp and the river (**Figure 3-3**). The results confirmed a significant reduction in the volume of river-to-swamp flows by as much as 40–64% under scenario D and an increase in the swamp-to-river outflows into the river by as much as 23%.

3.4.2 Effect on Water Surface Elevations (WSE) in the Main River. Figure 3-7

and **Figure 3-8** show longitudinal profiles of the maximum water surface elevation (WSE) along the river during the two simulation periods for the baseline scenario and the four dredging scenarios. For better clarity, the results for the four dredging scenarios are presented in the form of differences from those of the baseline scenario.

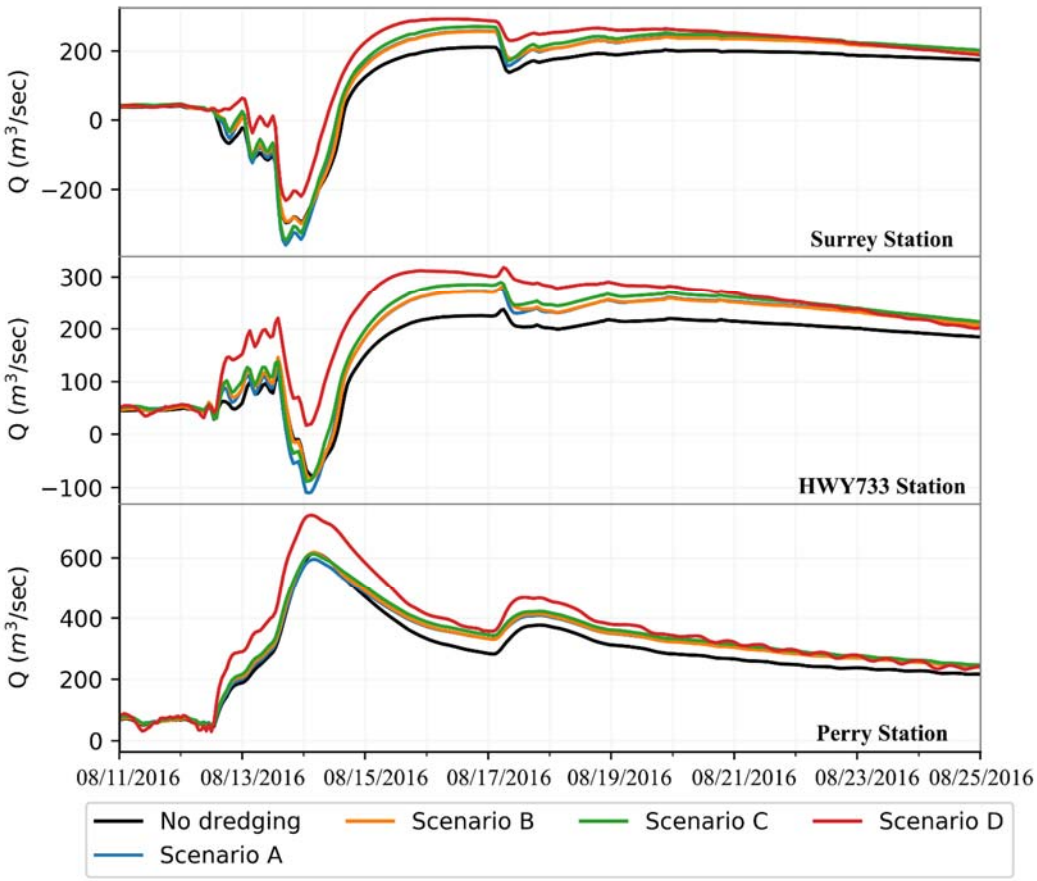

Figure 3-6: Simulated flow hydrographs at three key stations along the Vermilion River (top panel: Surrey, middle panel: HWY733, bottom panel: Perry; see Figure 1 for specific locations) during the August 2016 simulation period for the no-dredging baseline case and the four dredging scenarios.

In general, the dredging scenarios reduced water surface elevations along some reaches the river, but to various degrees. During the August 2016 period, maximum reductions in water surface elevation were 0.14, 0.22, 0.30, and 0.49 m for dredging scenarios A, B, C, and D, respectively. Smaller reductions (0.19, 0.21, 0.22, and 0.42 m) were obtained during the more-frequent storms of May–June 2014. The reductions are more noticeable over the middle section of the river (~river km 50 to river km 80). The reduction reached further downstream (~river km 5–20) under the most aggressive dredging scenario D. Despite the overall reduction in WSE, it is interesting to see that local dredging that doesn't extend downstream enough (e.g., Scenarios A and B), although may reduce water

surface elevations within the dredged reach, had actually triggered downstream increases in water surface elevations during the May–June 2014 period where up to a 0.2 m increase was observed in the last third of the river (~river km 10–45). During more frequent events, spatially-limited increases in the in-channel storage of the river offered localized relief to the water surface profiles but led to a significant backup in water volumes and thus an increase in downstream water surface elevations.

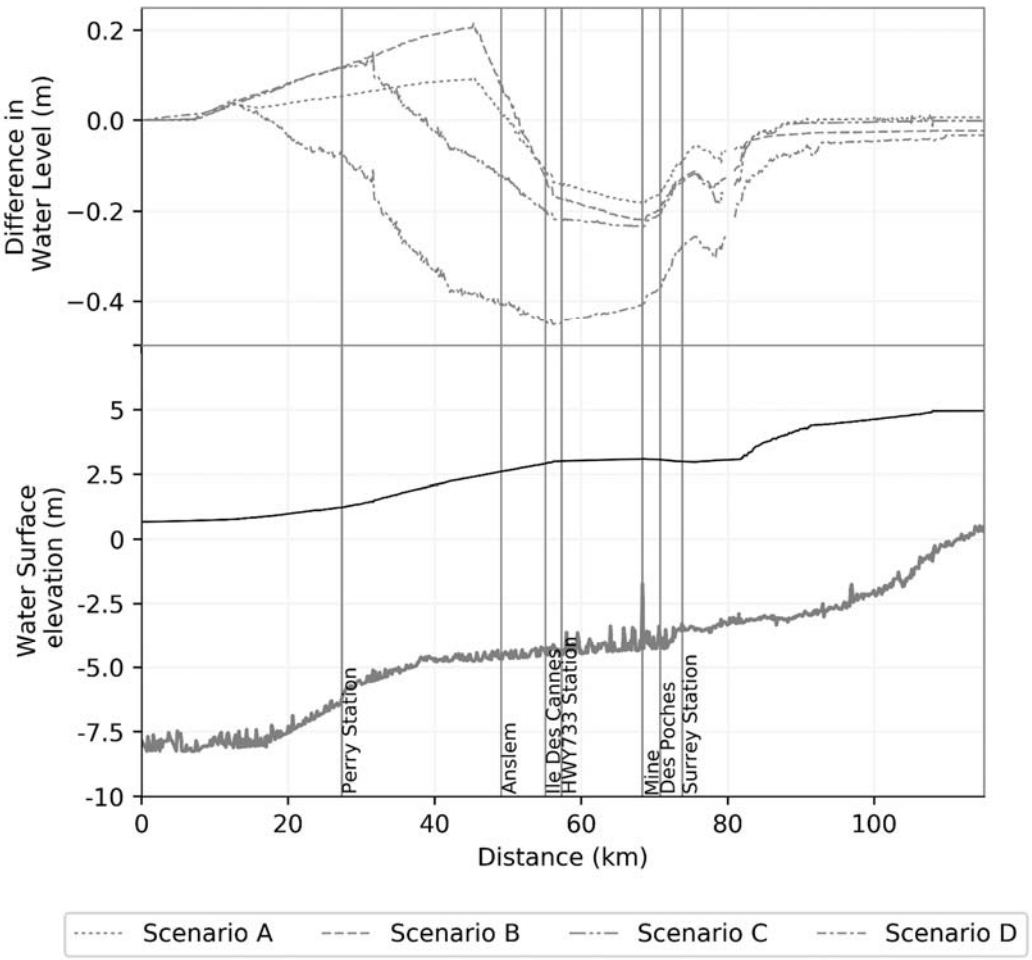

Figure 3-7: Lower Panel: Longitudinal profile of maximum water surface elevation (WSE) along the mainstem of the Vermilion River simulated under the baseline case during the May-June 2014 simulation period. The existing river bathymetry is also shown (irregular line). Top Panel: Longitudinal profile of the differences between the maximum WSE simulated under each dredging scenario and the baseline case.

Interestingly, the results obtained from Scenario C, despite being a full dredging scenario that extends for a longer distance down the river, also showed some increase (~0.15 m) in the water surface elevation in the last reach of the river (up to river km 25). Considering that Scenario C includes increasing the channel dimensions only, the lack of any enhancements to the channel bed slope as it approaches the Gulf didn't allow the river to benefit from the enlargement added to channel size. It is also noted that channel size enlargement implemented in Scenario C were actually much less needed in the last section of the river due it its already existing large channel.

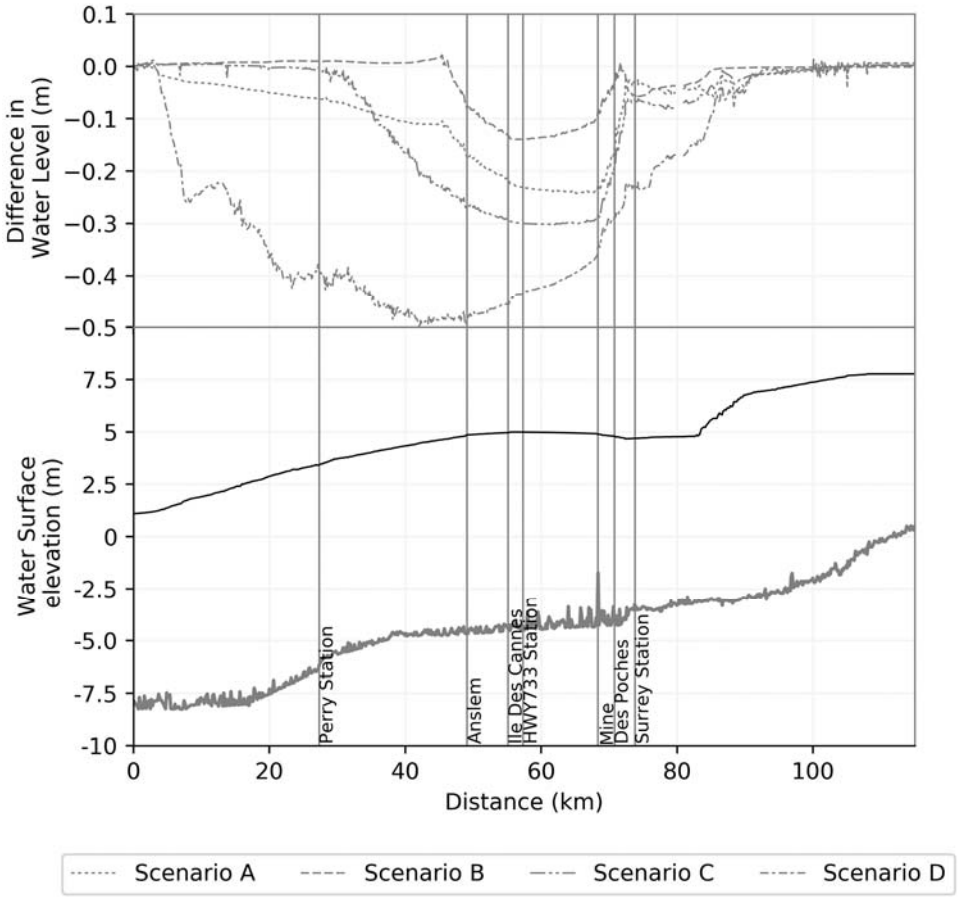

Figure 3-8: Lower Panel: Longitudinal profile of maximum water surface elevation (WSE) along the mainstem of the Vermilion River simulated under the no-dredging baseline case during the August 2016 simulation period. The existing river bathymetry is also shown (irregular line). Top Panel: Longitudinal profile of the differences between the maximum WSE simulated under each dredging scenario and the baseline case.

The negative consequences of increasing the water surface elevation were not obtained under more extreme storm of 2016. This is simply because the water elevations were already high and the large rainfall volumes created their own gradients regardless of the channel slope or its dimensions.

3.4.3 Effect on the WSE in the Tributaries. In addition to examining the impact of riverine dredging on the main stem of the river, it is also of interest to assess the propagation of such impacts into the tributaries that drain into the river. To allow such examination, five of the main tributaries that drain into the Vermilion River (Coulee Des Poches, Coulee Mine, Coulee Isaac Verot, Coulee Ile des Cannes, and Anslem Coulee) were explicitly modeled as part of the hydrodynamic model. The maximum WSE profiles along two of these tributaries (Coulee Ile des Cannes and Coulee Isaac Verot) are shown in **Figure 3-9** and **Figure 3-10**. Observations drawn from the profiles of these two tributaries were found consistent for the other tributaries as well.

Compared to the results inside the main river, generally, a lesser reduction in water stage across the tributaries are attained. The Ile des Cannes tributary showed larger drops in water surface elevation, both in magnitude and spatial extent. As expected, the maximum WSE reduction occurred at the outlet of the tributaries, with Scenario D showing the most WSE reduction in both events. Scenario A and Scenario B showed the least WSE reduction, similar to their in the main river. The reduction in WSE propagated upstream into the coulees for relatively limited distances of mostly ~2 km and no more than 10–13 km. The magnitude and spatial extent of the reduction within each tributary is largely dependent on the longitudinal bed slopes of each tributary and the hydraulic gradient during the flood event. The most downstream reach of Coulee Ile des Cannes is characterized by an average bed

slope of 0.037%, while the same reach in Coulee Isaac Verot exhibits a steeper average bed slope of 0.084%. The WSE reduction apparently increases in coulees that have milder slopes. Examining the hydraulic gradient provides some additional insight. During the more frequent storm, May–June 2014, the hydraulic gradient inside the Isaac Verot tributary was estimated as 5.4% for the baseline scenario, resulting in a minimal WSE reduction (0.015 m) that extended for a distance of <2 km under the most extensive dredging scenario (Scenario D). However, the same tributary had a milder hydraulic slope of 3% during the August 2016 extreme event, and thus resulted in a larger reduction in water surface elevation of 0.42 m that extended slightly further upstream under the same dredging Scenario D. Unlike Isaac Verot tributary, the hydraulic gradient in the Ile des Cannes tributary, under the baseline scenario, was 0.004 and 0.005% during the May–June 2014 and August-2016 periods, respectively. As such, these conditions resulted in larger reductions of 0.44 and 0.42 m that extended for longer distances of 13 and 12.1 km, respectively (Scenario D). The very flat bed slope for the Ile des Cannes tributary diminished the effects of differences in the hydraulic gradient between the periods of May–June 2014 and August 2016.

3.4.4 Effect on Tidal Propagation. Modifications to the river channel are expected to affect the propagation of tidal wave for rivers, such as the Vermilion River, especially with its connectivity to the Gulf of Mexico through the Vermilion Bay. To assess such potential effects, the model simulations were used to quantify the tidal amplitudes under the different dredging scenarios and compare them to the existing baseline condition.

Figure 3-11 illustrates the maximum tidal amplitude along the main stem of the river starting from its most downstream intersection with the bay. The amplitudes shown in **Figure 3-11** were calculated by taking the difference between the maximum and minimum water

elevation at each cross section along the river over the temporal span of the simulation period. However, this was performed for the pre-storm period only and without including the water stages during the main storm. The main reason for doing so is to isolate the potential impact of the dredging activities on the tidal hydrodynamics during non-flooding conditions and without including the effects of the inland rainfall storms.

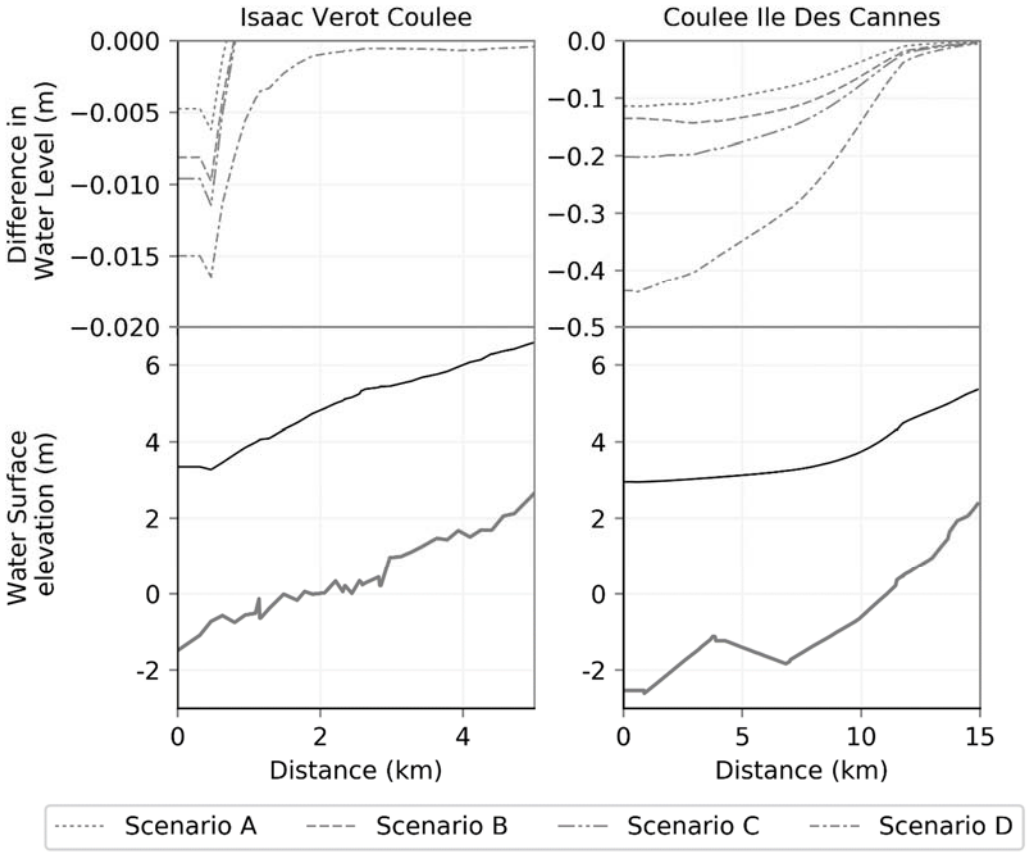

Figure 3-9: Lower panels: Longitudinal profiles of maximum water surface elevation (WSE) for the baseline case during the 2014 simulation period. The existing river bathymetry is shown (irregular line). Top panels: Longitudinal profile of differences between the maximum WSE of each dredging scenario and that of the baseline case.

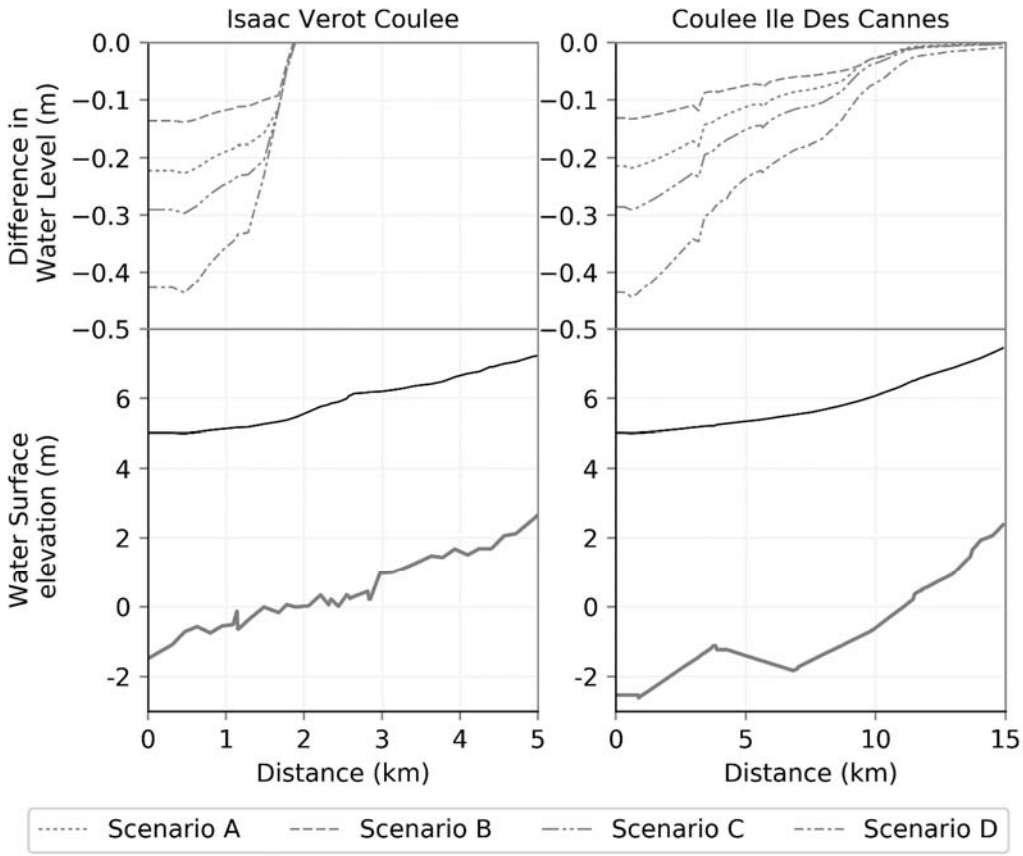

Figure 3-10: Lower panels: Longitudinal profiles of maximum water surface elevation (WSE) for the baseline scenario during the August 2016 simulation period; the existing river bathymetry is shown (irregular line). Top panels: Longitudinal profile of differences between the maximum WSE of each dredging scenario and the baseline case.

The results (**Figure 3-11**) obtained under the baseline scenario suggest that the tidal signal in the river is largely diminished around 65–70 km from its outlet to the Gulf. Generally, the results suggest that all dredging scenarios caused a significant alteration in the tidal range along the course of the main river. However, it is clear that dredging Scenario D has the most significant impact in allowing the tidal signal to propagate for longer distances upstream. Scenario D resulted in a drastic increase in the tidal amplitude that extended across the entire river, with an increase of as high as 1.8 times the magnitudes obtained under the baseline scenario. This amplification extended for significant distances upstream and as far as Surrey crossing, ~73 km landward into the heart of the City of Lafayette. Scenarios A, B, and C resulted in tidal amplitudes similar to the baseline condition, but with some minimal

attenuation in the downstream reaches of the river [0–50 km]. Starting at ~50 km and further north, an inflection in the tidal propagation starts to occur and the reach witnesses a relatively constant tidal amplitude that tends to be higher than the baseline scenario. Such increases are apparently triggered by the channel size enlargement and bed grading involved in this middle reach under scenarios A, B, and C. Also, the results shown in **Figure 3-11** highlight the value of the Bayou Tortue swamp as a coastal mitigation measure. Along the river reach where it has interconnections with the swamp (73–85 km), the maximum tidal wave height dropped sharply, especially under dredging scenarios B and D, which emphasizes the vital role of the swamp system in attenuating the tidal wave. The swamp storage capacity and its accessibility to the main river seems to have absorbed the effect of the tidal signal and reduced its propagation further upstream.

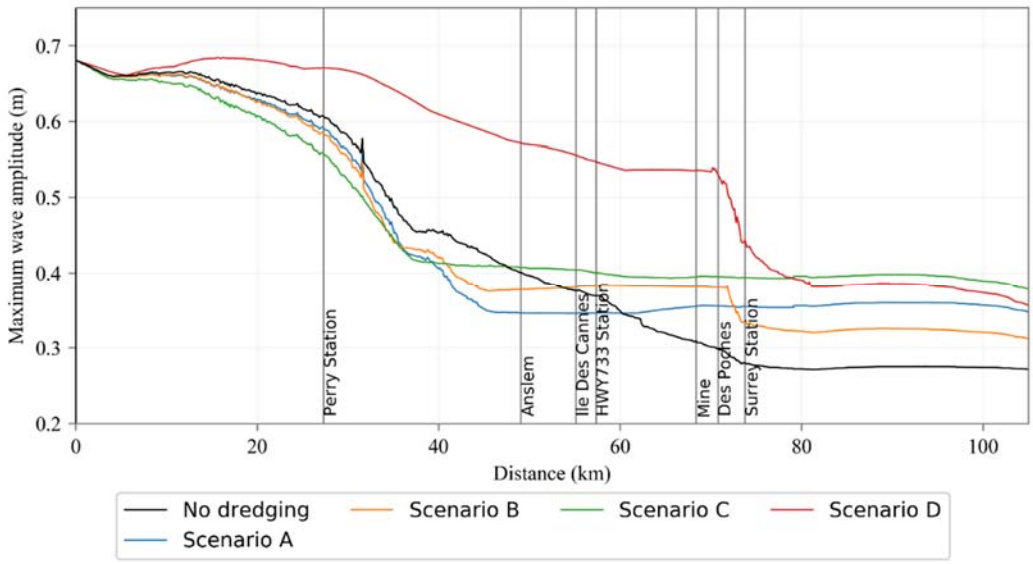

Figure 3-11: Propagation of tidal amplitude along the Vermilion River under the baseline case and each dredging scenario. Results are based on a non-flood period (07/25/2016 to 08/08/2016) that precedes the August 2016 flood. The vertical grey lines depict the inlet locations of key tributaries along the Vermilion River.

3.4.5 Effect on Inundation Extent and Duration. The impact of riverine dredging on flooding regime is further examined by assessing the flood inundation along the main river and its major tributaries. The maximum extent of flooded areas that would occur for each dredging scenario and for the baseline case were calculated during both simulation periods. The spatial extent of flood inundation was estimated by comparing the simulated water surface elevations and the LiDAR-based DEM. For the river channel and tributaries that were modeled as 1-D, a water surface model was developed by interpolating the maximum water stages at each cross-section on a grid that has the same spatial extent and resolution of the DEM surface. In areas that were simulated as 2D, the water surface grid is a direct output of the hydraulic model and no extra interpolation was required. After mosaicking the water surface grids estimated from 1D and 2D areas, the final water surface grid was overlaid onto the LiDAR grid to calculate differences between the surfaces and delineate the extent of the flood inundation. The results are summarized by calculating the total inundated areas for the entire domain of the river and its tributaries (**Table 3-2:** Inundation areas estimated for each dredging scenario.). As expected, the dredging scenarios resulted in some reductions in the inundated areas; however, such reductions appear rather minimal. The results report reductions in the flooded area in the order of (0.97–6.87 km2) and (0.48–2.29 km2) during the August 2016 and May–June 2014 periods, respectively. It is interesting to contrast these rather minimal reductions in inundation spatial extents vs. the more noticeable reductions in the water surface profiles reported earlier (~0.4–0.5 m reduction; **Figure 3-7** and **Figure 3-8**). These results indicate that the main river doesn't necessarily fully control the actual extent of inundation on adjacent floodplains, and further suggest that floodwaters of the river are mostly contained within its own main channel. These

results are also consistent with the earlier observations on the relatively small propagation of reductions in the water surface elevation from the river into its tributaries (**Figure 3-9** and **Figure 3-10**).

Table 3-2: Inundation areas estimated for each dredging scenario.

	Inundated Area (km^2)	
Approach	May-June 2014	August-2016
Baseline	181.26	269.1
Scenario A	180.78	268.1
Scenario B	180.39	267.8
Scenario C	180.09	264.2
Scenario D	178.97	262.2

Besides examining the spatial extent of inundation, it is also of interest to examine the duration of inundation. This becomes particularly relevant given the extreme slow recession of flood waters in low-gradient rivers, such as the Vermilion River (**Figure 3-5** and **Figure 3-6**). The duration of inundation was quantified by calculating the total number of hours each cell in the composite spatial inundation grid experienced a positive water depth. The number of hours were summed over the full duration of each simulation period. When compiled over the entire domain of the model, scenarios A, B, and C resulted in average reductions of 2–4 days in the inundation duration, while scenario D showed average reductions of 4–6 days. Example of the results are shown in **Figure 3-12** and **Figure 3-13** for selected areas within the model domain. In these areas and depending on the dredging scenario, the average reduction in inundation duration was in the range of 9.5–28.6 and 6.7–33.3% for the May–June 2014 and the August-2016 periods, respectively. Reductions as high as 6–8 days were obtained, especially with scenario D and in areas around the City of Lafayette and before the river enters connects to the Bayou Tortue Swamp system. Such results reveal that while the dredging activities didn't significantly reduce the spatial extent of inundation, they seem to

reduce the duration of such inundations. The reduced inundation durations have implications for communities who are impacted by flooding conditions that last for several days after the peak of the storms.

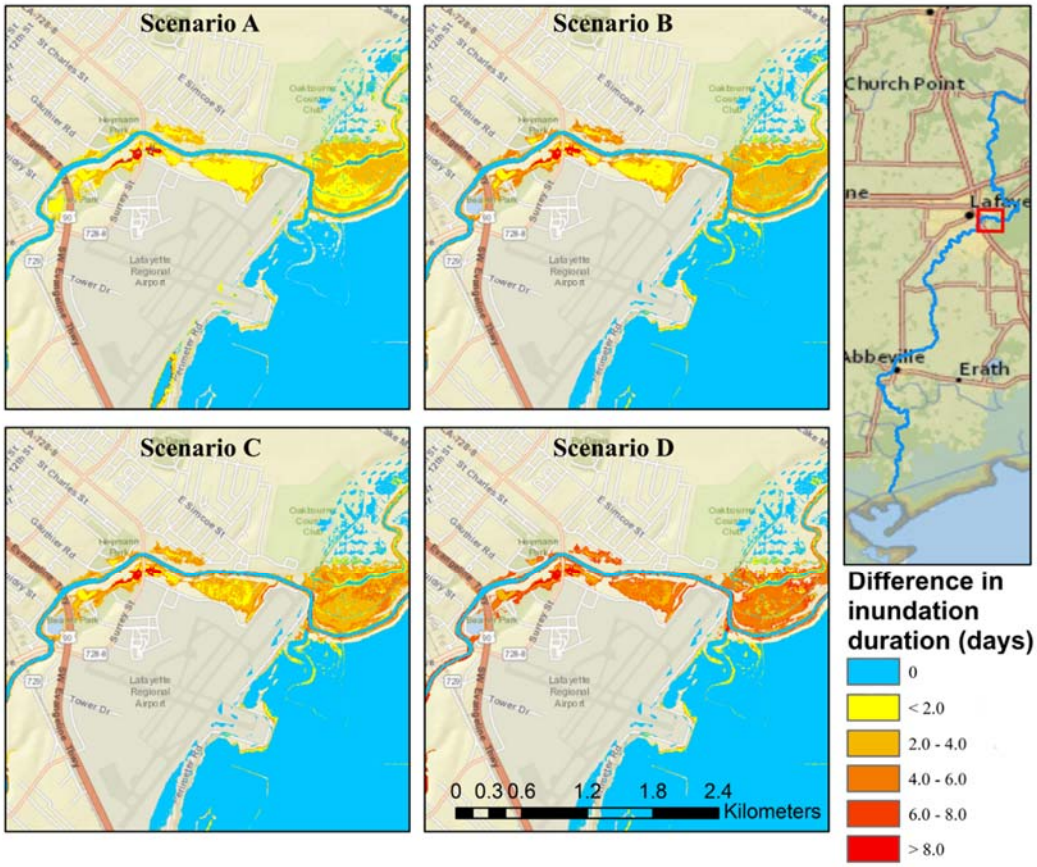

Figure 3-12: Differences in inundation duration between the baseline case and each dredging scenario during the May-June 2014 simulation period.

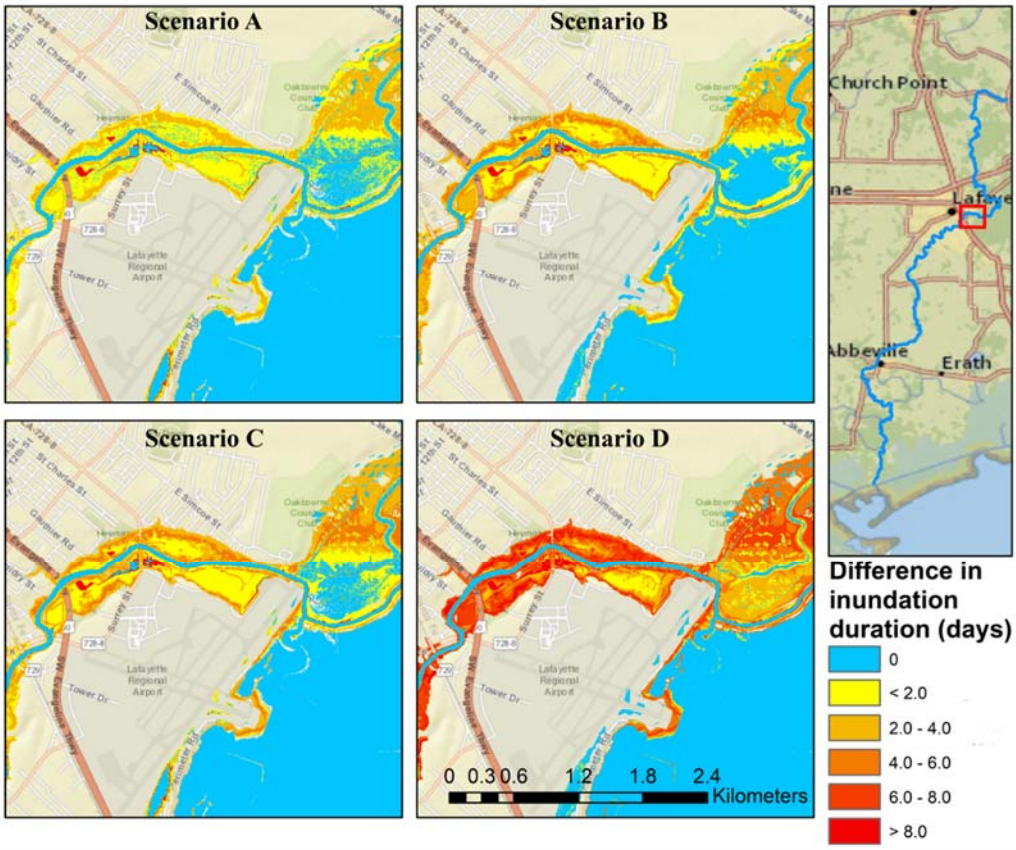

Figure 3-13: Differencesin inundation duration between the baseline condition and each dredging scenario during the August 2016 simulation period.

3.5 Conclusions And Recommendations

This study investigated how large-scale channel modifications via riverine dredging may alter flood dynamics in the Vermilion River in southern Louisiana, a representative of low-gradient tidally-influenced river systems. With the presence of large swamp system within its watershed, the river is characterized by complex flow dynamics where frequent reverse (upstream) flows occur allowing flood waters to travel upstream for temporary storage in the swamps. The study examined the impacts of four different dredging scenarios that represent varying degrees of spatial extent and modifications to the channel cross section and longitudinal bed slope. A hybrid 1D/2D numerical model was used to simulate the impact of dredging activities on the flow hydrodynamics along the main course of the river and five of its major tributaries. The analysis was performed on two flooding periods, May-

June 2014 and August 2016, which are classified as <10-year and >100-year storms, respectively. The four different dredging scenarios were assessed by evaluating key characteristics of the flow regime, including changes in flow hydrographs at key locations, reductions in water surface profiles and flood inundation, alterations to river-swamp interactions, and impact on tidal amplitudes and propagation. The results from each dredging scenario were compared against those obtained under the existing no-dredging scenario.

Overall, the results suggest that a watershed-centered approach, instead of a riverine-centered approach is needed for assessment of flood mitigation alternatives in such riverine systems. The following conclusions can be formulated based on the findings of the study:

1. The effect of large-scale riverine dredging on the flow regime in the river and the resultant flood conditions is highly controlled and modulated by inter-related and often competing factors, such as extent of the dredging in both volume and spatial coverage, flow exchanges between the river and the inter-connected natural swamps, bed slopes and hydraulic gradients, and the large volumes of runoff contributions from river tributaries and how they compare to induced changes to the river in-channel capacity.
2. Dredging scenarios that modified the river channel modifications and the riverbed slope lead to significant changes to the river flow regime. Overall, reverse river flows that travel to the swamp during the peak period of the storms were reduced. Such impacts have significantly altered the flow exchanges between the river and the swamp and severed the river-to-swamp inflows and increased the swamp outflows. This is expected to affect the hydroperiod of the swamp system and its residence time and may eventually affect its viability as a natural ecosystem.

3. Dredging approaches that were spatially extensive and included modifications to the river slope can result in sizeable reductions in water surface profiles (40–50 cm) along the river during flood conditions. However, such extensive dredging brings significant increase in the amplitude and propagation of the Gulf tidal wave that extended as far as 70 km inland.
4. While less-extensive, spatially-limited dredging approaches can also reduce the water surface profiles to some extent (10–30 cm), they tend to cause an increase in the water surface elevations downstream of the dredged river reaches. Such increases can extend over 20–40 km along the river, exposing downstream communities to increased flooding especially during more frequent events.
5. The results reveal that while the dredging activities can increase the hydraulic conveyance of the river system and improve its drainage characteristics, the large runoff volumes delivered by the contributing tributaries eventually overwhelm the river and outweigh the added improvement in terms of in-channel storage, thus reducing the anticipated flood relief benefit expected from the dredging.
6. Reductions in water surface profiles in the Vermilion River propagated along the tributaries that drain into the river, but only to limited spatial extents. The degree of reduction inside the tributaries was dependent on the hydraulic gradient and longitudinal bed slopes of each tributary.
7. While there is evidence that dredging can increase channel conveyance and reduce water levels inside the Vermilion River, such reduction was not reflected in a parallel reduction in the spatial extent of flood inundation boundaries under any of the four dredging scenarios. On the other hand, reductions in the duration

of inundation were found to be substantial, suggesting that while dredging didn't significantly reduce the maximum extent of inundation, it seems to reduce the duration that flooded areas get inundated.

8. Generally, the results suggest that, regardless of the specific scenario, dredging activities caused a noticeable alteration in the tidal wave range along the river. Extensive dredging scenarios caused a substantial amplification in the tidal signal along the main course of the river, which can facilitate the landward penetration of storm surges into the river.

Acknowledgments

This material is based upon work supported by the National Oceanic and Aviation Administration (NOAA) UCAR Subaward No. SUBAED001383 to the University of Louisiana at Lafayette and by the Louisiana Board of Regents Support Fund (BoRSF) under Award # LEQSF (2019-22)-RD-B-05. The author would like to thank Mr. Donald Sagrera, the Executive Director of Teche-Vermilion Freshwater District, for providing information on the characteristics and operation of the Vermilion River hydraulic structures. The author also thanks Mr. Clyde Barre and Mr. Jeffrey Varisco from the United States Army Corps of Engineers–New Orleans District, for the valuable discussions that informed this study.

Chapter 4: Evaluation of the Role of Large Natural Storage Areas on Flood Dynamics in Low-gradient Coastal Rivers

4.1 Introduction

Communities are increasingly depending on their surrounding peri-urban and rural ecosystems for various services, particularly flood mitigation and control. The capacity of such ecosystems to reduce flood risk or reduce flood impacts provides a regulating service and benefit of enhanced safety to human life (de Groot et al., 2002). One of the well-known ecosystems that provide such flood mitigation services to communities is large natural storage areas such as swamps and wetlands. These systems represent natural green infrastructures that influence the hydrologic regime of the watershed where they exist (Mitsch et al., 2009). Mitsch has argued that wetlands serve "as nature's age-old method of flood control" by their short-and long-term water storage capacity, both of which are expected to reduce downstream flood peaks.

There is evidence that storage areas, especially those formed on the floodplains of rivers, reduce the frequency (Acreman et al., 2003) and magnitude (Ogawa and Male, 1986) of flood events and increase the time to peak of these events. Similar results have been obtained for headwater wetlands formed on the upstream reaches of a watershed. Draining wetlands in New Zealand was observed to significantly increase the frequency of flood peaks (Jackson, 1987). A study of wetlands in Illinois in the US estimated that as the peak flow to average precipitation ratio decreased by (on average) 3.7%, flood flow volume to total precipitation ratio decreased by ~1.4%, and low flow increased by 7.9% for an increase of one percent wetland area in a watershed (Demissie and Khan, 1993). Also, evidence from the impact of building dams upstream rivers, with storage effects analogous to that provided by swamps or wetlands, supports this conclusion.

On the other hand, there is evidence that wetland drainage has little impact on flooding (Bengtson and Padmanabhan, 1999), and somehow that wetlands may increase flood peaks (Acreman and Holden, 2013). As flood regulation relies on available water storage, permanently saturated swamps with little or no storage capacity may generate or convolute floods relative to unsaturated ones (Morris and Camino, 2011). Hence, it is unclear to what extent floods are attenuated or enhanced by wetlands of different types and sizes located in areas of different topographies (Smakhtin and Batchelor, 2005). This dependence of water storage capacity on wetland type and topography makes it difficult to generalize the flow regulation services offered by wetlands (Acreman and Holden, 2013). A synthesis of the hydrological functions of wetlands (Bullock and Acreman, 2003) showed that there are many qualitative assessments of the impact on flow regulation; however, there are few quantitative assessments.

Physically-based numerical hydrodynamic models provide a way to perform such quantitative assessments. These models are mathematical representations of the river system and the related natural storage areas, which provide insight into the water circulation dynamics along the river as well as inside the body of the wetlands itself. However, most of the hydraulic studies found in the literature used numerical models that depended on the one-dimensional (1D) representation of the wetland as a storage area (e.g., Tang et al., 2020). This 1D approach limits the ability of the numerical model to resolve key spatial dynamics (e.g., complex flow routes inside the wetland, travel time within the wetland, and variation in flood levels) and only considers the size of the available storage inside the wetland. Factors such as the wetland topography (Acreman and Holden, 2013), size (Kadykalo and Findlay, 2016), location relative to the watershed outlet (Fang et al., 2010), presence of discrete

lengths of spoil banks separating the river from the adjacent swamp area, in addition to the geometry and structure of the flow routes inside the wetland size, all play a role in the degree to the wetland may affect the flood flow in the river. In recent years, the demand for understanding the hydrological and hydrodynamic processes that govern wetlands located along the floodplains of rivers has been ever-increasing (Chomba et al., 2021). Besides being relatively under-studied in general, such wetlands, when located in low-lying topography, directly alter the flow dynamics of the passing-through rivers (Saad et al., 2020). In such regions, river systems are typically characterized by complex flow dynamics such as flow reversals and bi-directional flows (Watson et al., 2017), dynamic connectivity, and flow exchanges with large natural storage areas, such as swamps. As the flood stages in the river reach just downstream of the swamp areas start to build up because of the inflows from lateral tributaries, the elevated water stage causes the flow to overtop the upstream spoil banks towards the natural wetland areas located on both sides of the river. As this mechanism grows in low-lying topography, a steeper hydraulic gradient towards the swamp areas develops, and the floodwater favors to move upstream towards such an area rather than the normal downstream direction followed during low flow season, thus causing the reverse flow to occur. While that role is conceptually simple, the processes which define and drive such interactions between the river and the adjacent swamp area are exceedingly complex. In most rivers, inundation of floodplain swamps occurs when the discharge exceeds the channel's capacity and floodwater overtops the spoil banks. However, in some settings, flood waters leave the river via flow paths that laterally connect the river and the swamp and inundate the swamp prior to filling up the river section. Moreover, the flow exchange of water between adjacent storage areas and rivers involves mutualistic influences, which adds to the

complexity of the hydrodynamic processes. It is critical to have a thorough understanding of the significance of this relationship and the physical processes that drive the flow exchange in order to arrive at a consensus for sustainable management of the floodplain swamps.

This study deploys a hydrodynamic model to investigate the various impacts of floodplain swamps attributes such as size, lateral flow paths connecting the swamp with the river, and the spoil banks separating the river from the swamp and their implications for flood mitigation and how it may alter the overall flow regime. The study site is in the Vermilion River in southern Louisiana, US, a representative of low-gradient tidally influenced river systems that are located in flood transition zones. The study focuses on understanding the effect on flow regime and changes in water surface elevations under a suite of different setups that represent varying degrees of modification for the lateral connectivity between the swamp and the river, and changes to the size of the swamp through excavation. The analysis will be performed for different storm conditions (e.g., 10-year and >100-year return periods) to assess the dependence on the storm magnitude and the amount of runoff generated in the watershed.

4.2 Methods

4.2.1 Study Area. The Vermilion River study area is approximately 1560 km2 when estimated at the Gulf Intracoastal Waterway (GIWW). The GIWW is a navigable inland waterway running approximately 1,690 km east to west from Carrabelle, Florida, to Brownsville, Texas (**Figure 4-1**).

The Vermilion River intersects with the GIWW just 5.6 km before it drains into Vermilion Bay. The headwaters of the Vermilion River are the confluence of Bayou Bourbeux and Bayou Fusilier in the north, after which the river flows in a predominately

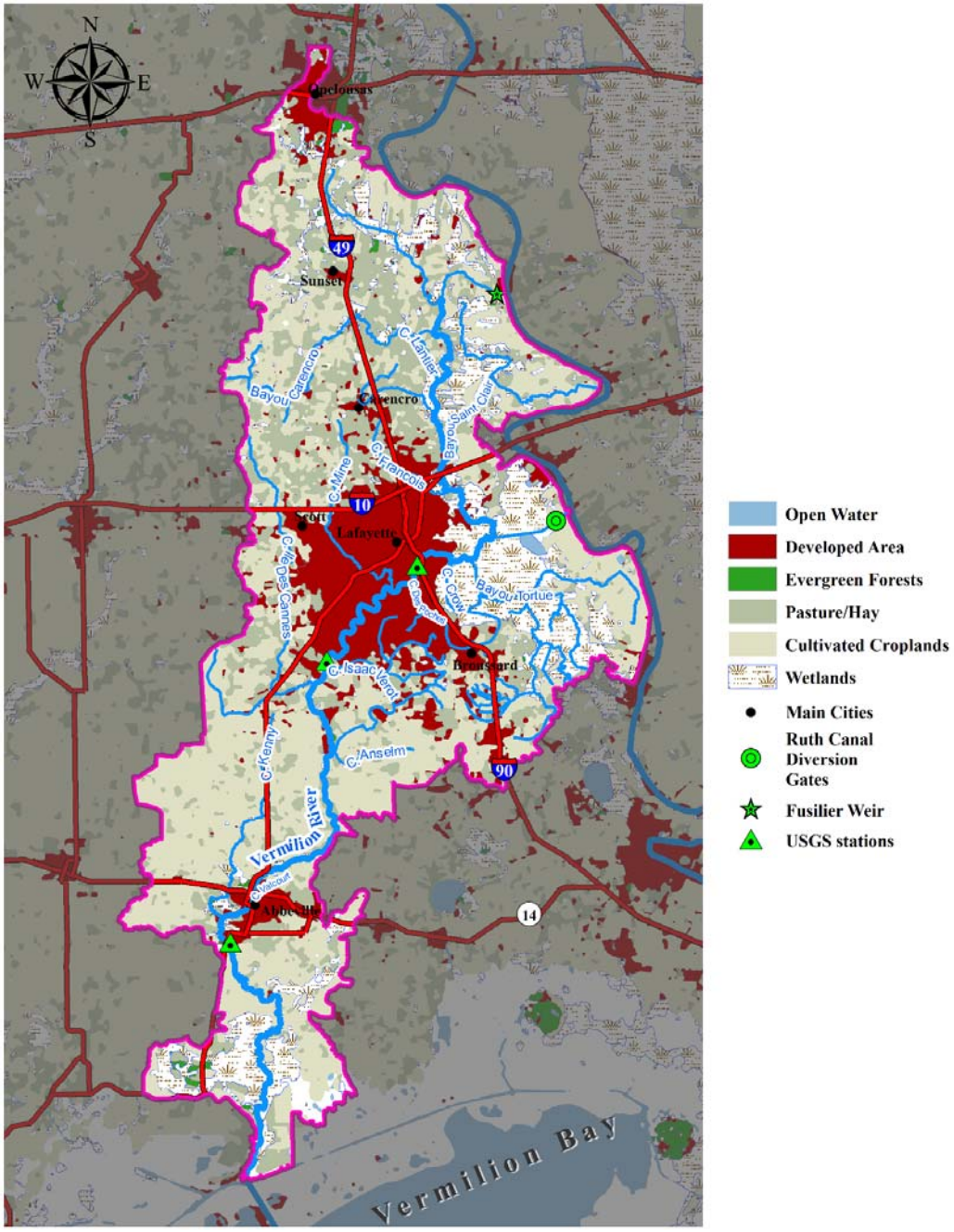

Figure 4-1: The Vermilion River watershed for the study site. The downstream end of the modeled reach of the river is at GIWW. The map shows different hydrologic features within the river basin, including the lateral coulees, Ruth Canal gates and Fuselier Weir that control flow from Bayou Teche to the Vermilion River.

south direction until it drains into the gulf through the Vermilion Bay. Agricultural practices dominate the watershed land use, but highly urbanized areas also exist with a significant concentration just south of a vast hardwood swamp system that is locally known

by Bayou Tortue swamp. Historical connections between the Vermilion River watershed and the former Mississippi River alluvial floodplain resulted in the formation of the Bayou Tortue Swamp. The Bayou Tortue swamp is a series of interconnected swamps and lakes that occupy an open-water surface area of ~35.2 km2 that is dissected by two main tributaries Coulee crow and Bayou Tortue (**Figure 4-2**). These two coulees have their outlets on the Vermilion River, and combined, they assemble the primary drainage system of the swamp area during non-flooding conditions. During flooding periods, the swamp system functions as a natural floodwater storage area by accepting overflow from the Vermilion River depending on the intensity of the storm event. This configuration of the Vermilion River caused it to exhibit a very complex and dynamic flood response. During normal river stages, the Vermilion River collects inflows from the different tributaries and transports them downstream (south) into the Vermilion Bay. However, the river becomes bidirectional during extreme rainfall events and shows a reverse flow along a certain reach towards the north, where it drains into the Bayou Tortue swamps. The division point location for flow downstream (toward the Vermilion Bay) and flow upstream (towards the Bayou Tortue swamps) depends on the severity of the rainfall event. During high frequency, less extreme events, the bidirectional flow often initiates where Coulee Mine enters the Vermilion. If the storm event is extreme enough, then a further-downstream change in bidirectional flow division in the Coulee Ile des Cannes/Isaac Verot Coulee reach of the Vermilion River may occur. In each case, flooding of residences and businesses on the floodplain within Lafayette city and upstream, northeast, of Lafayette along the Vermilion River and its tributaries may result. The migration of the division point in the reach extending between Coulee Mine and Coulee Ile des Cannes suggested that the coulees that drain into the Vermilion in this reach,

including Coulee Mine and Ile des Cannes, play an essential role in the river hydrodynamics. These coulees, namely; Coulee Des Poches, Coulee Mine, Coulee Isaac Verot, Coulee Ile des Cannes, and Anslem Coulee drain a major portion of the impermeable surface of the city of Lafayette, resulting in it being very flashy and delivering an early surge of water to the river. It is worth mentioning that Anslem Coulee is located downstream of Coulee Ile des Cannes. However, it shares a significant number of lower-order streams with Coulee Isaac Verot that make it necessary to be included in any analysis performed on Coulee Isaac Verot. Observations on river stage and streamflow are available at four locations within the model domain (Figure 4 1). Stage measurements are available at three road crossings over the Vermilion, namely Surrey, Hwy733, and Perry, while the fourth location is just upstream of the inlet control gates of Ruth canal. Streamflow (flow rate) data are available only at Surrey and Perry gauges.

4.2.2 Hydrodynamic Model. In this study, the Hydrologic Engineering Center's River Analysis System (HEC-RAS) is used to simulate the impact of different simulation scenarios. The model domain encompasses a total of 88 km of the mainstream of the Vermilion River, starting at its headwaters, where a flow hydrograph from the Fusilier weir provides an upstream boundary condition and terminates at its intersection with GIWW. Despite the absence of a gauging station at the intersection of the Vermilion River with the GIWW, a station that belongs to the Coastal Reference Monitoring System (CRMS) gauges network exists approximately 1.5 km northeast of the intersection. Water-stage data is collected from this station, Station ID: CRMS0552, and is used in the model as a downstream boundary condition.

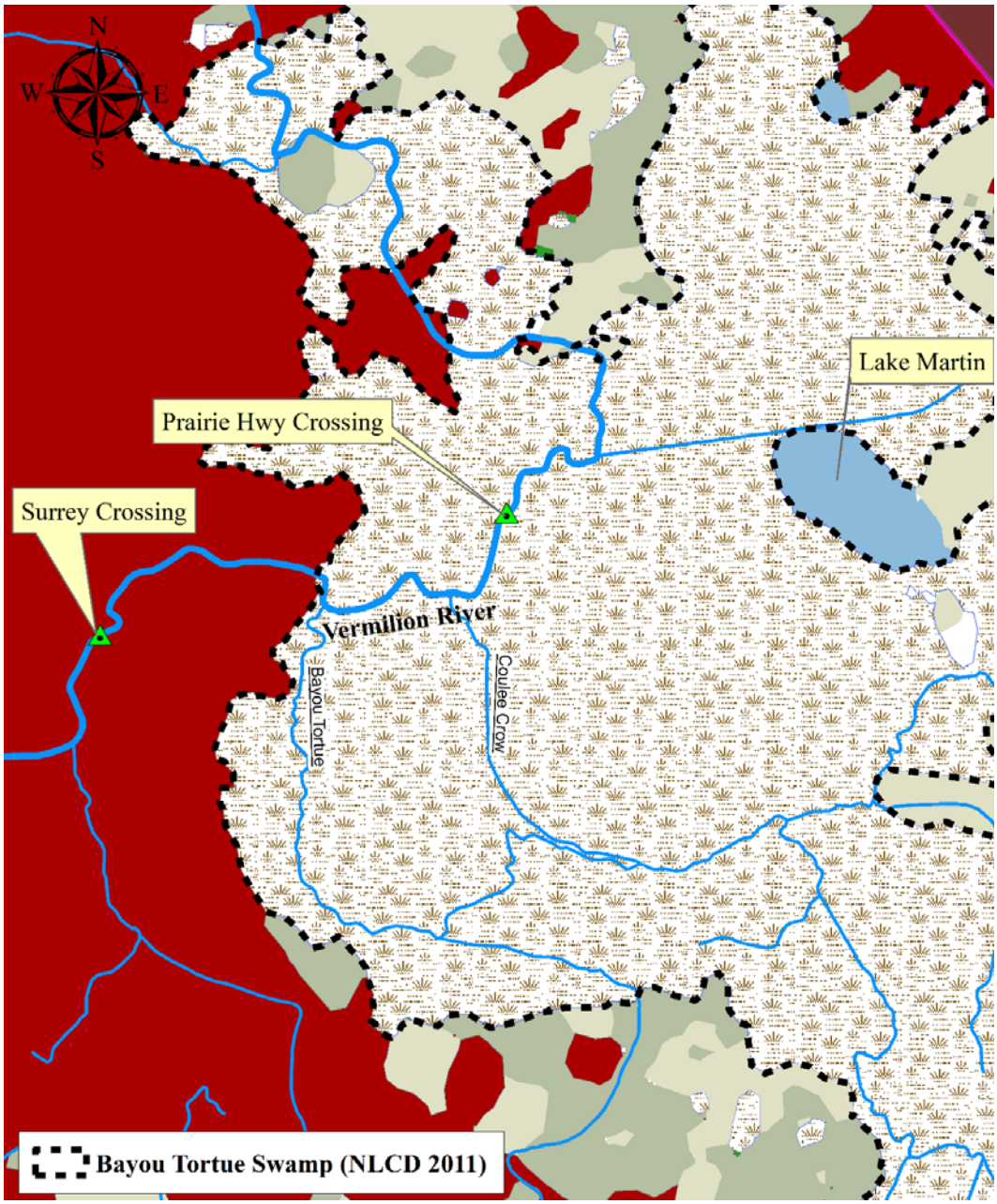

Figure 4-2: Close-up view on the Bayou Tortue swamp with the two Coulees Bayou Tortue and Coulee Crow.

This study modeled the mainstream of the Vermilion River with a hybrid 1D/2D representation. In the 1D part of the model, the Vermilion River mainstem is represented as a sequence of 1396 cross-sections that covers the whole length of the Vermilion river in a direction perpendicular to the longitudinal flow direction of the river. Despite that the 1D flow assumption is not entirely accurate in reality, the well-defined, narrow, and steep-sided

channel of the Vermilion River (Kinsland and Wildgen, 2006) validates, with acceptable accuracy, the 1D characterization for the Vermilion River in flood hydrodynamic studies.

The 2D part of the developed model consists of eight 2D Flow areas, which combined define the extent of the Bayou Tortue Swamp system. The 2D allows water to move in both longitudinal and lateral directions, while velocity is assumed to be negligible in the z-direction. However, unlike 1D models, these models represent the terrain as a continuous surface through a mesh or grid. This study used the ability of HEC-RAS to generate an irregular unstructured mesh and developed 2D computational meshes with varying resolutions ranging from 30m to 90m for the swamp area as necessary. Even in areas with relatively coarse computational grid, a good representation of the swamp hydrodynamics is achieved due to the HEC-RAS implementation of a sub-grid approach that uses a relatively coarse computational grid and more refined scale information of the underlying topography (Brunner, 2016). To further refine the 2D meshes in areas critical for the accurate simulation of overland flows, break lines have been used to enforce key features of the terrain and ensure that the model reasonably simulates the movement of overland flow. This includes break lines along recognized channels that concentrate flows and ridgelines that allow flows to spill from one area to another across features such as road embankments, levees, and natural ridgelines. The 1D and 2D parts of the model are coupled by setting up a lateral connection. This lateral connection is hydraulically represented in the model as a weir structure, and the flow over the structure is determined using the weir equation or 2D flow equations. Seeking a more stable model, this study used the standard weir equation to calculate the flow over the lateral weir. During the unsteady flow simulation, the solution algorithm allows for direct feedback at each time step between the 1D and 2D flow elements,

which enables a more accurate calculation of headwater, tailwater, flow, and any submergence that occurs at the hydraulic structure on a time-step-by-step basis. The developed hybrid 1D/2D scheme allows working on a more extensive river system, such as the case of the Vermilion River, through implementing the 2D modeling only in the areas that require a higher level of hydrodynamic flexibility.

4.2.3 Digital Terrain Model. The study adopted a previously-developed improved digital elevation model of the Vermilion River and the surrounding region to reflect the existing conditions of the bathymetry for the river and Bayou Tortue swamp. The improved digital elevation model integrated multiple sources of river bathymetry and floodplain topography. The bathymetric data primarily comprised the routine hydrographic surveys performed by the US Army Corps of Engineers (US Army Corps of Engineers, 2015) to monitor conditions of major navigational channels. The data collected for the bathymetry used the USACE survey conducted for the Vermilion River and Vermilion Bay during the 2015 period. Wherever the USACE survey data was unavailable, the bathymetric data were collected from the local cross-sectional surveys of the river included in the tributary hydraulic models developed earlier as part of the FEMA program on flood insurance rate maps for the Vermilion River.

The floodplain topography was extracted from the Louisiana Statewide LIDAR high-resolution elevation data Project. A 5-m horizontal resolution characterizes this LIDAR dataset with a vertical accuracy of ~ 15–30 cm RMSE (Cunningham et al., 2009). Finally, the bathymetric data for the Vermilion River corridor, in addition to the floodplain topography, were merged and hydrodynamically corrected, producing the improved digital elevation model. With the improved digital elevation model, the topographic information required

along the 1D cross-sections and at the 2D cells to run the hydrodynamic model is extracted, and a topographic scenario referred to hereinafter as a baseline scenario that represents the existing conditions is established.

4.2.4 Simulation Scenarios. This study aims to evaluate the significance of different attributes of the Bayou Tortue swamp on the flood dynamics along the Vermilion River and within the swamp area itself. Despite that the role of the swamp as a whole was investigated in previous research (Saad et al., 2020), the relative significance of factors such as the size of the available storage in the swamp, the role of the spoil banks that separates the river from the swamp and acts as a spillway during the flooding conditions, and the network of coulees that connects the swamp with the river is still not fully established. The study examined three different simulation scenarios.

4.2.4.1 Effect of Swamp Storage (Scenario A). The first scenario, Scenario A, includes enhancing the available storage volume of the swamp. As the Vermilion River crosses Prairie hwy traveling towards the City of Lafayette, it travels for ~1.5kms within the Bayou Tortue swamp areas before reaching the northern boundary of the City of Lafayette. This reach, more specifically the left-side banks of the Vermilion River, beholds the most floodwater exchange with Bayou Tortue swamp during moderate and extreme storm events. The proximity of this area to the City of Lafayette, the narrow bayous that allow for easier water exchange with the swamp (Coulee Crow and Bayou Tortue), the low elevations of the spoil banks of the Vermilion River, and the low-lying elevations inside the swamp itself along this reach, combined led for this particular southern reach to play an active role in the flood relief of the Lafayette City and flood dynamics in the river. However, the bathymetry of the swamp on this left-side of the river, observed through the Lidar, clearly shows that the

bottom elevation of the swamp is divided into two main low-lying compartments that are separated by a natural high ground ridge (

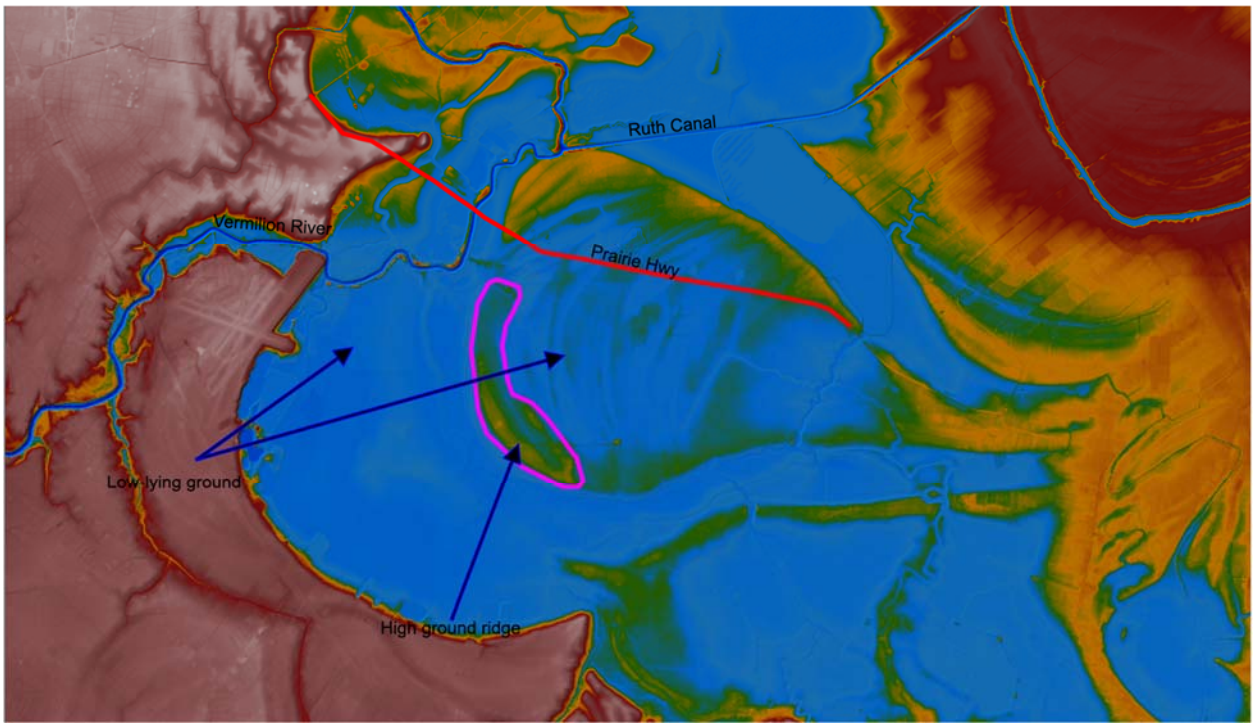

Figure **4-3**). The study considered removing this high ground barrier through excavation, aiming to ease the water flow between the two storage compartments and enhance the storage capacity of the swamp overall to allow for more flood relief from Vermilion River into the swamp.

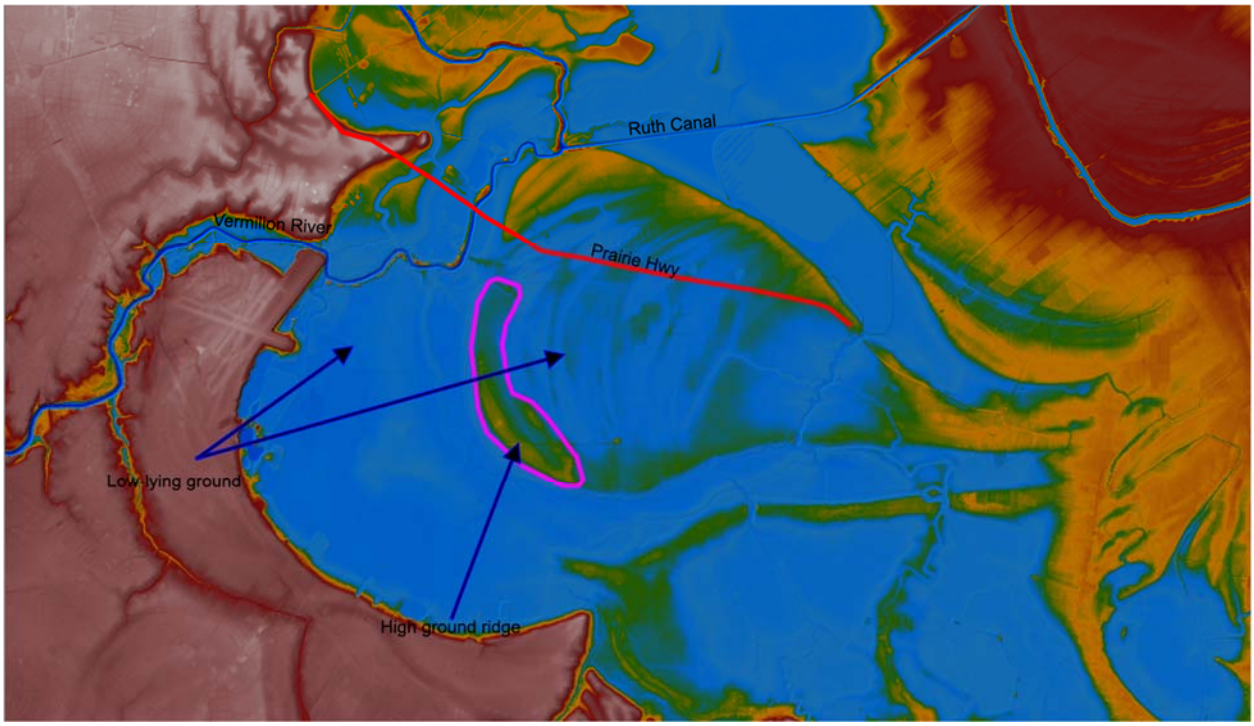

Figure 4-3: General Layout of the Bayou Tortue swamp showing the area to be dredged.

4.2.4.2 Effect of river-swamp connectivity through overbank flows (Scenario B).

The second scenario, scenario B, considered adjusting the heights of the southern portion of the spoil banks reach that extends for ~1.5km on the left-bank-side of the Vermilion River (**Figure 4-4**). The LiDAR data clearly shows the spoil banks bordering the Vermilion River and the Bayou Tortue swamp with an existing average elevation of +5.00m (NAVD88 datum). The study proposed lowering the heights of the southern spoil banks on the left-hand side to elevation (+3.00 NAVD88) for approximately 1km of the spoil banks' length. Scenario B seeks to manage the overflow level in the Bayou Tortue Swamp's southern portion by lowering the spoil banks elevation so to allow the river to exploit the Bayou Tortue swamp's detention storage capacity early on once the river's water level reaches elevation +3.00 in contrast to +5.00 as it is under the current conditions. **Figure 4-5** shows a sample cross-section across the Vermilion River that designates the spoil bank's current and proposed target elevation.

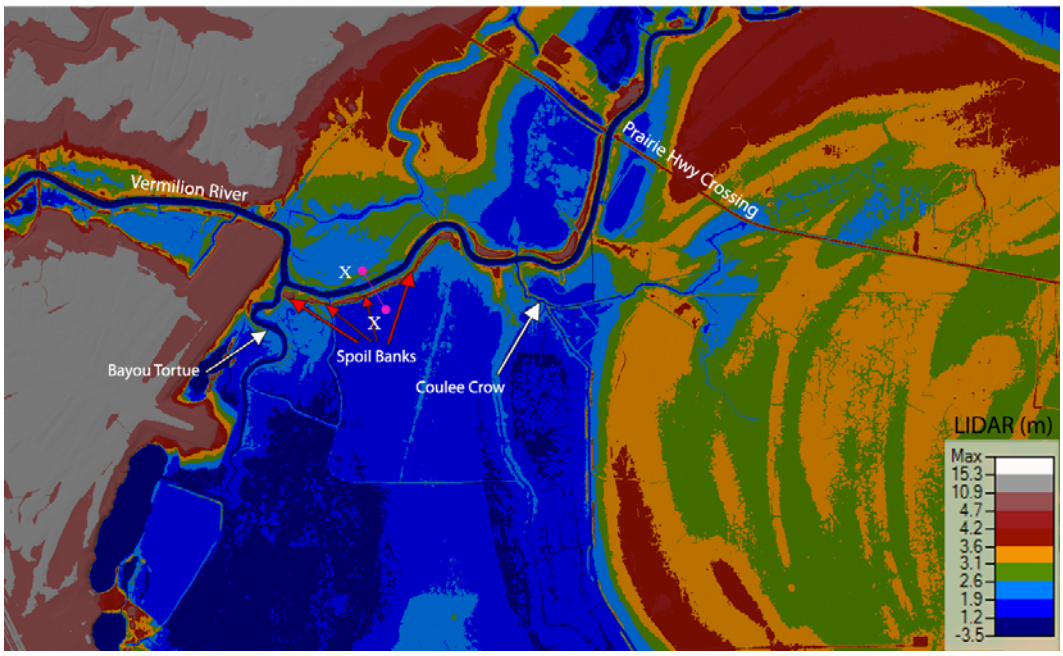

Figure 4-4: Map of the Vermilion River reach crosses through the Bayou Tortue swamp. The map shows the spoil banks that border the Vermilion River on the left side along this reach with the location of the X-X sample cross-section. The background is the LiDAR elevations for the reach between Prairie Hwy and the northern boundary of Lafayette.

4.2.4.3 Effect of river-swamp connectivity through lateral channels (Scenario C).

Finally, the third scenario, Scenario C, aimed to test the impact of the stream drainage network that connects the Vermilion River and the Bayou Tortue swamp. The scenario includes testing the alteration of the bathymetry of the two coulees, Coulee Crow and Bayou Tortue Coulee (**Figure 4-2**), that drain the swamp area into the Vermilion River. The bathymetry for these two coulees used in the baseline scenario is adopted from the Louisiana Statewide LIDAR high-resolution elevation data. The Louisiana Statewide LIDAR high-resolution elevation data project performed post-processing analysis on the captured raw lidar data to remove the forest canopy and any manmade features that prevented the laser beam from reaching bare earth. (Cunningham et al., 2009).

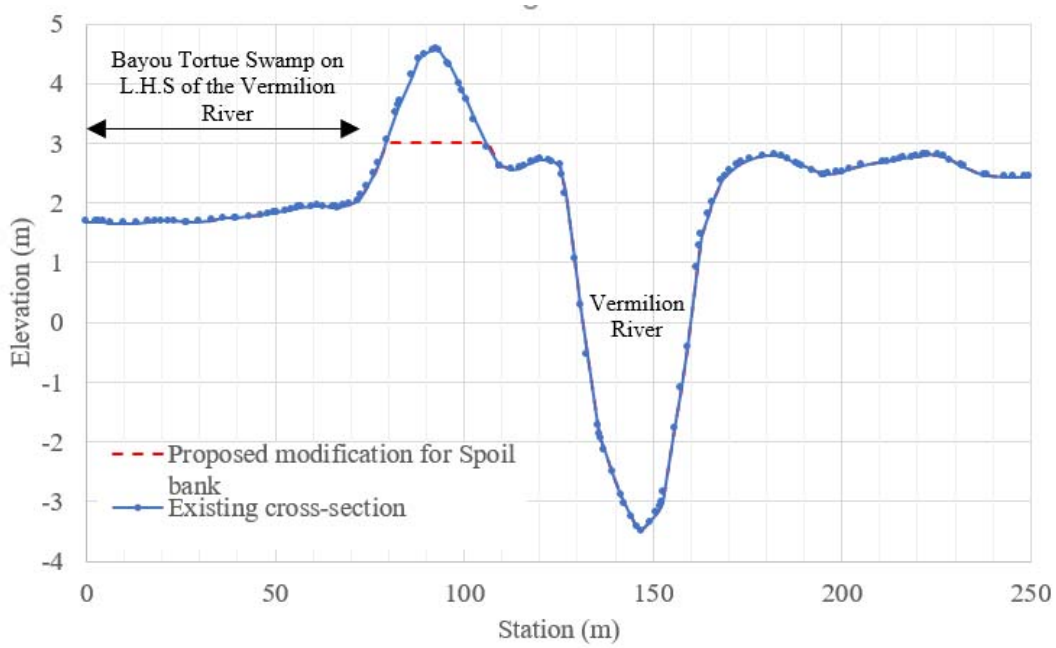

Figure 4-5: X-X sample cross-section across the Vermilion River showing the existing spoil banks located on the left-hand side of the river (looking downstream) proposed to be lowered under scenario B.

Performing this post-processing stage produced a map of the topography with the best possible representation of Bayou Tortue swamp topography and the bathymetry of Coulee Crow and Bayou Tortue Coulees. However, an older USGS report (Baker, 1988) that studied the hydrologic features and processes of the Vermilion River included some cross-sectional surveys for the bathymetry of Coulee Crow, and Bayou Tortue Coulees collected during the year 1985. The survey shows deeper cross-sections for these two coulees compared to the LIDAR model representation of the coulees. In the effort of investigating the significance of the uncertainty that underly the bathymetry information of the drainage network within the swamp, scenario C adopted the survey extracted from the USGS report for both coulees and ran the simulation events using this modified survey.

4.2.5 Simulation Periods. This study examined two flood events that occurred during 2014 and 2016. The first event occurred when a series of rainfall storms started on the 28th of May, 2014, when a late-season cold front and slow-moving upper-level system moved into the region (NCEI, 2015). The front pulled down deep atmospheric moisture across the area and caused heavy rain that lasted two days, resulting in widespread flooding. During these two days, the storm dropped a total rain accumulation of 220 mm with a maximum hourly intensity of 37 mm/hr. During this event, the maximum observed stage at Surrey, Hwy733, and Perry stations were 3.25, 3.38, and 1.88 m, respectively. These stages exceeded the flood stage of 2.21 m at Surrey station, as reported by the National Weather Service, causing significant flooding where lateral coulees meet the Vermilion River (AHPS, 2018). Additionally, the event is classified as a 10-yr return period flood based on the flood frequency analysis performed by the Federal Emergency Management Agency (FEMA) (FEMA, 2018) for the Vermilion River.

The second event took place in August 2016. During August 11–14, 2016, a slow-moving and low-pressure system accompanied by a high amount of atmospheric precipitable water (van der Wiel et al., 2017) resulted over Louisiana and southwestern Mississippi in an exceptional amount of rainfall of 20 to more than 31 inches (Watson et al., 2017). This event caused the river stages to rise and peaks to exceed the previous maxima formerly recorded at 10 USGS streamflow-gaging stations. During this event, the maximum observed stage at Surrey, Hwy733, and Perry stations were 4.54, 6.07, and 3.14 m, respectively. Accompanying this, historic flooding in numerous stream basins in Louisiana occurred, and many rivers, including the Vermilion River, witnessed spread, severe and long-duration flooding (Watson et al., 2017). The storm is considered to be around 500 years return period

is classified as a 100-yr return period flood based on the flood frequency analysis performed by the FEMA for the Vermilion River (FEMA 2018).

The study selected the May-2014 and August-2016 events to assess the impact of different scenarios because they represent a wide range of rainfall intensity. The 2016 event represents a heavy rainfall event (100-year) that spatially covered a large-scale extent of the Vermilion watershed, while the 2014 event represents a smaller, more frequent rain event (10-year).

The stage and streamflow hydrographs observed during both events clearly illustrate the reverse flows within the Vermilion River and the prolonged recession that continued for several days after the end of the rainfall storm.

4.3 Results

4.3.1 Effect on Flow Regime in the Main River. Figures 5 and 6 show the simulated longitudinal profile of the water surface elevation along the Vermilion obtained during the peak for the two simulation periods, May-2014 and August 2016. In general, the results of the different scenarios show a reduction in the water surface elevations along the river compared to the baseline scenario.

During the August 2016 period, maximum reductions obtained in water surface elevation were 0.063, 0.025, and 0.69 m for scenarios A, B, and C, respectively. Smaller reductions (almost null, 0.2, and 0.22 m) were obtained during the more-frequent storms of May-2014. The results from both events suggest that the maximum reductions are more significant in the reach of the river between the Surrey crossing (~km 72) and Prairie Hwy

crossing (~ km 82). However, such water surface elevation reductions also extended along the river downstream the swamp reach.

The results suggest the maximum water surface profile reduction under scenarios B and C extended downstream to reach approximately ~ 25 Km and 50 Km of the river during the May-2014 and August-2016 events, respectively. Moreover, the results show that scenario C's flood elevation reduction benefits also continued until ~km 90 upstream during the August-2016 event. Interestingly, Scenario A, which included maximizing the storage capacity of the swamp, despite being a typical flood mitigation measure, showed the least significant flood elevation reduction impact on the Vermilion River compared to scenarios B and C. This implies that the currently available storage capacity of the Bayou Tortue swamp is not a limiting factor on the flood control role of the swamp, and the flow restrictions caused by the lateral connectivity structures that control the flow exchange between the river and adjacent swamp did not allow the river to benefit from the enlargement added to swamp size.

In addition to examining the impact of altering different attributes of the swamp area on the longitudinal profile of the river's main stem, it is also of interest to assess this impact across time as the storm event progresses. To do so, the stage and flow hydrographs are extracted at three key locations along the river: Km 72 (At Surrey crossing, which is located downstream of Bayou Tortue), Km 77 (which is located halfway between Bayou Tortue and Coulee Crow), and Km 82 (which is at Prairie Hwy crossing located upstream of Coulee Crow).

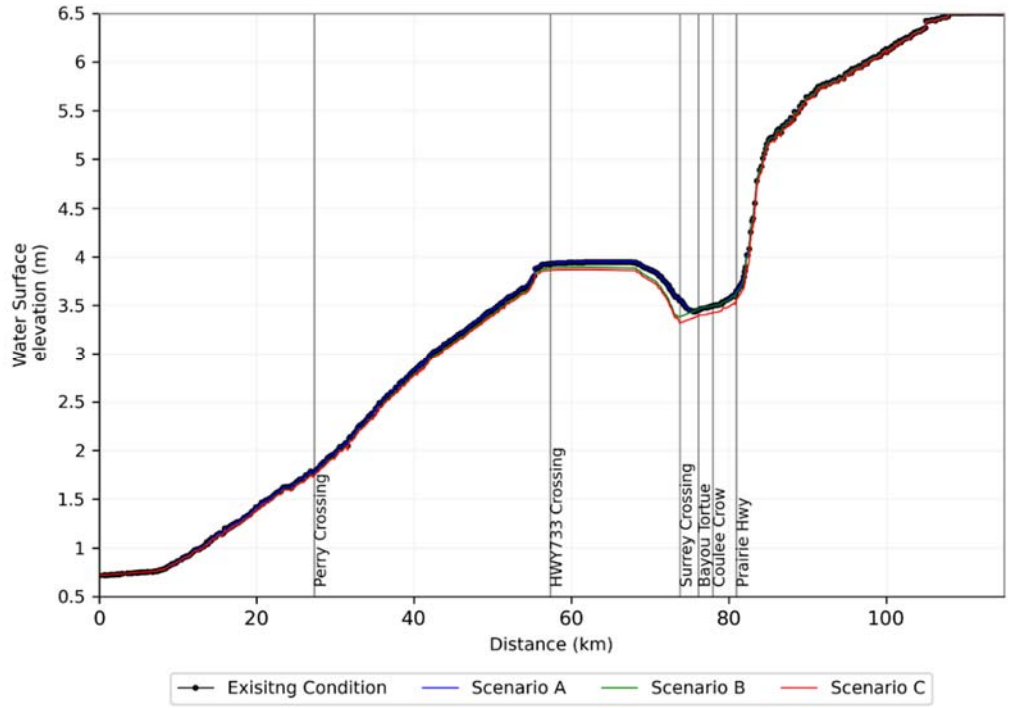

Figure 4-6: Longitudinal profiles of maximum water surface elevation (WSE) during the 2014 event. Distance is in km from the mouth of the river in the upstream direction. (The bottom elevations of the river are removed for clarity purposes)

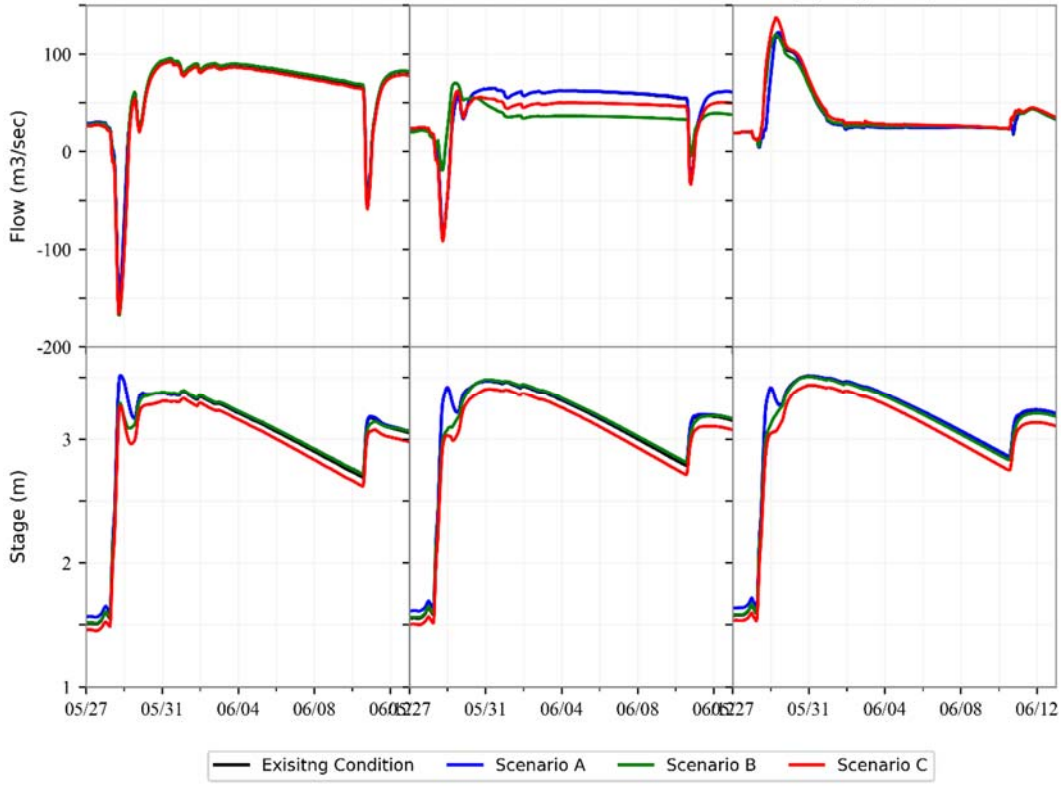

Figure 4-7: Stage and Flow hydrographs at three locations (km 72, 77, and 79) along the Vermilion River during the 2014 event.

The hydrographs were extracted for both simulation periods of May-2014 and August-2016 and presented in **Figure 4-7** and **Figure 4-9**. Several remarks can be inferred by investigating these two figures. First, the flow hydrographs at Surrey crossing reveal that, despite the reduction in the maximum water surface profile, all scenarios did not show any noticeable impact on the reverse flow phenomenon in the downstream reaches of the Vermilion River during both events, May-2104, and August-2016. The flow hydrographs simulated under each proposed scenario are similar in timing and peak value to the baseline scenario. This observation implies that the downstream reaches of the Vermilion River did not send additional floodwater volume towards the swamp area during any of the moderate or extreme events under any proposed scenarios and that the different modifications included in all scenarios only decreased the hydraulic gradient needed to drive the water flow towards the swamp causing a reduction in the water stage along the river with various degrees.

Examining the stage hydrographs at Surrey crossing during both events, May-2014 show that the gradient of the recession curve of the hydrograph is of the same magnitude for all scenarios to the baseline scenario. With the assumption that the swamp is the main supply of water right after the storm recedes, this observation suggests that, during more frequent storms such as May-2014, the rate at which the swamp drains into the Vermilion River did not change regardless of the scenario under investigation. However, during extreme events such as August-2016, increasing the flow capacity of Bayou Tortue and Coulee Crow caused the gradient of the recession curve to be steeper than the baseline scenario indicating that less volume of water was drained back to the river from the swamp during this phase of the storm. Such conclusions are also confirmed when investigating the falling limb of the flow

hydrographs at Surrey crossing during August-2016, where a reduction in the amount of flow is noted.

Investigating the flow and stage hydrographs at Prairie Hwy crossing (km 82), the results show a negligible impact for scenarios A and B during both simulation periods. Only Scenario C, through maximizing the flow capacity of Bayou Tortue and Coulee Crow, caused an increase in the peak flow heading towards the swamp from the northern sub watersheds by 14% and 45% during May-2014 and August-2016 respectively. Remarkably, such an increase in the upcoming flow did not translate into a corresponding increase in the maximum water stage, but the peak water stage dropped by 0.1 m and 0.18 m compared to the baseline scenario.

4.3.2 Effect on the Flow Exchange between the Swamp and the Main River.

Figure 4-10 and **Figure 4-11**demonstrate the simulated hydrographs of the flow exchange between the Vermilion River and the Bayou Tortue swamp during both May-2014 and August-2016 for all proposed and baseline scenarios. The figures are designed to include three panels, where the top one shows the flow exchange that occurred overtopping the spoil banks that extends between Bayou Tortue and Coulee Crow, while the middle and bottom panels show the flow exchange through Bayou Tortue and coulee crow, respectively.

Considering the baseline scenario, the results obtained from both simulation events show that the spoil banks play a primary role in the flow exchange between the Vermilion River and swamp compared to the Bayou Tortue and Coulee Crow under the existing conditions. The peak flow that overtopped the spoil banks into the swamp was 112 and 267 m3/s during the May-2014 and August-2016 events, respectively.

Concurrently, the simulations show a secondary role for both Bayou Tortue and Coulee crow in the flow exchange as the peak flows carried by these two coulees were found to be 25 and 21 m3/s (during the May-2014 event) and 92 and 87 m3/s (during the August-2016 event) respectively. This remark suggests that the spoil banks are of greater significance than the two coulees combined for the flow exchange between the main river and the swamp. However, introducing the modification that included increasing the conveyance of both coulees in scenario C seemed to reverse the relative importance of the spoil banks and the coulees in terms of the flow exchange. Results from scenario C show that the flows that traveled through Bayou Tortue from the Vermilion River to the swamp were 290 and 300 267 m3/s during the May-2014 and August-2016 events, respectively, compared to 135 and 295 m3/sec which are the peak flows simulated under scenario C to overtop the spoil banks during the same events.

Examining figures (10 and 11) reveals some consistent similarities in the performance of the floodwater dynamics under both events, May-2014 and August-2016. First, all proposed scenarios, except for scenario A, amplified the amount of flow that got diverted from the main river into the swamp area during the storm period (the positive values of flows shown in the hydrograph). For scenario A, which included maximizing the storage size available within the swamp area, the results show an insignificant change in the flow exchange between the main river and the swamp as the flow hydrographs simulated under this event completely coincided with the baseline scenario for the whole simulation period. This observation agrees with the remark made in the previous section that the currently available storage within the swamp has not been exhausted in either of the two events and

that increasing the size of storage inside the swamp is deemed ineffective because it is not critically needed.

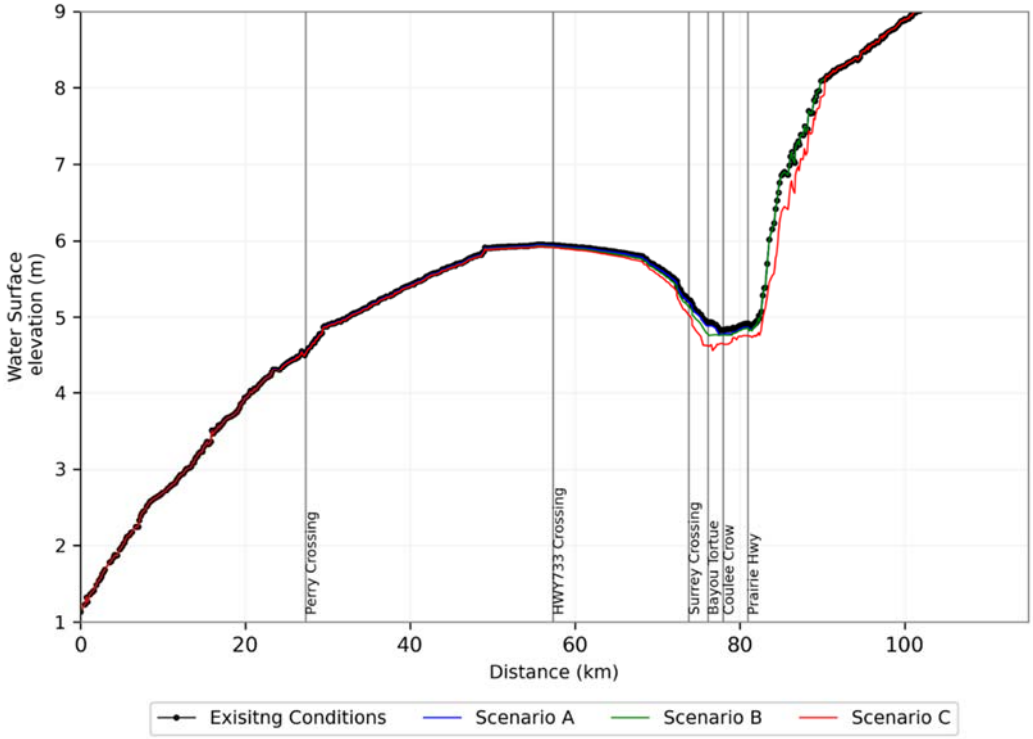

Figure 4-8: Longitudinal profiles of maximum water surface elevation (WSE) during the 2016 event. Distance is in km from the mouth of the river in the upstream direction. (The bottom elevations of the river are removed for clarity purposes)

Regarding the flow exchange that occurred overtopping the spoil banks (top panels in the figures), the results show that scenario B, which included lowering the height of the spoil banks, increased the peak positive (river-to-swamp) flow of exchange by ~ 94% and 47% during the May-2014 and August-2016 events, respectively. Interestingly, Scenario C, which only involved increasing the cross-section of both coulees Bayou Tortue and coulee crow, also increased the peak positive flow overtopping the spoil banks by ~ 23% and 11% during the two events. This increase can be attributed to the increase in the approach velocity head attained by the flowing water inside the Vermilion River upstream of the spoil banks resulting from the improved flow circulation that occurred along this reach of the Vermilion River following the enhanced flow capacity the lateral drainage network.

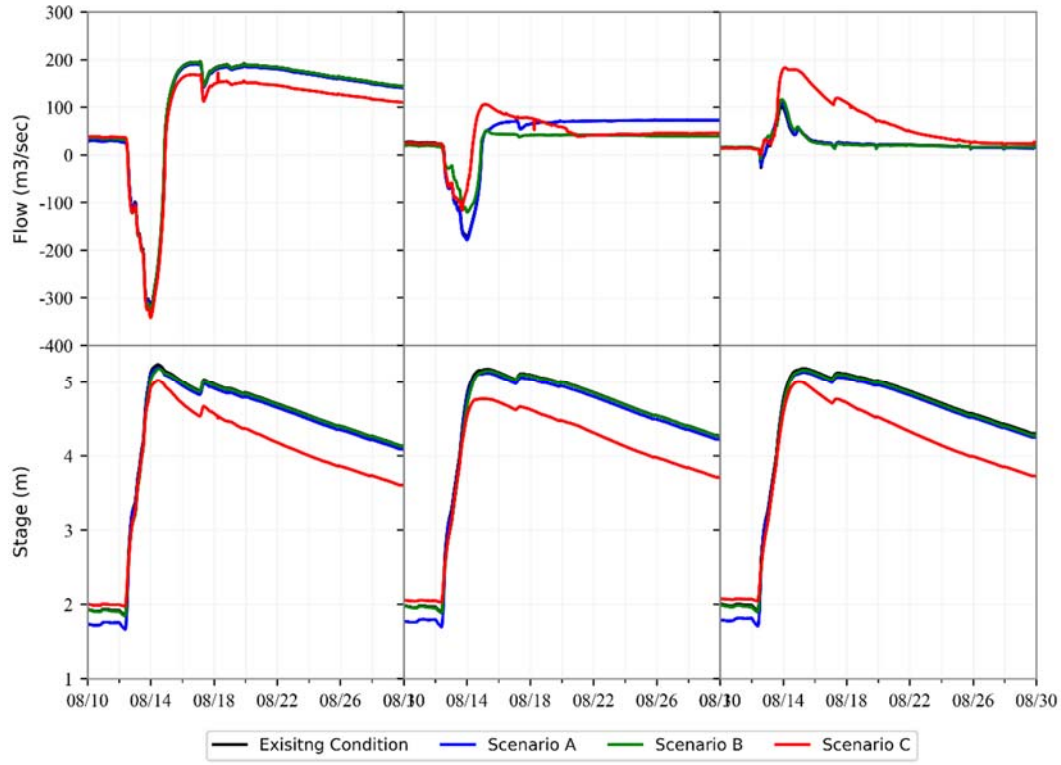

Figure 4-9: Stage and Flow hydrographs at three locations (km 72, 77, and 79) along the Vermilion River during the 2016 event.

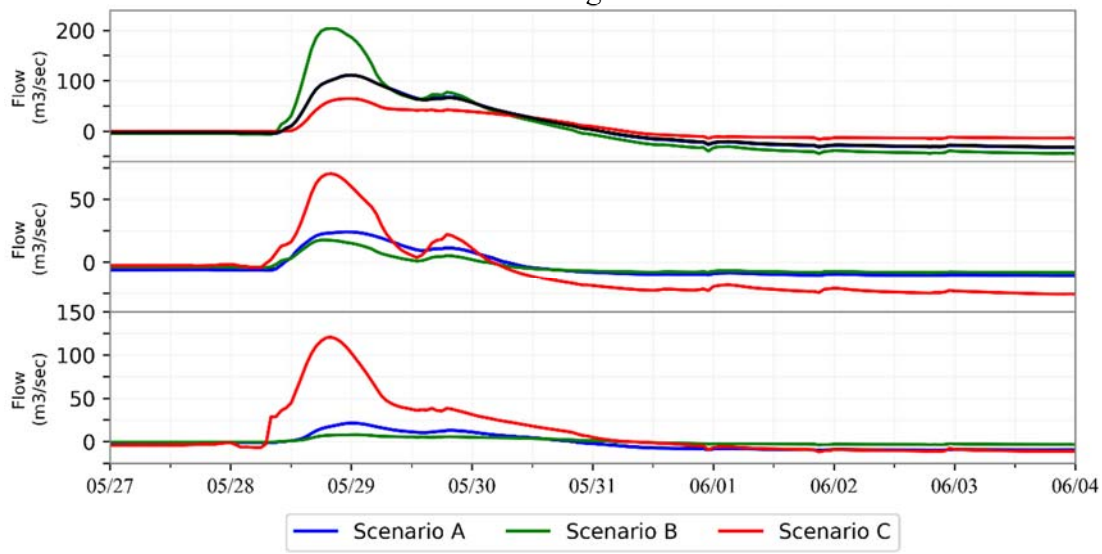

Figure 4-10: Stage and Flow hydrographs at Surrey crossing for all proposed and baseline scenarios during the 2014 event. (Top panel) Flow exchange overtopped the spoil banks between Bayou Tortue and Coulee Crow. (Middle panel) show the flow exchange through Bayou Tortue while (Bottom panel) show the flow exchange through coulee crow.

The results obtained under scenario C show a significant increase in the swamp-to-river flows (negative flows) that occurred after the storm receded during the August-2016

event. The results show that the flow overtopping the spoil banks back to the river increased to 712 m3/sec instead of 95 m3/sec in the baseline scenario. Given the severity of the August-2016 event being >100 years storm event, the excessive amount of flow that is drained from the river into the swamp under scenario C increased the amount of stored floodwaters within the swamp area compared to the baseline scenario. The very flat representation of the swamp topography altered the flow paths of the returned swamp-to-river flows and made it unnecessary for the flow to follow the same path it took to enter the swamp, explaining the reason behind the increase of the flow overtopping the spoil banks.

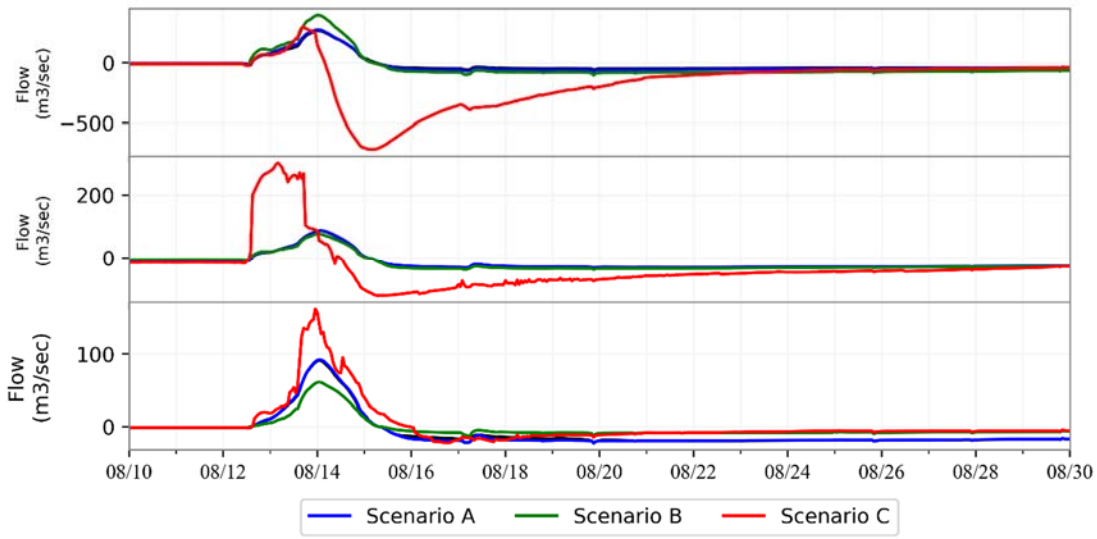

Figure 4-11: Stage and Flow hydrographs at Surrey crossing for all proposed and baseline scenarios during the 2016 event. (Top panel) Flow exchange overtopped the spoil banks between Bayou Tortue and Coulee Crow. (Middle panel) show the flow exchange through Bayou Tortue while (Bottom panel) show the flow exchange through coulee crow.

Let us consider the flow exchange through Bayou Tortue and coulee Crow shown in the middle and bottom panels in Figure 4-10 and Figure 4-11. The results suggest that increasing the flow capacity of the coulees by applying a wider cross-section for both led to a significant increase in the flow exchange between the swamp and the Vermilion River. This was expected as a typical response to the increase in the size of cross-sections of the coulees.

However, the results show different behavior in the negative flow that drains from the swamp toward the Vermilion River. During May-2014, no significant increase in the amount of the negative flow from the swamp to the river was obtained, despite the increase in the positive flow. This behavior suggests that during more frequent storm events such as in May-2014, the flow that goes into the swamp gets dispersed within the flat area of the swamp and may not necessarily return back to the river. However, during extreme events such as August-2016, and due to the heavy amount of flows that go into the swamp area, part of such flow finds its way back to the river during the recession period causing an increase in the amount of the negative flow exchange between the swamp and the river.

4.3.3 Effect on the water stage inside the swamp. In addition to examining the impact of modifying different swamp area attributes on the river's main stem, it is also of interest to assess the propagation of such impact into the swamp area that receives water from the river. The stage hydrographs at the centroid point of the swamp were sampled from each scenario during both events May-2014 and August-2016 (**Figure 4-12** and **Figure 4-13**). It is worth noting that there is nothing specific about the centroid of the swamp that led us to choose it for comparison; however, the same observation was drawn from six different points across the swamp area, and the results from all points came out to be consistent. Accordingly, and to avoid repetition, we chose to show the results drawn only at this specific point.

Generally, the modifications included in the different scenarios, except for scenario C that involved increasing the flow capacity of Bayou Tortue and Coulee Crow, did not show any significant change in the peak water surface elevation attained during the simulation period of both events May-2014 and August-2016. However, during May-2014, lowering

the spoil banks (Scenario B) revealed a quicker drain of the water surface elevation as the recession limb exhibited a steeper slope before starting to rise again due to the June 2014 storm, as shown in **Figure 4-12**. Similar behavior was also encountered under Scenario C that increased the capacity of the two channels between the river and the swamp; however, the recession limb exhibited a more aggressive slope compared to scenario B. Such a quicker drop in the water surface elevation inside the swamp is a direct result of more floodwaters being drained back into the main stem of the Vermilion River after the storm recedes. Even though the stage hydrograph at km 77 of the main river, **Figure 4-7**, did not show any significant increase of water stage inside the river due to the excess amount of water coming from the swamp area, this result indicates that the river system can have more flood control benefits from more dynamic management of water storage inside the swamp area. For example, management that includes gates on the outlets of both Bayou Tortue and Coulee Crow can impose more control on the timing and quantity of floodwater released right after any storm event recedes.

The results obtained from the simulation of the August-2016 event, **Figure 4-13**, showed similar behavior to the May-2014 event results. However, given that August-2016 is an extreme event with an intense amount of rainfall that fell over the swamp area, the extra amount of floodwaters that went from the river to the swamp area during the storm caused the peak stage inside the swamp under scenario C to slightly rise by 0.08 m compared to the baseline scenario.

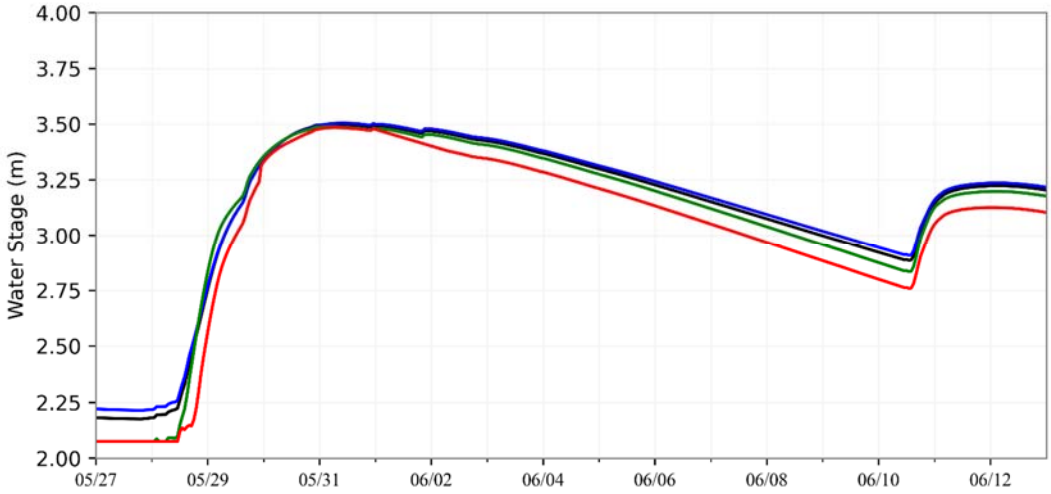

Figure 4-12: Water Stage Hydrograph at the point of centroid for Bayou Tortue swamp during the May-2014 event. The black line represents the baseline scenario while the blue, green and red lines represent Scenario A, B, and C respectively.

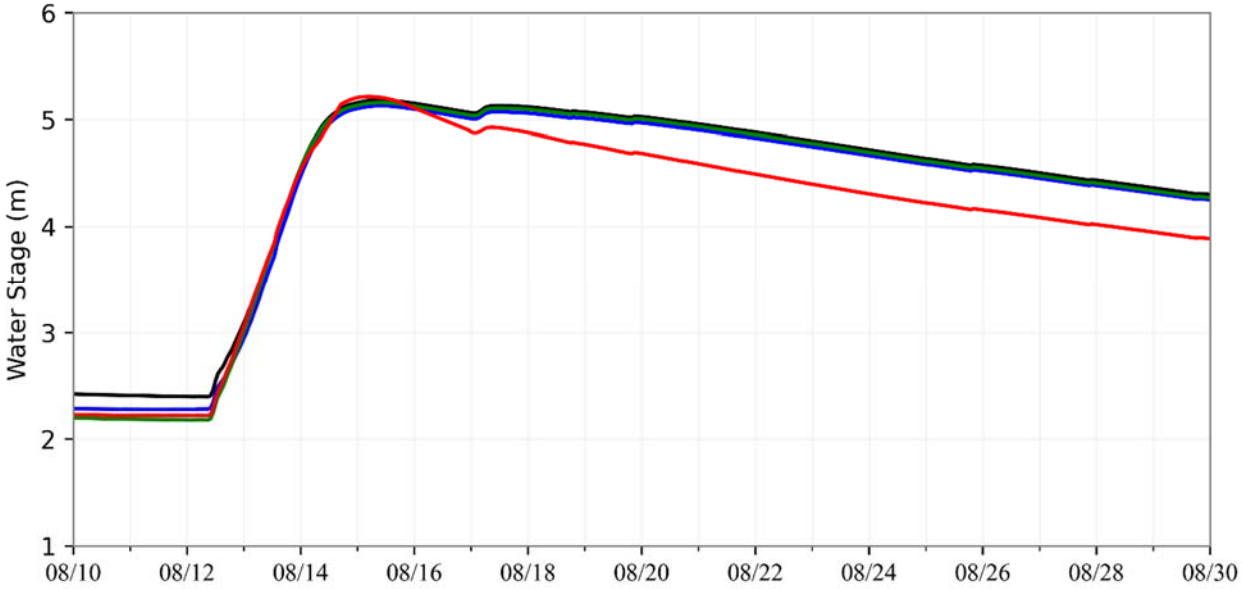

Figure 4-13: Water Stage Hydrograph at the point of centroid for Bayou Tortue swamp during the August-2016 event. The black line represents the baseline scenario while the blue, green and red lines represent Scenario A, B, and C respectively.

4.4 Conclusions And Recommendations

This study investigated the role of the attributes of a large natural storage area such as a connected swamp on flood dynamics in a low-gradient river system. The Vermilion River in southern Louisiana was chosen in the study as a representative of such systems. The Vermilion River has a long history of severe flooding since the major flood that occurred in

August 1940 until the most recent in August 2016. The presence of an on-channel large swamp system within its watershed, known as Bayou Tortue swamp, triggered complex flow dynamics along the river's main stem where frequent reverse (upstream) flows occur, allowing floodwaters to travel upstream for temporary storage in the swamps. The study examined the impacts of three different swamp-modification scenarios representing maximizing the storage capacity in the swamp, adjustment to the height of the spoil banks that separate the river from the swamp area and increasing the conveyance of the drainage network that laterally connect the river and swamp area. A hybrid 1D/2D numerical model was used to simulate the impact of these activities on the flow hydrodynamics along the main course of the river and the swamp itself. The analysis was performed on two flooding periods, May–June 2014 and August 2016, classified as <10-year and >100-year storms, respectively. The three different proposed scenarios were assessed by evaluating key characteristics of the flow regime, including changes in flow hydrographs at key locations along the river, reductions in water surface profiles, alterations to river-swamp flow exchanges, and impact on water stage inside the swamp. The results from each scenario were compared against those obtained under the existing baseline scenario. The following conclusions can be formulated based on the findings of the study:

1. Each attribute of an on-channel large natural storage area plays a role in the flood dynamics of a low-gradient river system; however, the significance of each attribute is a case-by-case dependent. For example, this study showed that enhancing the storage capacity of the natural storage area located along the Vermilion River did not show any extra flood mitigation benefit.

2. Scenarios that modified the lateral connectivity between the main stem of the river and the adjacent natural storage area impacted the river flow regime. Overall, the maximum water stage attained along the river was reduced even in reaches upstream of the swamp area where the flows traveling towards the swamp were amplified. Such impacts have significantly altered the flow exchanges between the river and the swamp, severed the river-to-swamp inflows, and increased the swamp outflows. This is expected to affect the hydroperiod of the swamp system and its residence time and may eventually affect its viability as a natural ecosystem.
3. The results reveal that the activities that can increase the hydraulic conveyance of the tributaries that laterally connect the river system with the swamp area have more significant impacts on the flood regime along the river than adjusting the heights of the spoil banks that separates the river from the swamp and controls the overflow exchange between the river and the swamp.
4. The flood control benefits for the river can be maximized by applying dynamic management of the flow exchange between the river and the swamp. A flood control management scheme that, for example, includes gates on the outlet of the coulees that drain the swamp into the main river would be able to control the release, in both timing and quantity, of the floodwaters from the swamp area into the main river during the recession limb of the storm event water storage inside the swamp area.

Chapter 5: Exploring the Progress and Implications in Coastal Hydrodynamic Modeling

5.1 Introduction

Understanding flood dynamics in coastal watersheds and the main drivers that control these dynamics is essential for designing proper flood mitigation measures. Such understanding is more eminent in watersheds located in low-gradient coastal areas where flood hazard is often more complex and challenging to model and study than in non-coastal watersheds with more significant topographic relief. Additionally, such understanding is necessary for integrated watershed-centered flood risk management approaches that incorporate the development of flood modeling tools. Besides the role these tools play in assessing current flooding conditions, they can be used over time to assess the impacts of climate variability and anthropogenic activities on flooding patterns. Several flood modeling techniques and flood control measures have been assessed in this study, and an adequate modeling framework that suits the conditions of low-lying coastal watersheds was developed. This chapter explains the significance of this framework and its future implications in low-gradient coastal environments by applying it over the Vermilion River watershed in south Louisiana as a case study.

5.2 The Economic Cost of Flooding

Coastal regions are vital for the advancement of society by supporting capital flows for tourism, industrialization, transportation, and urban development. Current projections for the United States (US) population in low-gradient coastal zones indicate that more than 1 billion are forecast to live in the coastal zone by 2060 (Neumann et al., 2015). In addition, the US has 17 port cities with a population greater than 1 million (Wahl et al., 2015). Extreme coastal flooding is one of the hazardous elements that pose a significant threat to

human life and infrastructure (Bates et al., 2005; Bhaskaran et al., 2014). Low-gradient coastal watersheds are vulnerable to flooding hazards from intense rainfall and coastal storm surge penetration, produced from extreme meteorological events (e.g., tropical cyclones, low-pressure systems). Hurricanes were responsible for 40% of the total global deaths for all weather-related disasters from 1995 to 2015 (CrED, 2015). Also, three of the five costliest hurricanes that have impacted the US mainland and its territories occurred in the 2017 hurricane season (NOAA, 2018). Hurricanes Harvey, Irma, and Maria affected the Texas and Louisiana coasts, the Florida peninsula, and Puerto Rico and the U.S. Virgin Islands, respectively, in less than a month. These three hurricanes produced total damage of $265 billion (2017 USD) and were directly responsible for the loss of 183 human lives (NOAA, 2018). These natural hazards can be devastating with wide-ranging social (Comer et al., 2017; Olbert et al., 2017), economic (Karamouz et al., 2015; Wang et al., 2015), and environmental (Park et al., 2011) consequences in low-gradient coastal watersheds around the world.

The long history of flooding, often poorly understood and understudied flood dynamics of low-lying coastal watersheds, the uncertain climate projections, and the recent higher frequency of compound flooding are all factors that call for watershed management that goes beyond conventional mitigation measures. This study bridges this gap and lays down the foundation for developing flood models to understand flood risk better and help select mitigation projects best suited for investment in coastal watersheds that have been long-suffering from such a lack.

5.3 Enhancing Flood Hazard Assessments in Coastal Louisiana

The great Louisiana flood of 2016 resulted in immediate and lingering flooding impacts that exemplify a need to understand better the interplay between hydrologic, riverine, off-coast tidal, and surge processes. The storm-induced overland and riverine flows resulted in prolonged flooding that lasted almost a month after the extreme rainfall event receded (USGS, 2016). Significant runoff contributions from the tributaries, in addition to the relatively elevated water stages in the gulf produced severe backwater flooding that led to inundation in dense urban regions. Areas in the southern parts of the watershed are also vulnerable to hurricane storm surges, which warrants consideration of the contribution from both overland and coastal flows to flood hazards and, ultimately, flood risk (Wu et al., 2018).

Historically events resulting in complex interactions between rainfall- and coastal-induced flooding have occurred. An example of that is the devastation of Hurricane Ike that was exacerbated by having Gustav hit Louisiana 12 days prior. Hurricane Harvey (2017) caused record rainfalls (1,539 mm) in Texas, along with a 3m coastal storm surge (Blake and Zelinsky, 2018). Similarly, Hurricane Florence (2018) caused 3m surges along the North Carolina coast, with over 900 mm of rainfall (Bilskie et al., 2021). Hurricane Laura (2020) was the tenth-strongest, by windspeed, U.S. hurricane to make landfall on record. The effects of Laura across Louisiana were devastating. Nearly 3.5m of storm surge was recorded in Cameron Parish, in addition to a total of 203mm of rainfall. A better understanding of flood dynamics in coastal watersheds is needed to better prepare for such outcomes. Flood models that incorporate overland and riverine flood processes from rainfall-runoff (including antecedent conditions) and a representation of tropical cyclone (TC) induced storm tides

(presented in adequate boundary conditions) can fill such gap, especially under uncertain future climates (Santiago-Collazo et al., 2019)

A shortcoming of most coastal flood studies (both return period and risk analyses) assumes that coastal and fluvial floods are mutually exclusive events (Santiago-Collazo et al., 2019). Damage caused by recent TC and unnamed storm events (e.g., August-2016 flood) that resulted in compound floods has pushed the research community to work on improved representations of combined hydrologic and surge processes to quantify flood hazards and risk. Furthermore, flood hazards and risks need to be readily furnished to policymakers and emergency managers. The increasing availability of accurate and spatially detailed datasets, along with advances in computational resources will, allow for developing more representative flood models and thus timely and informing flood predictions. This study presents an effort to develop an adequate holistic modeling framework to simulate the compound effects of rainfall-runoff and storm surge flooding in complex watersheds. We aimed in the study to address the fundamental issues that face flood modeling in low-lying coastal watersheds via the development of a coupled hydrologic and hydrodynamic model that was tested against past storm events with different severity and found adequate. Such a setup can be used to analyze the impact of different return period storms to enable more comprehensive enhanced flood zone assessments.

5.4 Making Coastal Communities More Flood Resilient

The rate at which flooding occurs in recent times has been unprecedented, with the implication that only a few coastal, rural, and urban environments still have their natural states unaltered (Hirabayashi et al., 2013b). During flooding, water broadly covers land areas not usually covered by water, destroying farmland and critical infrastructure, displacing

human populations, disrupting economic activities, and in the worst cases, leading to epidemics and death (Smith, 2013). Large-scale flood disasters in recent years vividly demonstrate the need to invest in flood risk management measures before such events happen. However, it can be difficult for a community to decide to invest in such measures, as these decisions usually involve several options and multiple stakeholders with different short- and long-term objectives and priorities. A variety of decision-support tools are available to organize and evaluate options, which can assist in making a case for pre-event risk reduction to flooding and other hazards. The most widely used for assessing flood risk reduction measures among these tools is cost-benefit analysis (CBA). Cost-benefit analysis is based on the economic efficiency criteria of maximizing benefits net of costs over time. CBA has been the primary analytical approach to provide quantitative information when prioritizing risk reduction solutions.

Using CBA in the context of analyzing risk reduction requires four main steps: (1) Estimating the amount of flood losses expected in the future under the status quo (that is, without risk reduction); (2) identifying possible risk reduction measures and their associated costs; (3) estimating how much of the future flood losses would be reduced with such measures in place (that is, estimation of benefits); (4) calculating the economic efficiency of the measures. The measures are said to be economically efficient if benefits exceed the cost. In this context, it is seen that steps two and three heavily depend on the capacity to estimate the flood risk and losses under the current conditions and proposed flood mitigation measures. Best practices in flood risk management are generally supported by adequate flood modeling (Liu et al., 2015), and consequently, a better understanding and modeling of the relationship between precipitation, surface runoff, urbanization, climate change, and urban

pluvial flooding is becoming an essential requirement for decision-makers, investors and developers.

This study develops a modeling framework for coastal watersheds that can explore the relationship mentioned above by coupling a sophisticated spatially distributed hydrologic model with a high-resolution hybrid 1D/2D hydrodynamic model. The developed model captured the spatial and temporal variation in the produced runoff under different storm events with varying severity and delineated its impact over the watershed and into the main river and its tributaries while fully capturing the complex riverine flood dynamics that occur. The model outcome included many flow parameters to aid decision-makers: flood flow, water stage, flood inundation duration, and extent. This application was employed in the Vermilion River watershed as a case study. Watercourse dredging for the main river was proposed as a part of a suite of flood mitigation measures. Several dredging alternatives included different combinations of removing instream sediment and vegetation as well as bed slope grading were presented. Under this study, a model developed for the Vermilion River was used to evaluate the flood benefits out of each alternative. Flood inundation maps for the baseline simulations (pre-dredging conditions) and each alternative were generated based on the estimated maximum water surface profile. To further assess the potential value of the dredging scenarios, a flood consequence assessment was performed based on the results obtained from the inundation maps produced by the hydraulic model. The analysis simply keeps track of the number of inundated structures within the Vermilion River basin under each scenario and compares that to the baseline condition. The analysis utilized the Microsoft U.S. building footprint dataset released in June 2018 as an Open Database for OpenStreetMap (https://www.microsoft.com/en-us/maps/building-footprints). This dataset

has approximately 125 million building footprint polygon geometries in all 50 US States, 118,396 of which are located within the Vermilion River basin. Comparing the total number of the buildings flooded under each scenario to that of the baseline scenario would provide an estimate of the number of structures removed from flooding due to each dredging alternative.

5.5 Development of Street-level Flood Forecasting System

Floods are one of the deadliest natural hazards in the United States. Since 2010, floods have killed 950 people in the US. Such patterns are expected to continue as climate, and land-use pressures amplify (Hirabayashi et al., 2013). While flood damage cannot be eliminated, it can be mitigated. This is particularly true when populations are given advanced warning, have faith in the accuracy of forecast, and are provided actionable intelligence. When emergency responders are given maps showing where water is and where it might be in the future, better choices can be made that systematically save time, energy, and resources (National Research Council, 2009). Combined, these challenges and opportunities suggest a need to better understand and forecast flood events across the United States, with special attention to high flood hazard areas such as coastal regions.

Developing the National Water Model (NWM) was a part of the national efforts to develop a viable flood forecast system. The NWM serves as a cornerstone of the new NOAA Water Initiative to provide integrated predictive capabilities that promote resilience and mitigation of water risks. In August 2016, version 1.0 was made operational, expanding the nation's forecasting domain from approximately 9000 gaged locations to 2.7 million reach outlets along the NHDPlusV2. The National Water Model uses the Noah Multi-Parameterization (Noah-MP) land surface model (LSM) to simulate land surface processes across a 1 km grid and a separate 250 m grid to perform diffusive wave surface and saturated

subsurface flow routing. Once water is in the channel, WRF-Hydro implements a standard 1-D Muskingum–Cunge (MC) hydrograph routing method using time-varying parameter estimates. Despite that, the in-channel hydrograph routing scheme implemented in the NWM allows only for the evaluation of downstream-headed streamflows and limits its ability to estimate any flood stages.

Complementary efforts towards producing real-time and future flood inundation forecasts for the US have resulted in the compilation of a 10 m resolution Height Above Nearest Drainage (HAND) layer for the continental United States (Liu et al., 2018). The methodology depends on coupling streamflow predictions from the National Water Model (NWM) and HAND to produce rapid flood predictions for disaster warning and guidance. However, a study that was performed to investigate the accuracy of the coupled NWM-HAND methodology (Johnson et al., 2019) found out that such a scheme performs poorly in low-relief coastal watersheds. The study found that the HAND cannot conserve volume through space or time, and in areas of low relief, where many cells have similar if not equal HAND values, minor errors in the water stage can have disproportionate errors in inundation. Additionally, storm surge and tidal influences play a significant role in the water stage characterization in coastal regions, requiring more advanced in-channel flow routing not currently supported by the NWM. The study also suggested that physically based models are needed in these cases. The modeling framework suggested in our study for the low-lying coastal watersheds bridges this gap and provides a specification for the minimum level of detail needed to model similar cases. Ongoing research effort at the Louisiana Watershed Flood Center is being carried out to produce a watershed-based medium-range flood forecast

system. The Flood center is currently experimenting with the Vermilion River flood model developed under this study.

5.6 Transferable Knowledge and Skills

Despite that the work done under this study was developed and tested in coastal watersheds located in Louisiana, the study included understanding, skills, and procedural knowledge transferable to other areas that share some commonalities. For example, this study highlighted the role of large natural storage areas, such as swamps and wetlands, in flood dynamics and how that is incorporating such storage areas, which in our case study was the Bayou Tortue swamp, in the flood model was required to capture the complex flow dynamics of the Vermilion River. However, such a conclusion is not limited to the Vermilion River. Instead, it can be applied in other low-gradient watersheds with vast swamps or wetlands. For example, following this study, developing a flood model for Withlacoochee River, Florida, requires to include the green swamp (Pride et al., 1966) as part of the model for accurate estimates of peak flow parameters (stage and flow rate).

Additionally, this study provided an insight into the performance of traditional flood mitigation measures such as riverine dredging and swamp management in low-gradient river systems. These flood mitigation measures are often sought and considered by communities living alongside rivers, such as Cypress Creek Watershed (Houston, TX), to alleviate riverine-induced flooding (Tang et al., 2020). This study emphasizes the benefits and the drawbacks of implementing riverine dredging or swamp management in similar watersheds.

The study closed in on some existing modeling tool gaps as it developed a modeling architecture that seamlessly integrated the outputs from a nationwide scale hydrologic model, the National Water Model (NWM) outputs, to drive a 1D/2D hybrid hydrodynamic model

developed using the HEC-RAS. The developed modeling architecture is a numerical modeling setup that can be used as a tool to simulate flood events using NWM-driven simulations (Saad and Habib, 2019).

Chapter 6: Summary, Limitations, and Future Work

This study sought to understand the drivers behind the complex flood dynamics in low-lying coastal watersheds and investigate the minimum level of detail needed to adequately simulate them using a hydrodynamic modeling approach. The study also sought to evaluate the impact of different flood mitigation measures such as large-scale channel modifications via riverine dredging, and modification of large natural storage areas (swamps) with significant river-swamp interactions. This chapter summarizes procedures performed to attain the research objectives and discusses the synthesis of the findings from the study. In addition, the scientific contribution and how the study findings could influence further understanding of the research subject is addressed. Implications of the research questions and how they can be extended in future investigations are also discussed.

6.1 Summary

To provide a thorough understanding of the flood dynamics in low-lying coastal watersheds, the study started by addressing the question of model complexity in modeling applications in low-gradient watersheds with complex flood regimes. The study chose the Vermilion River basin in South Louisiana, USA, which represents a typical low-lying coastal watershed, to be the case study. The study aimed to assess the value of increasing complexity in the hydraulic model setup by testing a range of; spatial dimensionality and resolution to represent the main river and its linkage combinations (1-D only and hybrid 1-D/2-D), boundary conditions, and the representation of sizeable natural storage areas. A series of numerical experiments are developed using a range of model setups featuring the HEC-RAS hydraulic model of varying complexity driven by hydrologic inputs furnished by the National Water Model (NWM). The model results are compared against available stage and

streamflow observations during a series of flooding events that occurred in late spring of 2014 and Summer 2016. Based on the comparisons, the study adopts the model setup that shows the most accurate predictive skill to represent the baseline scenario (i.e., existing conditions) in the proposed flood mitigation measures evaluations. Following that, four different riverine dredging scenarios that represent different combinations of spatial extents and changes to the dimensions of the river channel and its longitudinal slope are developed using the HEC-RAS hydraulic model. Similarly, three additional scenarios simulate increasing the size of the available storage in the swamp, lowering the height of banks separating the river from the swamp, and enhancing the conveyance of the river-to-swamp network of coulees that connects the swamp with the main river are developed. Finally, each developed scenario is treated as a proposed flood mitigation scheme. The performance of each scheme is evaluated compared to the baseline scenario according to some flood benefits metrics such as the alteration of the reverse flow, the drop in the maximum flood stage, the reduction in the flooding duration. The main findings from this study can be summarized as follows:

- By adopting a more advanced flow routing approximation, increasing the model complexity led to only minor improvements in capturing the river's flow dynamics, such as the reverse flow. However, improved representation of the physical hydraulic processes led to a more realistic simulation of the stages and flow rates along the river.
- Imposing a normal-depth assumption as a downstream boundary condition can significantly impact the stage and flow simulations in low-gradient rivers. It can result in an inaccurate representation of the water surface profile and the

extent of river-induced flooding at locations well within the domain of interest.

- Incorporating large natural storage areas, such as swamps and wetlands, into the model domain was required to capture the complex flow dynamics, especially the reverse flows. Incorporating storage elements also significantly improved the estimates of peak flow parameters (stage and flow rate). Such natural areas play a significant role in rivers with low transport capacity and flat gradients. During the active part of the rainstorm, these areas offer significant temporary storage for the floodwater, and after the storm peak recedes, it drains back into the usual downstream direction resulting in a prolonged attenuation of the flood.
- Increasing the model dimensionality along the river's mainstream by representing the floodplain along the main channel using 2D did not necessarily improve the model performance. Instead, it resulted in a slight deterioration in capturing the prolonged flood receding and the spatial extent of the reversal flows. These unexpected results are attributed to the added challenges in characterizing flow exchanges between the main channel and the floodplains, especially with the absence of calibration data at scales necessary to capture such fine-resolution local effects.
- The results obtained during the study from evaluating traditional flood mitigation measures such as riverine dredging revealed that such dredging could increase the hydraulic conveyance of the river system and improve its drainage characteristics. However, the large runoff volumes delivered by the

contributing tributaries eventually overwhelm the river and outweigh the added improvement in terms of in-channel storage, thus reducing the anticipated flood relief benefit expected from the dredging.

- While there is evidence that dredging can increase channel conveyance and reduce water levels inside the main river itself, such reduction was not reflected in a parallel reduction in the spatial extent of flood inundation boundaries. On the other hand, reductions in the duration of inundation were substantial, suggesting that while dredging didn't significantly reduce the maximum extent of inundation, it seems to reduce the duration that flooded areas get inundated.
- Generally, the dredging activities caused a noticeable alteration in the tidal wave range along the river. Extensive dredging caused a substantial amplification in the tidal signal along the main course of the river, which can facilitate the landward penetration of storm surges into the river.
- In low-gradient environments, mitigation strategies that rely on maximizing the function of natural storage areas are more effective than traditional riverine and channel modifications.
- Enhancing the lateral connectivity between the river and the adjacent swamp did have a more significant impact on reducing the flood stages inside the river compared to maximizing the size of available storage inside the swamp.
- The impact of flood mitigation measures that include modifications to the swamp seemed to have more impact on the recession limb of the stage hydrograph compared to the peak stage.

6.2 Limitations and Future Work

Efforts were made in this study to develop a comprehensive and reliable modeling-based evaluation of the physical processes that underlies flood dynamics in low-gradient systems and evaluate the performance of different mitigation measures in the context of such dynamics. However, the physics-based modeling approach adopted in this study generally has high data volume and quality input requirements, a high level of complexity, and high computational cost, which are not always available. Accordingly, some simplifications and assumptions had to be made, which pose some limitations on the current work and might need to be revisited in future studies. The following summarizes the main limitations of the current work:

- The hydrodynamic model depends on topographic information to simulate the overland flow routing in areas modeled using 2D flow elements. The current study adopted the latest available LIDAR data to provide the model with the needed topographic information. However, the LIDAR data did not represent the bare earth or bathymetry of the flow paths inside the swamp; instead, the horizontally-leveled terrain information found in the LIDAR for this area suggests that the elevations provided are more for the stagnant water levels. Another sign of that was found in an older report prepared by the USGS in 1985, which revealed deeper cross-sectional surveys for the bayous dissecting the swamp area. The current study showed a high sensitivity of the results to how the cross-sectional information of the lateral river-to-swamp network is actually represented in the model. Adjustments to the LiDAR data, augmented

by ground surveys, which are beyond the scope of this study, are needed to address such limitations.

- Building a 1D/2D hybrid model using the HEC-RAS requires defining lateral structures representing the hydraulic connections between the 1D river reaches and the adjacent 2D areas. The numerical experiments performed during this study showed that the model's stability highly depends on the parameters assigned for these lateral structures. However, due to the absence of any field observations on the amount of flow exchanges between the river and the adjacent swamp, the study depended on the recommended values for the lateral structure parameters provided in the HEC-RAS manual. Gauging the actual flow exchanges between the river and swamp and calibrating the lateral weir parameters accordingly would improve the reliability and performance of the model.
- The hydrologic model (NWM) and the HEC-RAS hydrodynamic model were coupled independently in an offline mode. In this configuration, the output of one model (NWM) is used as input for the next model (RAS). The one-directional passing of information may ignore possible dynamic feedbacks between two sets of models.
- This study was centered on understanding the flow dynamics inside the river itself and evaluating the impact of different mitigation measures on the flooding mechanism inside the river. However, no direct attention was given to verify the flow dynamics and circulation inside the swamp, mainly due to

the lack of reliable topographic and bathymetric data in these areas, as well as to the lack of hydrologic data on water stages.

- The research did not study the effect of flood mitigation measures, especially those that alter the river-to-swamp interactions, on the ecological function of the swamp.
- Future work needs to investigate the effectiveness of flood mitigation measures in low-gradient settings in the context of future climate change and variability, as well as the historic and future changes in the land use and urbanization.

References

Abbot, J., Marohasy, J., 2014. Input selection and optimisation for monthly rainfall forecasting in Queensland, Australia, using artificial neural networks. Atmospheric Research, 138: 166-178. DOI:https://doi.org/10.1016/j.atmosres.2013.11.002

Abderrezzak, K.E.K., Paquier, A., Mignot, E., 2009. Modelling flash flood propagation in urban areas using a two-dimensional numerical model. Natural Hazards, 50(3): 433-460.

Acreman, M., Holden, J., 2013. How Wetlands Affect Floods. Wetlands, 33(5): 773-786. DOI:10.1007/s13157-013-0473-2

Acreman, M.C., Riddington, R., Booker, D.J., 2003. Hydrological impacts of floodplain restoration: a case study of the River Cherwell, UK. Hydrol. Earth Syst. Sci., 7(1): 75-85. DOI:10.5194/hess-7-75-2003

Advanced Hydrologic Prediction Service [AHPS], National Weather Service, 2018. Historic Crests at Surrey Station, LA.

Afshari, S. et al., 2018. Comparison of new generation low-complexity flood inundation mapping tools with a hydrodynamic model. Journal of Hydrology, 556: 539-556. DOI:https://doi.org/10.1016/j.jhydrol.2017.11.036

Ahilan, S., Guan, M., Sleigh, A., Wright, N., Chang, H., 2018. The influence of floodplain restoration on flow and sediment dynamics in an urban river. Journal of Flood Risk Management, 11(S2): S986-S1001. DOI:10.1111/jfr3.12251

Alemseged, T., Rientjes, T., 2007. Uncertainty issues in hydrodynamic flood modeling, Proceedings of the 5th international symposium on spatial data quality SDQ, pp. c43.

Babcock, M., 2013. State hazard mitigation plans and climate change: rating the states.

Baker, N.T., 1988. Hydrologic features and processes of the Vermilion River, Louisiana. 88-4019. DOI:10.3133/wri884019

Barbier, E.B., Georgiou, I.Y., Enchelmeyer, B., Reed, D.J., 2013. The value of wetlands in protecting southeast Louisiana from hurricane storm surges. PloS one, 8(3): e58715.

Bates, P.D., 2004. Remote sensing and flood inundation modelling. Hydrological processes, 18(13): 2593-2597.

Bates, P.D. et al., 2005. Simplified two-dimensional numerical modelling of coastal flooding and example applications. Coastal Engineering, 52(9): 793-810.

Bates, P.D., Marks, K.J., Horritt, M.S., 2003. Optimal use of high-resolution topographic data in flood inundation models. Hydrological Processes, 17(3): 537-557. DOI:doi:10.1002/hyp.1113

Bengtson, M.L., Padmanabhan, G., 1999. A review of models for investigating the influence of wetlands on flooding. North Dakota Water Resources Research Institute, North Dakota State University.

Benjankar, R., Tonina, D., McKean, J., 2015. One-dimensional and two-dimensional hydrodynamic modeling derived flow properties: impacts on aquatic habitat quality predictions. Earth Surface Processes and Landforms, 40(3): 340-356.

Berlin, C., Handley, J., 2007. Wetlands as Flood Control: The Case of the La Crosse River Marsh. Focus on Geography, 50(2): 7-15. DOI:https://doi.org/10.1111/j.1949-8535.2007.tb00191.x

Bermúdez, M. et al., 2017. Quantifying local rainfall dynamics and uncertain boundary conditions into a nested regional-local flood modeling system. Water Resources Research, 53(4): 2770-2785.

Beven, K.J., 2011. Rainfall-runoff modelling: the primer. John Wiley & Sons.

Bhaskaran, P.K., Gayathri, R., Murty, P., Bonthu, S., Sen, D., 2014. A numerical study of coastal inundation and its validation for Thane cyclone in the Bay of Bengal. Coastal Engineering, 83: 108-118.

Bhuiyan, C., 2004. Various drought indices for monitoring drought condition in Aravalli terrain of India, Proceedings of the XXth ISPRS Congress, Istanbul, Turkey, pp. 12-23.

Bilskie, M., Hagen, S., 2018. Defining flood zone transitions in low-gradient coastal regions. Geophysical Research Letters, 45(6): 2761-2770.

Bilskie, M.V. et al., 2021. Enhancing Flood Hazard Assessments in Coastal Louisiana Through Coupled Hydrologic and Surge Processes. Frontiers in Water, 3. DOI:10.3389/frwa.2021.609231

Blake, E.S., Zelinsky, D.A., 2018. National Hurricane center tropical cyclone report: Hurricane Harvey. National Hurricane Center, National Oceanographic and Atmospheric Association.

Boisier, J.P., Rondanelli, R., Garreaud, R.D., Muñoz, F., 2016. Anthropogenic and natural contributions to the Southeast Pacific precipitation decline and recent megadrought in central Chile. Geophysical Research Letters, 43(1): 413-421.

Brauman, K.A., Daily, G.C., Duarte, T.K.e., Mooney, H.A., 2007. The Nature and Value of Ecosystem Services: An Overview Highlighting Hydrologic Services. Annual Review of Environment and Resources, 32(1): 67-98. DOI:10.1146/annurev.energy.32.031306.102758

Brookes, A., 1988. Channelized rivers: perspectives for environmental management.

Brown, M.E., de Beurs, K., Vrieling, A., 2010. The response of African land surface phenology to large scale climate oscillations. Remote Sensing of Environment, 114(10): 2286-2296.

Brunner, G.W., 2016. HEC-RAS River Analysis System. Hydraulic Reference Manual. Version 5.0, Hydrologic Engineering Center Davis CA.

Buizza, R. et al., 2005. A Comparison of the ECMWF, MSC, and NCEP Global Ensemble Prediction Systems. Monthly Weather Review, 133(5): 1076-1097. DOI:10.1175/mwr2905.1

Bullock, A., Acreman, M., 2003. The role of wetlands in the hydrological cycle. Hydrology and Earth System Sciences, 7(3): 358-389.

Cai, H., Savenije, H., Yang, Q., Ou, S., Lei, Y., 2012. Influence of River Discharge and Dredging on Tidal Wave Propagation: Modaomen Estuary Case. Journal of Hydraulic Engineering, 138: 885-896. DOI:10.1061/(ASCE)HY.1943-7900.0000594

Cai, H., Savenije, H.H.G., Yang, Q., Ou, S., Lei, Y., 2012. Influence of River Discharge and Dredging on Tidal Wave Propagation: Modaomen Estuary Case. Journal of Hydraulic Engineering, 138(10): 885-896. DOI:doi:10.1061/(ASCE)HY.1943-7900.0000594

Candel, A., Parmar, V., LeDell, E., Arora, A., 2016. Deep learning with H2O. H2O. ai Inc.

Center, N.H., 2018. Costliest US tropical cyclones tables updated. NOAA Tech. Memo. NWS NHC-6.

Chanson, H., 2004. Hydraulics of open channel flow. Elsevier.

Chen, W.-B., Liu, W.-C., 2014. Modeling flood inundation induced by river flow and storm surges over a river basin. Water, 6(10): 3182-3199.

Chomba, I.C. et al., 2021. A Review of Coupled Hydrologic-Hydraulic Models for Floodplain Assessments in Africa: Opportunities and Challenges for Floodplain Wetland Management. Hydrology, 8(1): 44.

Chow, V.T., 1959. Open-channel hydraulics. McGraw-Hill, New York.

Comer, J., Olbert, A.I., Nash, S., Hartnett, M., 2017. Development of high-resolution multi-scale modelling system for simulation of coastal-fluvial urban flooding. Natural Hazards and Earth System Sciences, 17(2): 205-224.

Cook, A., Merwade, V., 2009. Effect of topographic data, geometric configuration and modeling approach on flood inundation mapping. Journal of Hydrology, 377(1-2): 131-142.

Costabile, P., Costanzo, C., Macchione, F., 2013. A storm event watershed model for surface runoff based on 2D fully dynamic wave equations. Hydrological processes, 27(4): 554-569.

Council, N.R., 2009. Mapping the Zone: Improving Flood Map Accuracy. The National Academies Press, Washington, DC, 136 pp. DOI:doi:10.17226/12573

Council, N.R., 2013. Levees and the national flood insurance program: improving policies and practices. National Academies Press.

CrED, U., 2015. The human cost of weather-related disasters, 1995–2015. United Nations, Geneva.

Crossett, K., Ache, B., Pacheco, P., Haber, K., 2013. National coastal population report, population trends from 1970 to 2020. NOAA State of the Coast Report Series, US Department of Commerce, Washington.

Cunningham, R., Gisclair, D., Craig, J., 2009. THE LOUISIANA STATEWIDE LIDAR PROJECT.

Dai, A., Wigley, T., 2000. Global patterns of ENSO-induced precipitation. Geophysical Research Letters, 27(9): 1283-1286.

Dalrymple, R.W., Choi, K., 2007. Morphologic and facies trends through the fluvial–marine transition in tide-dominated depositional systems: A schematic framework for environmental and sequence-stratigraphic interpretation. Earth-Science Reviews, 81(3): 135-174. DOI:https://doi.org/10.1016/j.earscirev.2006.10.002

de Groot, R.S., Wilson, M.A., Boumans, R.M.J., 2002. A typology for the classification, description and valuation of ecosystem functions, goods and services. Ecological Economics, 41(3): 393-408. DOI:https://doi.org/10.1016/S0921-8009(02)00089-7

Demissie, M., Khan, A., 1993. Influence of wetlands on streamflow in Illinois. ISWS Contract Report CR 561.

Deo, R.C., Şahin, M., 2015. Application of the extreme learning machine algorithm for the prediction of monthly Effective Drought Index in eastern Australia. Atmospheric Research, 153: 512-525. DOI:https://doi.org/10.1016/j.atmosres.2014.10.016

Dore, M.H., 2005. Climate change and changes in global precipitation patterns: what do we know? Environment international, 31(8): 1167-1181.

Ehsanzadeh, E., van der Kamp, G., Spence, C., 2012. The impact of climatic variability and change in the hydroclimatology of Lake Winnipeg watershed. Hydrological Processes, 26(18): 2802-2813. DOI:https://doi.org/10.1002/hyp.8327

Eldardiry, H., Habib, E., Zhang, Y., Graschel, J., 2017. Artifacts in Stage IV NWS Real-Time Multisensor Precipitation Estimates and Impacts on Identification of Maximum Series. Journal of Hydrologic Engineering, 22(5): E4015003. DOI:doi:10.1061/(ASCE)HE.1943-5584.0001291

ElSaadani, M., Krajewski, W.F., 2017. A time-based framework for evaluating hydrologic routing methodologies using wavelet transform. Journal of Water Resource and Protection, 9(7): 723-744.

Fang, Z. et al., 2010. Using a Distributed Hydrologic Model to Evaluate the Location of Urban Development and Flood Control Storage. Journal of Water Resources Planning and Management, 136(5): 597-601. DOI:doi:10.1061/(ASCE)WR.1943-5452.0000066

FAO. Soils resources, m., service, c., 1983. Guidelines: land evaluation for rainfed agriculture. FAO.

Federal Emergency Management Agency (FEMA), 2018. Flood Insurance Study (LAFAYETTE PARISH, LOUISIANA).

Ferrari, M.R., Miller, J.R., Russell, G.L., 1999. Modeling the effect of wetlands, flooding, and irrigation on river flow: Application to the Aral Sea. Water Resources Research, 35(6): 1869-1876. DOI:https://doi.org/10.1029/1999WR900035

Garreaud, R., Battisti, D.S., 1999. Interannual (ENSO) and interdecadal (ENSO-like) variability in the Southern Hemisphere tropospheric circulation. Journal of Climate, 12(7): 2113-2123.

Gochis, D. et al., 2018. The WRF-Hydro modeling system technical description, (Version 5.0) . NCAR Technical Note. 107 pages.

Godschalk, D. et al., 1999. Natural hazard mitigation: Recasting disaster policy and planning. Island press.

Habib, E., Henschke, A., Adler, R.F., 2009. Evaluation of TMPA satellite-based research and real-time rainfall estimates during six tropical-related heavy rainfall events over Louisiana, USA. Atmospheric Research, 94(3): 373-388. DOI:https://doi.org/10.1016/j.atmosres.2009.06.015

Habib, E. et al., 2008. Effect of rainfall spatial variability and sampling on salinity prediction in an estuarine system. Journal of Hydrology, 350(1): 56-67. DOI:https://doi.org/10.1016/j.jhydrol.2007.11.034

Habib, E.H., Meselhe, E.A., 2006. Discharge Relations for Low-Gradient Tidal Streams Using Data-Driven Models. Journal of Hydraulic Engineering, 132(5): 482-492. DOI:doi:10.1061/(ASCE)0733-9429(2006)132:5(482)

Hillman, G.R., 1998. Flood wave attenuation by a wetland following a beaver dam failure on a second order boreal stream. Wetlands, 18(1): 21-34. DOI:10.1007/BF03161439

Hirabayashi, Y. et al., 2013. Global flood risk under climate change. Nature climate change, 3(9): 816-821.

Hodges, B.R., 2014. Hydrodynamical Modeling☆, Reference Module in Earth Systems and Environmental Sciences. Elsevier. DOI:https://doi.org/10.1016/B978-0-12-409548-9.09123-5

Homer, C. et al., 2015. Completion of the 2011 National Land Cover Database for the Conterminous United States - Representing a Decade of Land Cover Change Information, 81, 346-354 pp. DOI:10.14358/PERS.81.5.345

Hooper, R.P., Nearing, G., Condon, L.S., 2017. Using the National Water Model as a Hypothesis-Testing Tool, CUAHSI Hydroinformatics Conference (2017: Tuscaloosa, Alabama).

Ingram, K.T., Dow, K., Carter, L., Anderson, J., Sommer, E.K., 2013. Climate of the Southeast United States: variability, change, impacts, and vulnerability. Springer.

IPCC, W., 2007. Climate change 2007: the physical science basis contribution of working group I. Fourth assessment report of the intergovernmental panel on climate change. Cambridge University Press, Cambridge.

Jackson, R., 1987. Hydrology of an acid wetland before and after draining for afforestation, western New Zealand. Forest hydrology and watershed management: 465-474.

Jardine, A., Merideth, R., Black, M., LeRoy, S., 2013. Assessment of climate change in the southwest United States: A report prepared for the National Climate Assessment. Island press.

Jarihani, A.A., Callow, J.N., McVicar, T.R., Van Niel, T.G., Larsen, J.R., 2015. Satellite-derived Digital Elevation Model (DEM) selection, preparation and correction for hydrodynamic modelling in large, low-gradient and data-sparse catchments. Journal of Hydrology, 524: 489-506.

Johnson, J.M., Munasinghe, D., Eyelade, D., Cohen, S., 2019. An integrated evaluation of the National Water Model (NWM)–Height Above Nearest Drainage (HAND) flood mapping methodology. Nat. Hazards Earth Syst. Sci., 19(11): 2405-2420. DOI:10.5194/nhess-19-2405-2019

Juan, A., Gori, A., Sebastian, A., 2020. Comparing floodplain evolution in channelized and unchannelized urban watersheds in Houston, Texas. Journal of Flood Risk Management: e12604.

Kadykalo, A.N., Findlay, C.S., 2016. The flow regulation services of wetlands. Ecosystem Services, 20: 91-103. DOI:https://doi.org/10.1016/j.ecoser.2016.06.005

Kadykalo, A.N., Findlay, C.S., 2016. The flow regulation services of wetlands. Ecosystem Services, 20: 91-103.

Karamouz, M., Ahmadvand, F., Zahmatkesh, Z., 2017. Distributed hydrologic modeling of coastal flood inundation and damage: nonstationary approach. Journal of Irrigation and Drainage Engineering, 143(8): 04017019.

Karamouz, M., Zahmatkesh, Z., Goharian, E., Nazif, S., 2015. Combined impact of inland and coastal floods: Mapping knowledge base for development of planning strategies. Journal of Water Resources Planning and Management, 141(8): 04014098.

Kim, J., Warnock, A., Ivanov, V.Y., Katopodes, N.D., 2012. Coupled modeling of hydrologic and hydrodynamic processes including overland and channel flow. Advances in Water Resources, 37: 104-126.

Kinsland, G.L., Wildgen, J., 2006. Evolution of the morphology of the Vermilion River near Lafayette, Louisiana, USA; consequent flooding problems and a mitigation plan; some features on the surface of the Prairie Complex: All illustrated with LIDAR imagery.

Koussis, A.D., 2009. Assessment and review of the hydraulics of storage flood routing 70 years after the presentation of the Muskingum method. Hydrological Sciences Journal, 54(1): 43-61. DOI:10.1623/hysj.54.1.43

LA Department of Wildlife & Fisheries, 2005. Louisiana Comprehensive Wildlife Conservation Strategy (LA CWCS).

Labat, D., 2005. Recent advances in wavelet analyses: Part 1. A review of concepts. Journal of Hydrology, 314(1-4): 275-288.

Leandro, J., Chen, A.S., Djordjević, S., Savić, D.A., 2009. Comparison of 1D/1D and 1D/2D coupled (sewer/surface) hydraulic models for urban flood simulation. Journal of hydraulic engineering, 135(6): 495-504.

Lester, G.D., Sorensen, S.G., Faulkner, P.L., Reid, C.S., Maxit, I.E., 2005. Louisiana comprehensive wildlife conservation strategy.

Lewis, M., Horsburgh, K., Bates, P., Smith, R., 2011. Quantifying the Uncertainty in Future Coastal Flood Risk Estimates for the U.K. Journal of Coastal Research, 27(5): 870-881. DOI:10.2112/jcoastres-d-10-00147.1

Liao, K.-H., Chan, J.K.H., Huang, Y.-L., 2019. Environmental justice and flood prevention: The moral cost of floodwater redistribution. Landscape and Urban Planning, 189: 36-45. DOI:https://doi.org/10.1016/j.landurbplan.2019.04.012

Lin, Y., Mitchell, K., 2005. The NCEP stage II/IV hourly precipitation analyses: Development and applications.

Liu, L. et al., 2015. Developing an effective 2-D urban flood inundation model for city emergency management based on cellular automata. Natural hazards and earth system sciences, 15(3): 381-391.

Liu, Y., Brown, J., Demargne, J., Seo, D.-J., 2011. A wavelet-based approach to assessing timing errors in hydrologic predictions. Journal of hydrology, 397(3-4): 210-224.

Marj, A.F., Meijerink, A.M., 2011. Agricultural drought forecasting using satellite images, climate indices and artificial neural network. International Journal of Remote Sensing, 32(24): 9707-9719.

Maskell, J., Horsburgh, K., Lewis, M., Bates, P., 2013. Investigating River–Surge Interaction in Idealised Estuaries. Journal of Coastal Research, 30(2): 248-259. DOI:10.2112/jcoastres-d-12-00221.1

Masood, M., Takeuchi, K., 2011. Assessment of flood hazard, vulnerability and risk of mid-eastern Dhaka using DEM and 1D hydrodynamic model, 61. DOI:10.1007/s11069-011-0060-x

McKay, L. et al., 2012. NHDPlus Version 2 : User Guide.

Meroni, M., Rembold, F., Fasbender, D., Vrieling, A., 2017. Evaluation of the Standardized Precipitation Index as an early predictor of seasonal vegetation production anomalies in the Sahel. Remote sensing letters, 8(4): 301-310.

Mitsch, W.J., Dorge, C.L., Wiemhoff, J.R., 1977. Forested wetlands for water resource management in southern Illinois.

Mitsch, W.J., Gosselink, J.G., 2015. Wetlands. John Wiley & Sons.

Mitsch, W.J., Gosselink, J.G., Zhang, L., Anderson, C.J., 2009. Wetland ecosystems. John Wiley & Sons.

Morris, J., Camino, M., 2011. Economic assessment of freshwater, wetland and floodplain (FWF) ecosystem services. UK National Ecosystem Assessment Working Paper, Cranfield University.

Morss, R.E., Demuth, J.L., Lazo, J.K., 2008. Communicating uncertainty in weather forecasts: A survey of the US public. Weather and forecasting, 23(5): 974-991.

Moussa, R., Bocquillon, C., 2009. On the use of the diffusive wave for modelling extreme flood events with overbank flow in the floodplain. Journal of hydrology, 374(1-2): 116-135.

National Center For Environmental Information [NCEI], 2015. Storm Events Database For Louisiana.

NCEI, N., 2018. US billion-dollar weather and climate disasters. Retrieved 22/10/18 from https://www. ncdc. noaa. gov/billions.

Neal, J. et al., 2012. How much physical complexity is needed to model flood inundation? Hydrological Processes, 26(15): 2264-2282. DOI:10.1002/hyp.8339

Nelson, B.R., Prat, O.P., Seo, D.-J., Habib, E., 2016. Assessment and Implications of NCEP Stage IV Quantitative Precipitation Estimates for Product Intercomparisons. Weather and Forecasting, 31(2): 371-394. DOI:10.1175/waf-d-14-00112.1

Neumann, B., Vafeidis, A.T., Zimmermann, J., Nicholls, R.J., 2015. Future coastal population growth and exposure to sea-level rise and coastal flooding-a global assessment. PloS one, 10(3): e0118571.

Nunnally, N.R., 1978. Stream renovation: an alternative to channelization. Environmental Management, 2(5): 403-411.

Office Of Water Prediction, 2018. National Water Model.

Ogawa, H., Male, J.W., 1986. Simulating the Flood Mitigation Role of Wetlands. Journal of Water Resources Planning and Management, 112(1): 114-128. DOI:doi:10.1061/(ASCE)0733-9496(1986)112:1(114)

Olbert, A.I., Comer, J., Nash, S., Hartnett, M., 2017. High-resolution multi-scale modelling of coastal flooding due to tides, storm surges and rivers inflows. A Cork City example. Coastal Engineering, 121: 278-296.

O'Sullivan, J.J., Ahilan, S., Bruen, M., 2012. A modified Muskingum routing approach for floodplain flows: Theory and practice. Journal of Hydrology, 470: 239-254. DOI:10.1016/j.jhydrol.2012.09.007

Özçelik, C., Doğan, M., 2009. Investigation of wave attenuation mechanism under the downstream backwater effect. Flow Measurement and Instrumentation, 20(4): 180-188. DOI:https://doi.org/10.1016/j.flowmeasinst.2009.06.004

Pappenberger, F. et al., 2006. Influence of uncertain boundary conditions and model structure on flood inundation predictions. Advances in Water Resources, 29(10): 1430-1449. DOI:https://doi.org/10.1016/j.advwatres.2005.11.012

Park, G., Kim, I., Suh, K., Lee, J., 2011. Prediction of storm surge and runoff combined inundation. Journal of Coastal Research: 1150-1154.

Patel, D.P., Ramirez, J.A., Srivastava, P.K., Bray, M., Han, D., 2017. Assessment of flood inundation mapping of Surat city by coupled 1D/2D hydrodynamic modeling: a case application of the new HEC-RAS 5. Natural Hazards, 89(1): 93-130. DOI:10.1007/s11069-017-2956-6

Pattison, I., Lane, S.N., Hardy, R.J., Reaney, S.M., 2014. The role of tributary relative timing and sequencing in controlling large floods. Water Resources Research, 50(7): 5444-5458.

Pettorelli, N., 2013. The normalized difference vegetation index. Oxford University Press.

Pierce, A.R., King, S.L., 2013. 12.14 Valley Plugs, Land Use, and Phytogeomorphic Response. In: Shroder, J.F. (Ed.), Treatise on Geomorphology. Academic Press, San Diego, pp. 221-235. DOI:https://doi.org/10.1016/B978-0-12-374739-6.00330-4

Prestegaard, K.L. et al., 1994. Spatial variations in the magnitude of the 1993 floods, Raccoon River basin, Iowa. Geomorphology, 10(1): 169-182. DOI:https://doi.org/10.1016/0169-555X(94)90015-9

Pride, R., Meyer, F.W., Cherry, R.N., 1966. Hydrology of Green Swamp area in central Florida. Florida Geological Survey.

Quirogaa, V.M., Kurea, S., Udoa, K., Manoa, A., 2016. Application of 2D numerical simulation for the analysis of the February 2014 Bolivian Amazonia flood: Application of the new HEC-RAS version 5. Ribagua, 3(1): 25-33.

R. Miller, 2019. Numerical Simulation of Nonstationary River Backwater Effects on Regional Flood Characteristics in Regulated Basins. (Submitted).

Ralston, D.K., Talke, S., Geyer, W.R., Al-Zubaidi, H.A.M., Sommerfield, C.K., 2019. Bigger Tides, Less Flooding: Effects of Dredging on Barotropic Dynamics in a Highly Modified Estuary. Journal of Geophysical Research: Oceans, 124(1): 196-211. DOI:10.1029/2018jc014313

Reilly, J. et al., 2003. U.S. Agriculture and Climate Change: New Results. Climatic Change, 57(1): 43-67. DOI:10.1023/A:1022103315424

Rose, S., Peters, N.E., 2001. Effects of urbanization on streamflow in the Atlanta area (Georgia, USA): a comparative hydrological approach. Hydrological Processes, 15(8): 1441-1457. DOI:10.1002/hyp.218

Rose, S., Peters, N.E., 2001. Effects of urbanization on streamflow in the Atlanta area (Georgia, USA): a comparative hydrological approach. Hydrological Processes, 15(8): 1441-1457.

Saad, H.A., Habib, E.H., Miller, R.L., 2020. Effect of Model Setup Complexity on Flood Modeling in Low-Gradient Basins. JAWRA Journal of the American Water Resources Association, n/a(n/a). DOI:10.1111/1752-1688.12884

Saad, H.A., Habib, E.H., 2019. NWM-driven hydrodynamic simulations to resolve complex flow dynamics in low gradient watersheds, CUAHSI Conference on Hydroinformatics, Brigham Young University, Provo, Utah.

Saha, S. et al., 2014. The NCEP Climate Forecast System Version 2. Journal of Climate, 27(6): 2185-2208. DOI:10.1175/jcli-d-12-00823.1

Sandbach, S.D. et al., 2018. Hydrodynamic modelling of tidal-fluvial flows in a large river estuary. Estuarine, Coastal and Shelf Science, 212: 176-188. DOI:https://doi.org/10.1016/j.ecss.2018.06.023

Santiago-Collazo, F.L., Bilskie, M.V., Hagen, S.C., 2019. A comprehensive review of compound inundation models in low-gradient coastal watersheds. Environmental Modelling & Software, 119: 166-181. DOI:https://doi.org/10.1016/j.envsoft.2019.06.002

Scharffenberg, W.A., Kavvas, M., 2011. Uncertainty in flood wave routing in a lateral-inflow-dominated stream. Journal of Hydrologic Engineering, 16(2): 165-175.

Schoof, R., 1980. ENVIRONMENTAL IMPACT OF CHANNEL MODIFICATION 1. JAWRA Journal of the American Water Resources Association, 16(4): 697-701.

Shankman, D., Pugh, T.B., 1992. Discharge response to channelization of a coastal plain stream. Wetlands, 12(3): 157-162. DOI:10.1007/BF03160604

Shankman, D., Samson, S.A., 1991. CHANNELIZATION EFFECTS ON OBION RIVER FLOODING, WESTERN TENNESSEE 1. JAWRA Journal of the American Water Resources Association, 27(2): 247-254.

Shastry, A., Luo, C., Aristizabal, F., Egbert, R., 2017. Comparing NWM Inundation Predictions with Hydrodynamic Modeling. National Water Center Innovators Program Summer Institute Report 2017: 49.

Sheffield, J., Wood, E.F., Roderick, M.L., 2012. Little change in global drought over the past 60 years. Nature, 491(7424): 435-438.

Singh, S., Srivastava, P., Mitra, S., Abebe, A., 2016. Climate and anthropogenic impacts on stream flows—A systematic evaluation. J Hydrol Reg Stud, 8: 274-286.

Smakhtin, V.U., Batchelor, A., 2005. Evaluating wetland flow regulating functions using discharge time-series. Hydrological Processes: An International Journal, 19(6): 1293-1305.

Smith, K., 2013. Environmental hazards: assessing risk and reducing disaster. Routledge.

Svoboda, M., Fuchs, B., 2016. Handbook of drought indicators and indices.

Svozil, D., Kvasnicka, V., Pospichal, J.í., 1997. Introduction to multi-layer feed-forward neural networks. Chemometrics and Intelligent Laboratory Systems, 39(1): 43-62. DOI:https://doi.org/10.1016/S0169-7439(97)00061-0

Tadesse, T., Demisse, G.B., Zaitchik, B., Dinku, T., 2014. Satellite-based hybrid drought monitoring tool for prediction of vegetation condition in Eastern Africa: A case study for Ethiopia. Water Resources Research, 50(3): 2176-2190.

Tang, Y., Leon, A.S., Kavvas, M.L., 2020. Impact of Dynamic Storage Management of Wetlands and Shallow Ponds on Watershed-scale Flood Control. Water Resources Management, 34(4): 1305-1318. DOI:10.1007/s11269-020-02502-x

Tarlock, A.D., 2012. United States flood control policy: The incomplete transition from the illusion of total protection to risk management. Duke Envtl. L. & Pol'y F., 23: 151.

Tayefi, V., Lane, S.N., Hardy, R.J., Yu, D., 2007. A comparison of one- and two-dimensional approaches to modelling flood inundation over complex upland floodplains. Hydrological Processes, 21(23): 3190-3202. DOI:10.1002/hyp.6523

Thampapillai, D.J., Musgrave, W.F., 1985. Flood Damage Mitigation: A Review of Structural and Nonstructural Measures and Alternative Decision Frameworks. Water Resources Research, 21(4): 411-424. DOI:10.1029/WR021i004p00411

The National Weather Service, N., 1993. The Great Flood of 1993.

Timbadiya, P.V., Patel, P.L., D Porey, P., 2014. One-dimensional hydrodynamic modelling of flooding and stage hydrographs in the lower Tapi River in India, 106, 708-716 pp.

Torrence, C., Compo, G., 1998. A practical guide to wavelet analysis. bulletin of the American Meteorological Society 79: 61–78. doi: 10.1175/1520-0477 (1998) 079\0061: APGTWA [2.0. Co.

Tsai, C.W., 2005. Flood routing in mild-sloped rivers—wave characteristics and downstream backwater effect. Journal of Hydrology, 308(1): 151-167. DOI:https://doi.org/10.1016/j.jhydrol.2004.10.027

U.S. Geological Survey Gap Analysis Program, 2016. GAP/LANDFIRE National Terrestrial Ecosystems 2011. In: U.S. Geological Survey (Ed.). DOI:https://doi.org/10.5066/F7ZS2TM0

US Army Corps of Engineers, New Orleans District, Operations Division, 2015. Navigation Condition Surveys.

US Army Corps of Engineers New Orleans District, 1995. Lafayette Parish, Louisiana Flood Control: Reconnaissance Report.

USACE, 2016. HEC-RAS River Analysis System Hydraulic Reference Manual. Version 5.0. Institute of Water Resources, Hydrological Engineering Center Davis.

van der Wiel, K. et al., 2017. Rapid attribution of the August 2016 flood-inducing extreme precipitation in south Louisiana to climate change. Hydrol. Earth Syst. Sci., 21(2): 897-921. DOI:10.5194/hess-21-897-2017

Van Leeuwen, W.J., Hartfield, K., Miranda, M., Meza, F.J., 2013. Trends and ENSO/AAO driven variability in NDVI derived productivity and phenology alongside the Andes Mountains. Remote Sensing, 5(3): 1177-1203.

Vanderkimpen, P., Melger, E., Peeters, P., 2008. Flood modeling for risk evaluation: a MIKE FLOOD vs. SOBEK 1D2D benchmark study.

W. Brunner, G., 2016. HEC-RAS River Analysis System. Hydraulic Reference Manual. Version 5.0, 538 pp.

Wahl, T., Jain, S., Bender, J., Meyers, S.D., Luther, M.E., 2015. Increasing risk of compound flooding from storm surge and rainfall for major US cities. Nature Climate Change, 5(12): 1093-1097. DOI:10.1038/nclimate2736

Waldon, M., 2018. High Water Elevations on the Vermilion River During the Flood of August 2016.

Wang, H.V., Loftis, J.D., Forrest, D., Smith, W., Stamey, B., 2015. Modeling storm surge and inundation in Washington, DC, during Hurricane Isabel and the 1936 Potomac River Great Flood. Journal of Marine Science and Engineering, 3(3): 607-629.

Wang, X., Kinsland, G., Poudel, D., Fenech, A., 2019. Urban flood prediction under heavy precipitation. Journal of Hydrology, 577: 123984. DOI:https://doi.org/10.1016/j.jhydrol.2019.123984

Watson, K.B., Ricketts, T., Galford, G., Polasky, S., O'Niel-Dunne, J., 2016. Quantifying flood mitigation services: The economic value of Otter Creek wetlands and floodplains to Middlebury, VT. Ecological Economics, 130: 16-24. DOI:https://doi.org/10.1016/j.ecolecon.2016.05.015

Watson, K.M., Storm, J.B., Breaker, B.K., Rose, C.E., 2017. Characterization of peak streamflows and flood inundation of selected areas in Louisiana from the August 2016 flood. 2017-5005, Reston, VA. DOI:10.3133/sir20175005

Webster, P., Rangeley-Wilson, C., Juniper, T., Harrison, P., 2014. Floods and dredging a reality check. CIWEM, Feb.

Wolter, K., Timlin, M.S., 2011. El Niño/Southern Oscillation behaviour since 1871 as diagnosed in an extended multivariate ENSO index (MEI.ext). International Journal of Climatology, 31(7): 1074-1087. DOI:https://doi.org/10.1002/joc.2336

Wu, K., A. Johnston, C., 2008. Hydrologic comparison between a forested and a wetland/lake dominated watershed using SWAT. Hydrological Processes, 22(10): 1431-1442. DOI:https://doi.org/10.1002/hyp.6695

Wu, W. et al., 2018. Mapping dependence between extreme rainfall and storm surge. Journal of Geophysical Research: Oceans, 123(4): 2461-2474.

Wu, Y., Zhang, G., Rousseau, A.N., Xu, Y.J., Foulon, É., 2020. On how wetlands can provide flood resilience in a large river basin: A case study in Nenjiang river Basin, China. Journal of Hydrology, 587: 125012. DOI:https://doi.org/10.1016/j.jhydrol.2020.125012

Zhang, Y., Wallace, J.M., Battisti, D.S., 1997. ENSO-like Interdecadal Variability: 1900–93. Journal of Climate, 10(5): 1004-1020. DOI:10.1175/1520-0442(1997)010<1004:eliv>2.0.co;2

Zhao, C. et al., 2017. Temperature increase reduces global yields of major crops in four independent estimates. Proceedings of the National Academy of Sciences, 114(35): 9326-9331.

Saad, Haitham Abdel Hakeem. Bachelor of Science, Ain Shams University, Egypt, Spring 2006; Master of Science, Ain Shams University, Egypt, Spring 2013; Master of Science, University of Louisiana at Lafayette, Spring 2018; Doctor of Philosophy, University of Louisiana at Lafayette, Spring 2022
Major: Systems Engineering
Title of Dissertation: Understanding Complex Flooding Dynamics in Low-Gradient Coastal Watersheds Using Hybrid 1D/2D Hydrodynamic Modeling and Implications for Flood Risk Mitigation
Dissertation Director: Dr. Emad Habib
Pages in Dissertation: 162, Words in Abstract: 330

Abstract

Extreme flooding in coastal watersheds poses a significant threat to human life and infrastructure. When combined with low-gradient topographies, such flooding conditions exhibit a complex hydrodynamic nature in rivers and connected tributaries. Reverse flows, local stagnations, prolonged flooding, and slow recessions are often witnessed. However, the relative significance of the different physical drivers behind complex flood dynamics in low-gradient systems is challenging to discern. In addition to its research significance, developing a comprehensive understanding of complex flood dynamics in low-gradient riverine systems is essential for designing effective flood mitigation strategies in such environments.

The overall goal of this dissertation is to develop a comprehensive understanding of the complex flood dynamics in low-gradient riverine systems using a modeling-based approach. Using this approach, the study will also provide a deep insight into the value of different strategies for flood mitigation and how they perform under extreme rainfall events and changing landscapes. The study starts by investigating the level of model complexity required for reproducing complex flood regimes in low-gradient watersheds. Following that, the best-performing modeling approach is used to evaluate the performance of different mitigation strategies, including: riverine dredging as a traditional flood mitigation strategy in

response to decreased channel capacities, and using nature-based approaches via maximizing the role of riverine-connected natural storage areas in mitigating the flooding impact.

The study highlighted the significance of incorporating large swamp areas within the basin in the model to successfully capture the complex flow dynamics in the river. Additionally, the slow recession of the flood peaks was accurately reproduced by the model with the use of 2D representation of the swamp areas. The results showed that riverine dredging can significantly alter the flood dynamics in the river. Despite its potential benefits, riverine dredging can significantly increase the amplitude and inland propagation of the Gulf tidal waves. The results also suggested that dynamic management of swamp areas appeared to be more effective in mitigating floods than traditional solutions, without any unintended negative consequences to the river.

Biographical Sketch

Haitham Saad received a Bachelor of Science with degree of honor in civil engineering from Ain Shams University. He joined Ain Shams University as a teaching assistant and earned his Master of Science degree in civil engineering from the same university in 2013. He then pursued the Ph.D. degree in systems engineering, civil engineering at the University of Louisiana at Lafayette. In Spring 2018, he earned his second master's degree. His research in the program has centered on understanding the flood dynamics in low-gradient watersheds. He graduated in the Spring of 2022 from UL Lafayette with a Doctor of Philosophy degree in systems engineering with a concentration in civil engineering.